TECHNISCHE
UNIVERSITÄT
WIEN

DIPLOMARBEIT

Geometric Multigrid Method with *hp*-Robust Contraction

ausgeführt am

Institut für
Analysis und Scientific Computing
TU Wien

unter der Anleitung von

Univ.-Prof. Dr. Dirk Praetorius

und

Dr. Ani Miraçi

durch

Paula Hilbert Bsc.

[redacted]

Wien, am 18. Dezember 2024

Kurzfassung

Im Kontext numerischer Methoden für symmetrische lineare elliptische PDEs ermöglicht die adaptive Finite-Elemente-Methode (AFEM) eine effiziente Diskretisierung des Problems, was zu optimalen Konvergenzraten in Bezug auf die Größe des Finite-Elemente-Raums führt. Um jedoch auch optimale Konvergenzraten in Bezug auf den Gesamtrechenaufwand zu erreichen, ist ein iteratives Verfahren erforderlich, das zur Lösung der auftretenden diskreten Probleme eingesetzt wird. In dieser Arbeit betrachten wir ein geometrisches Mehrgitterverfahren als iterativen Löser für AFEM, dessen Kontraktion pro Schritt unabhängig von den Ebenen der inhärenten Netzhierarchie und dem Polynomgrad p der FEM-Basisfunktionen ist. Obwohl er hp-robust ist, hängt der Kontraktionsfaktor von dem globalen Diffusionskontrast der gegebenen PDE ab. Ziel dieser Arbeit ist es, die Abhängigkeit des Kontraktionsfaktors so zu verbessern, dass er nur noch vom lokalen Kontrast des Diffusionskoeffizienten abhängt.

Zuerst wird die Analyse des Mehrgitterlösers von [Innerberger, Miraçi, Praetorius, Streitberger; ESAIM Math. Model. Numer. Anal. 58 (2024)] untersucht und festgestellt, dass die wichtigsten Werkzeuge für den Nachweis der hp-robusten Kontraktion des Lösers eine hp-robuste stabile Zerlegung und eine verschärfte Cauchy-Schwarz-Ungleichung sind. Beide Ergebnisse sind für die H^1-Seminorm formuliert, die eine Abhängigkeit vom globalen Diffusionskontrast einführt. Daher konzentrieren wir uns auf die Ableitung analoger Ergebnisse für die diffusionsgewichtete Energienorm, die sich aus der schwachen Formulierung der PDE ergibt. Die größte Herausforderung besteht darin, eine h-robuste stabile Zerlegung in diesem neuen Rahmen zu beweisen. Um dies zu erreichen, werden zusätzliche Konzepte wie das sogenannte K-Funktional, gewichtete L^2-Normen und Fortsetzungsoperatoren für Sobolev-Räume eingeführt. Unter Verwendung dieser Werkzeuge sowie durch Anpassung der Analyse der p-robusten stabilen Zerlegung im zweidimensionalen Fall können wir nachweisen, dass der Kontraktionsfaktor tatsächlich (zusätzlich zur hp-Robustheit) nur lokal vom Diffusionskontrast abhängig ist.

Schließlich werden die theoretischen Erkenntnisse durch entsprechende numerische Experimente validiert.

Abstract

In the context of numerical methods for symmetric linear elliptic PDEs, the adaptive finite element method (AFEM) enables an efficient discretization of the problem, leading to optimal convergence rates with respect to the size of the finite element space. However, to achieve optimal convergence rates with respect to the total computational cost, an iterative method is required to solve the arising discrete problems. In this work, we consider a geometric multigrid method as an iterative solver for AFEM, whose contraction per step is independent of the number of levels in the inherent mesh hierarchy and the polynomial degree p of the FEM basis functions. Though it is hp-robust, the contraction factor depends on the global diffusion-contrast of the inherent PDE. This thesis aims to improve the dependence of the contraction factor so that it depends only on the local contrast of the diffusion coefficient.

First, the analysis of the multigrid solver of [Innerberger, Miraçi, Praetorius, Streitberger; ESAIM Math. Model. Numer. Anal. 58 (2024)] is examined, establishing that the key ingredients for proving hp-robust contraction of the solver are an hp-robust stable decomposition and a strengthened Cauchy–Schwarz inequality. Both results are formulated for the H^1-seminorm, which leads to the dependence on the global diffusion-contrast. Therefore, we focus on deriving analogous results for the diffusion-weighted energy norm arising from the weak formulation of the PDE. The main challenge lies in proving an h-robust stable decomposition in this new setting. To address this, additional concepts such as the so-called K-functional, weighted L^2-norms, and extension operators for Sobolev spaces are introduced. Using these tools as well as adapting the analysis of the p-robust stable decomposition in the two-dimensional case, we are able to prove, that, indeed, the contraction factor is (in addition to hp-robust) only locally dependent on the diffusion-contrast.

Finally, the theoretical findings are validated through appropriate numerical experiments.

Danksagung

Zunächst möchte ich mich herzlich bei Professor Dirk Praetorius und Dr. Ani Miraçi für die exzellente Betreuung dieser Diplomarbeit sowie für das umfangreiche Korrekturlesen bedanken. Beide haben sich immer Zeit genommen, um meine Fragen zu beantworten, und haben mir durch zahlreiche lehrreiche Gespräche wertvolle Unterstützung geboten.

Ein besonderer Dank gilt Julian Streitberger für die vielfältige Unterstützung bei allen Herausforderungen, die während des Schreibens dieser Arbeit aufgetreten sind. Ebenso danke ich meiner Arbeitsgruppe für die großartige Arbeitsatmosphäre und für die nötige geistige Erholung an den anstrengenden Bürotagen.

Darüber hinaus möchte ich meinen Mitstudenten und Freunden für die vielen schönen Erfahrungen sowohl im Studium als auch in der Freizeit danken. Ein spezieller Dank geht an Sascha für seine kontinuierliche Unterstützung und zahllosen Hilfestellungen, die er mir seit Beginn des Studiums zuteilwerden ließ.

Abschließend danke ich meinen Eltern von Herzen für ihre unerschütterliche moralische und finanzielle Unterstützung. Dank ihres ständigen Rückhalts konnte ich mich voll auf mein Studium konzentrieren, mich weiterentwickeln und schließlich dieses bedeutende Kapitel meines Lebens erfolgreich vollenden.

Diese Arbeit wurde finanziell durch die TU Wien im Rahmen der Mittel zur Förderung von Frauen in der Mathematik sowie durch das TU Commitment SFB F65 Projekt *Taming Complexity in PDE Systems* unterstützt.

Eidesstattliche Erklärung

Ich erkläre an Eides statt, dass ich die vorliegende Diplomarbeit selbstständig und ohne fremde Hilfe verfasst, andere als die angegebenen Quellen und Hilfsmittel nicht benutzt bzw. die wörtlich oder sinngemäß entnommenen Stellen als solche kenntlich gemacht habe.

Wien, am 18. Dezember 2024

Paula Hilbert

Contents

1 Introduction

A large variety of scientific and technological advances rely on numerical simulations of partial differential equations (PDEs). A versatile discretization method is the finite element method (FEM), which solves the weak formulation of the PDE with exact solution $u^* \in \mathcal{X}$ on a finite dimensional subspace $\mathcal{X}_H \subset \mathcal{X}$. However, standard FEM relies on computational meshes $\mathcal{T}_H$ where all elements have comparable sizes and convergence rates can only be shown under additional regularity assumptions on the exact weak solution, see, e.g. [EG21b]. The pursuit of optimal convergence rates with respect to the size of the finite element space without additional assumptions is one reason to consider adaptive finite element methods (AFEMs). The adaptive algorithm consists of four modules. In the `SOLVE` module, the discrete solution $u_H^* \in \mathcal{X}_H$ on a given mesh $\mathcal{T}_H$ is calculated. Afterwards, a-posteriori error indicators for every element of the mesh are computed in the `ESTIMATE` module. These are then used in the `MARK` module to decide which elements require refinement. For this, a marking strategy and adaptivity parameter θ, which is given as an input to the algorithm, are needed. In the `REFINE` module, a new mesh, where at least every marked element is refined, is calculated: AFEM thus takes the following feedback loop structure

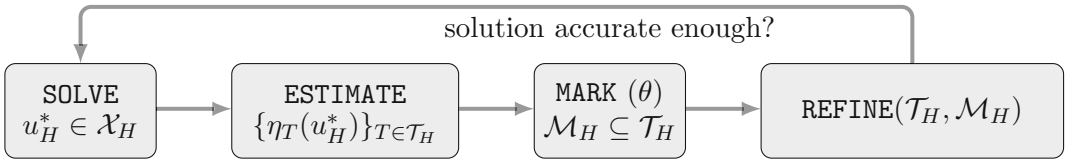

and allows to obtain a sequence of meshes and corresponding discrete solutions. Under reasonable assumptions on every module, it can be shown that AFEM even for minimal regularity of the exact solution yields optimal convergence rates with respect to the number of elements in the mesh, see, e.g. [CFP+14]. Although this result is a significant improvement compared to standard FEM, one can even obtain optimal convergence rates with respect to the overall computational cost and thus time, provided the algorithm is slightly modified. This leads to the introduction of iterative solvers. The adaptive loop is modified so that the `SOLVE` and `ESTIMATE` modules are combined and the discrete solution is not solved via direct solve anymore, but an iterative solver is utilized until the estimated algebraic error is sufficiently reduced compared to the estimated discretization error. This is implemented via a stopping criterion balancing the error components, which uses a solver-stopping parameter λ. Hence, the structure becomes

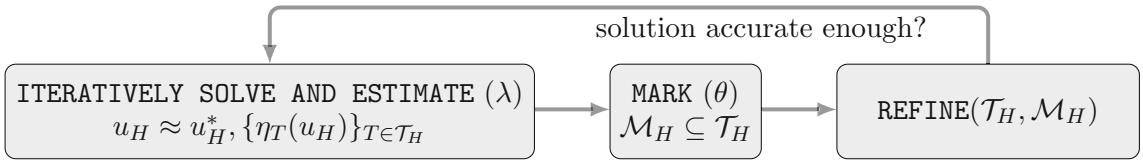

In order for the adaptive algorithm to be optimal with respect to the overall cost, i.e., of optimal complexity, the solver must be chosen suitably. More precisely, we require that the solver satisfies the following two properties:

(i) linear complexity,

(ii) uniform contraction.

Let us denote by $u_H \in \mathcal{X}_H$ a given approximation to the discrete solution $u_H^* \in \mathcal{X}_H$ and by $\Phi_H : \mathcal{X}_H \to \mathcal{X}_H$ the iteration operator of the solver on the finite element space $\mathcal{X}_H$. Then, we say that the solver contracts uniformly if there exists a constant $q_{\mathrm{ctr}} \in (0, 1)$ independent of $\mathcal{X}_H$ such that

$$\|\!| u_H^* - \Phi_H(u_H) |\!\| \leq q_{\mathrm{ctr}} \, \|\!| u_H^* - u_H |\!\|.$$

The contraction factor needs to be uniform, in particular, it is independent of the refinement level, and hence the mesh size h. Furthermore, q_{ctr} should even be independent of the polynomial degree p used in the FEM discretization. Then, we say that the multigrid solver is *hp*-robust. The motivation behind considering higher polynomial degrees is that they yield better convergence rates for AFEM; see, e.g. [BDD04; CKN$^+$08]. In this thesis, we consider a specific geometric multigrid solver, which satisfies the required properties (i)–(ii) and was introduced in [IMP$^+$24].

We will study the symmetric linear elliptic diffusion problem

$$\begin{aligned} -\operatorname{div}(\mathbf{K}\nabla u^*) &= f \quad \text{in } \Omega, \\ u^* &= 0 \quad \text{on } \partial\Omega, \end{aligned}$$

with $\mathbf{K}$ being symmetric, bounded, and uniformly elliptic. The analysis in [IMP$^+$24] yields that the contraction factor depends on the ratio of the biggest to smallest eigenvalue of the diffusion coefficient $\mathbf{K}$ *over the whole domain*. However, numerical experiments gave the indication that q_{ctr} actually depends only on *local* variations of the diffusion coefficient. The main objective and contribution of this thesis is to prove that the dependency is indeed local.

We conclude this introduction with a short overview on the structure of the work. The preliminary Chapters 2 and 3 introduce the underlying concepts of AFEM and geometric multigrid methods. Furthermore, the actual setting for the main results is described and the geometric multigrid solver is proposed. Afterwards, the existence of an *hp*-robust contraction factor q_{ctr} is shown in Chapter 4. For this, the proofs from [IMP$^+$24] are presented, but more details are added so that we can improve specific results accordingly in the following chapter. Finally, in Chapter 5 we show the main result of the thesis: the contraction factor q_{ctr} indeed depends only on local variations of the diffusion coefficient $\mathbf{K}$ for $d \in \{2, 3\}$, see Theorem 5.1. Moreover, for $d = 2$ we also prove that the main result holds p-robustly. The original proof of algebraic error contraction in Theorem 4.13 requires two main ingredients namely an *hp*-robust stable decomposition and a strengthened Cauchy–Schwarz inequality. In order to improve the dependency on the diffusion coefficient, we had to revisit both components. In Chapter 5, we first show that indeed the constant in the strengthened Cauchy–Schwarz inequality is influenced only by local diffusion-contrasts. Subsequently, we

turn to the *hp*-stable decomposition, where we first prove an *h*-robust stable decomposition for both $d = 2$ and $d = 3$ with the desired local dependency. Moreover, for $d = 2$ we are also able to show a *p*-robust stable decomposition with constants depending only locally on the diffusion. Analogously to the original proofs from [IMP+24], these two decompositions can be combined to obtain an *hp*-robust stable decomposition with the improvement that the stability constant now depends only on the local variations of the diffusion coefficient. Since the purpose of establishing a uniformly contractive solver was to use it in AFEM, we discuss how the proposed multigrid solver fits into the AFEM framework from [GHP+21] in Chapter 6. Furthermore, the theory in [GHP+21] immediately implies optimal complexity of AFEM with the proposed geometric multigrid solver. Lastly, Chapter 7 presents numerical experiments that corroborate the analysis developed in Chapter 5.

2 Model problem and adaptive algorithm

In this chapter, we first define some essential properties of meshes. Afterwards, we present the model problem, for which we will prove the analytical results. Subsequently, a short introduction to the finite element method (FEM) is given and it is used in the discretization of the model problem. Lastly, we describe the adaptive finite element method (AFEM) in Algorithm 2.11.

2.1 Mesh properties

First, we give some definitions concerning simplicial triangulations.

Definition 2.1. For a bounded domain $\Omega \subset \mathbb{R}^d$, a finite set $\mathcal{T}$ is called a *mesh* of Ω if

- every $T \in \mathcal{T}$ is a compact subset of Ω with $|T| > 0$,
- the elements cover the closure of Ω, i.e., $\bigcup_{T\in\mathcal{T}} T = \overline{\Omega}$,
- the intersection of two elements $T, T' \in \mathcal{T}$ with $T \neq T'$ has measure zero, i.e., $|T \cap T'| = 0$.

Definition 2.2. A set $T \subset \mathbb{R}^d$ is called a *non-degenerate simplex* if there exists $z_0, \dots, z_d \in \mathbb{R}^d$ such that $T = \operatorname{conv}(z_0, \dots, z_d)$ and $|T| > 0$. We denote by $\mathcal{V}_T := \{z_0, \dots, z_d\}$ the *set of vertices* of T.

Definition 2.3. Let $\Omega \subset \mathbb{R}^d$ be a bounded Lipschitz domain with polytopal boundary $\partial\Omega$. A set $\mathcal{T}$ is a *conforming simplicial triangulation* of Ω if it fulfills

- $\mathcal{T}$ is a finite set of simplices,
- the simplices cover the closure of Ω, meaning $\bigcup_{T\in\mathcal{T}} T = \overline{\Omega}$,
- the intersection of two elements $T, T' \in \mathcal{T}$ is either empty or there exists a set $M \in \mathcal{V}_T \cap \mathcal{V}_{T'}$ with $T \cap T' = \operatorname{conv}(M)$. In the last case, we call $\operatorname{conv}(M)$ a joint k-dimensional hyperface of T and T' with $k := \#M - 1$.

We denote by

$$\mathcal{V} := \bigcup_{T\in\mathcal{T}} \mathcal{V}_T$$

the *set of vertices* of $\mathcal{T}$.

Definition 2.4. Let $\mathcal{T}$ be a conforming simplicial triangulation of $\Omega \subset \mathbb{R}^d$ with $d \geq 2$. Define the *shape regularity constant* of $\mathcal{T}$ by

$$\sigma(\mathcal{T}) := \max_{T \in \mathcal{T}} \frac{\operatorname{diam}(T)}{|T|^{1/d}} > 0 \tag{2.1}$$

If there exists $\gamma > 0$ such that $\sigma(\mathcal{T}) \leq \gamma < \infty$, we say that $\mathcal{T}$ is γ-*shape regular*.

Shape-regular triangulations have the following important property.

Proposition 2.5 (γ-comparable neighbor diameters)**.** *Let $\mathcal{T}$ be a conforming simplicial triangulation of $\Omega \subset \mathbb{R}^d$ with $d \geq 2$, which is γ-shape regular for $\gamma > 0$. Then, there exists $C > 0$ depending only on γ and the dimension d such that*

$$\max_{T \in \mathcal{T}} \max_{\substack{T' \in \mathcal{T} \\ T \cap T' \neq \emptyset}} \frac{\operatorname{diam}(T)}{\operatorname{diam}(T')} \leq C. \tag{2.2}$$

Proof. We start with the case that $T \cap T'$ contains a 1-dimensional hyperface, which we call E. Such a hyperface is a shared edge between the two simplices and we denote its length by $|E|$. For the volume, it holds

$$|T| \leq \operatorname{diam}(T)^{d-1}|E| \leq \operatorname{diam}(T)^{d-1} \operatorname{diam}(T').$$

The γ-shape regularity (2.1) implies $\operatorname{diam}(T) \leq \gamma |T|^{1/d}$ for every $T \in \mathcal{T}$. Hence, we get

$$|T| \leq \operatorname{diam}(T)^{d-1} \operatorname{diam}(T') \leq \gamma^d |T|^{(d-1)/d} |T'|^{1/d}$$

and therefore $|T|^{1/d} \leq \gamma^d |T'|^{1/d}$. Moreover, for every simplex, we have $|T| \leq \operatorname{diam}(T)^d$. Combining this with γ-shape regularity (2.1) and the above estimate, we see

$$\operatorname{diam}(T) \leq \gamma |T|^{1/d} \leq \gamma^{d+1} |T'|^{1/d} \leq \gamma^{d+1} \operatorname{diam}(T'). \tag{2.3}$$

The case where T and T' only share a vertex still needs to be discussed. Because $\mathcal{T}$ is γ-shape regular, the number of simplices that share a vertex is bounded by an integer n that depends only on γ. Therefore, we can find n simplices $\{T_i\}_{i=1}^n$ with $T = T_1$, $T' = T_n$ such that the dimension of the hyperface $T_i \cap T_{i+1}$ is at least one for all $i = 1, \dots, n-1$. Iterating the established estimate (2.3) for the first case, we get

$$\operatorname{diam}(T) \leq \gamma^{n(d+1)} \operatorname{diam}(T').$$

Dividing by $\operatorname{diam}(T')$ and taking the maximum gives the result (2.2). □

Remark 2.6. *We want to emphasize that for $d = 1$ the estimate (2.2) needs to be enforced by the refinement algorithm. We will discuss this in more detail in Section 2.4.1.*

2.2 Model problem

Let $d \in \{1, 2, 3\}$ and $\Omega \subset \mathbb{R}^d$ be a bounded Lipschitz domain with polytopal boundary $\partial\Omega$. We consider the second-order symmetric linear elliptic diffusion problem

$$\begin{aligned} -\operatorname{div}(\mathbf{K}\nabla u^*) &= f \quad \text{in } \Omega, \\ u^* &= 0 \quad \text{on } \partial\Omega, \end{aligned} \tag{2.4}$$

where $f \in L^2(\Omega)$ and $\mathbf{K} \in [L^\infty(\Omega)]^{d\times d}_{\mathrm{sym}}$ is symmetric and uniformly positive definite. Let $\mathcal{T}_0$ be an initial conforming simplicial triangulation of Ω. We actually require the stronger regularity $\mathbf{K}|_T \in [W^{1,\infty}(T)]^{d\times d}$ for all $T \in \mathcal{T}_0$. More precisely, this is needed in Lemma 4.11 and for the residual error estimator (2.17). For $x \in \Omega$, the expressions $\lambda_{\max}(\mathbf{K}(x))$ and $\lambda_{\min}(\mathbf{K}(x))$ denote the maximal and minimal eigenvalue of $\mathbf{K}(x) \in \mathbb{R}^{d\times d}$ respectively. Furthermore, it is useful to define

$$0 < \Lambda_{\min} := \operatorname{ess\,inf}_{x\in\Omega} \lambda_{\min}(\mathbf{K}(x)) \le \Lambda_{\max} := \operatorname{ess\,sup}_{x\in\Omega} \lambda_{\max}(\mathbf{K}(x)) < \infty$$

by assumption on $\mathbf{K}$. For any measurable set $\omega \subseteq \Omega$, we denote the $L^2(\omega)$-scalar product with $\langle\cdot,\cdot\rangle_\omega$. The weak formulation of (2.4) is given by: Find $u^* \in \mathcal{X} := H^1_0(\Omega)$ that solves

$$\langle\!\langle u^*, v\rangle\!\rangle_\Omega := \langle \mathbf{K}\nabla u^*, \nabla v\rangle_\Omega = \langle f, v\rangle_\Omega =: F(v) \quad \text{for all } v \in \mathcal{X}. \tag{2.5}$$

From here on, we omit the index ω for $\omega = \Omega$.

Proposition 2.7 (Equivalent energy norm)**.** *The bilinear form $\langle\!\langle\cdot,\cdot\rangle\!\rangle$ is a scalar product on $\mathcal{X}$ and the induced semi-norm $|\!|\!|u|\!|\!|^2 := \langle\!\langle u, u\rangle\!\rangle$ is an equivalent norm on $\mathcal{X}$. More precisely, there holds*

$$\Lambda_{\min}^{1/2}\|\nabla u\| \le |\!|\!|u|\!|\!| \le \Lambda_{\max}^{1/2}\|\nabla u\| \quad \textit{for all } u \in \mathcal{X} \tag{2.6}$$

Proof. The bilinearity and symmetry of $\langle\!\langle\cdot,\cdot\rangle\!\rangle$ are clear as $\mathbf{K}$ is symmetric. Next, we show that $|\!|\!|\cdot|\!|\!|$ is equivalent to $\|\nabla\cdot\|$. For a symmetric matrix $A \in \mathbb{R}^{d\times d}$,it holds

$$\lambda_{\min}(A) = \min_{\substack{v\in\mathbb{R}^d \\ v\neq 0}} \frac{v^T A v}{|v|^2} \quad \text{and} \quad \lambda_{\max}(A) = \max_{\substack{v\in\mathbb{R}^d \\ v\neq 0}} \frac{v^T A v}{|v|^2}. \tag{2.7}$$

Applying this property to $\mathbf{K}(x)$ for every $x \in \Omega$ yields

$$\begin{aligned} |\!|\!|u|\!|\!|^2 &= \int_\Omega \mathbf{K}\nabla u\cdot\nabla u \,\mathrm{d}x \le \int_\Omega \lambda_{\max}(\mathbf{K}(x))\nabla u\cdot\nabla u \,\mathrm{d}x \le \Lambda_{\max}\|\nabla u\|^2, \\ \|\nabla u\|^2 &= \int_\Omega \nabla u\cdot\nabla u \,\mathrm{d}x \le \int_\Omega \frac{1}{\lambda_{\min}(\mathbf{K}(x))}\mathbf{K}\nabla u\cdot\nabla u \,\mathrm{d}x \le \frac{1}{\Lambda_{\min}}|\!|\!|u|\!|\!|^2. \end{aligned}$$

Finally, we note that $\|\nabla\cdot\|$ is a norm on $H^1_0(\Omega)$ so that $\langle\!\langle\cdot,\cdot\rangle\!\rangle$ is positive definite and hence a scalar product. This concludes the proof of (2.6). □

Proposition 2.7 allows us to apply the Lax–Milgram theorem, therefore yielding the existence of a unique solution $u^* \in \mathcal{X}$ to the problem (2.5).

2.3 Finite element method and discrete problem

In this section, we give a short introduction to the finite element/Galerkin method in an abstract framework. Afterwards, we formulate the discretization of the model problem.

2.3.1 Galerkin method

Let X be a Hilbert space and $\langle\!\langle \cdot, \cdot \rangle\!\rangle_X$ a scalar product on X such that the induced norm $|\!|\!| v |\!|\!|_X^2 := \langle\!\langle v, v \rangle\!\rangle_X$ admits constants $C_1, C_2 > 0$ that satisfy

$$C_1 \|v\|_X \leq |\!|\!| v |\!|\!|_X \leq C_2 \|v\|_X \quad \text{for all } v \in X. \tag{2.8}$$

For any $L \in X^*$, the Riesz theorem provides a unique solution $u \in X$ of

$$\langle\!\langle u, v \rangle\!\rangle_X = L(v) \quad \text{for all } v \in X. \tag{2.9}$$

The Galerkin method considers the problem (2.9) on a finite dimensional subspace $X_h \subseteq X$. Again, the Riesz theorem proves the existence and uniqueness of the solution $u_h \in X_h$ to

$$\langle\!\langle u_h, v_h \rangle\!\rangle_X = L(v_h) \quad \text{for all } v_h \in X_h. \tag{2.10}$$

We call u_h the Galerkin solution. This gives rise to the definition of the Galerkin projection $\mathbb{G}_h : X \to X_h$, where

$$\langle\!\langle \mathbb{G}_h u, \cdot \rangle\!\rangle_X = \langle\!\langle u, \cdot \rangle\!\rangle_X \in X_h^*.$$

The defining characteristic of the projection is the Galerkin orthogonality

$$\langle\!\langle u - \mathbb{G}_h u, v_h \rangle\!\rangle_X = 0 \quad \text{for all } v_h \in X_h. \tag{2.11}$$

This implies the Pythagorean identity

$$\begin{aligned} |\!|\!| u - v_h |\!|\!|_X^2 &= |\!|\!| u - \mathbb{G}_h u + \mathbb{G}_h u - v_h |\!|\!|_X^2 \\ &= |\!|\!| u - \mathbb{G}_h u |\!|\!|_X^2 + |\!|\!| \mathbb{G}_h u - v_h |\!|\!|_X^2 + 2\langle\!\langle u - \mathbb{G}_h u, \mathbb{G}_h u - v_h \rangle\!\rangle \\ &\overset{(2.11)}{=} |\!|\!| u - \mathbb{G}_h u |\!|\!|_X^2 + |\!|\!| \mathbb{G}_h u - v_h |\!|\!|_X^2 \quad \text{for all } v_h \in X_h. \end{aligned} \tag{2.12}$$

Ultimately, we want to state two well-known properties of the Galerkin method. The proofs can be found, e.g., in [Pra17].

Lemma 2.8 (Céa lemma)**.** *The Galerkin error is quasi-optimal, i.e., there holds*

$$\|u - \mathbb{G}_h u\|_X \leq \frac{C_1}{C_2} \min_{v_h \in X_h} \|u - v_h\|_X \quad \textit{for all } u \in X,$$

with C_1 and C_2 from (2.8)*. Furthermore, for the energy norm, we have that*

$$|\!|\!| u - \mathbb{G}_h u |\!|\!|_X = \min_{v_h \in X_h} |\!|\!| u - v_h |\!|\!|_X \quad \textit{for all } u \in X. \qquad \square \tag{2.13}$$

Lemma 2.9 (Galerkin approximation property)**.** *For all $h > 0$, we assume X_h to be a finite dimensional subspace of X. Let $D \subseteq X$ be a dense subspace of X, such that the approximation property*

$$\lim_{h \to 0} \min_{v_h \in X_h} \|u - v_h\|_X = 0 \quad \textit{for all } u \in D$$

is satisfied. Then, for every $u \in X$ it holds that

$$\lim_{h \to 0} \|u - \mathbb{G}_h u\|_X = 0. \qquad \square$$

2.3.2 Discretization of the model problem

Next, we define the finite element spaces for the discretization of the model problem (2.5).

Definition 2.10. Let $\mathcal{T}_h$ be a conforming simplicial triangulation, $p \in \mathbb{N}$ a fixed polynomial degree, and $T \in \mathcal{T}_h$ a simplex. We denote by $\mathbb{P}^p(T)$ the space of all polynomials on T, whose degree is at most p. The discrete space $\mathbb{S}^p(\mathcal{T}_h)$ is defined as

$$\mathbb{S}^p(\mathcal{T}_h) := \{v_h \in C(\Omega) : v_h|_T \in \mathbb{P}^p(T) \text{ for all } T \in \mathcal{T}_h\}.$$

Furthermore, we write $\mathcal{X}_h^p := \mathbb{S}_0^p(\mathcal{T}_h) := \mathbb{S}^p(\mathcal{T}_h) \cap H_0^1(\Omega)$.

The finite element method for the model problem is just the Galerkin method with the Hilbert space $\mathcal{X} = H_0^1(\Omega)$ and the discrete spaces $\mathcal{X}_h^p$. It is important to note, that the finite element spaces $\mathcal{X}_h^p$ rely on two parameters: The subscript h represents the inherent mesh $\mathcal{T}_h$ used in the discretization, while p gives the maximal polynomial degree of discrete functions aiming to approximate the solution u^* of (2.5) in the space $\mathcal{X}_h^p$. The discrete problem reads as follows: Find the solution $u_h^* \in \mathcal{X}_h^p$ to

$$\langle\!\langle u_h^*, v_h \rangle\!\rangle = \langle \mathbf{K}\nabla u_h^*, \nabla v_h \rangle = \langle f, v_h \rangle = F(v_h) \quad \text{for all } v_h \in \mathcal{X}_h^p. \tag{2.14}$$

If we choose a basis of $\mathcal{X}_h^p$, the discrete problem (2.14) can be rewritten as a linear system with a symmetric and positive definite matrix. Therefore, the solution u_h^* can be computed provided that computational resources suffice.

2.4 Adaptive algorithm

We first state the adaptive finite element algorithm. Subsequently, we explain the steps in the adaptive loop in more detail.

Algorithm 2.11 (Adaptive finite element method)**.** ***Input:*** *An initial mesh* $\mathcal{T}_0$.
Adaptive loop: *repeat the following steps* (i)–(iv) *for all* $\ell = 0, 1, \ldots$:

(i) `SOLVE:` *Compute the discrete solution* u_ℓ^* *associated to the mesh* $\mathcal{T}_\ell$.

(ii) `ESTIMATE:` *Compute local contributions* $\eta_\ell(T, u_\ell^*)$ *of an error estimator*

$$\eta_\ell(u_\ell^*)^2 := \sum_{T \in \mathcal{T}_\ell} \eta_\ell(T, u_\ell^*)^2$$

for all $T \in \mathcal{T}_\ell$.

(iii) `MARK:` *Depending on* $(\eta_\ell(T, u_\ell^*))_{T \in \mathcal{T}_\ell}$, *choose a set* $\mathcal{M}_\ell \subseteq \mathcal{T}_\ell$ *via a suitable criterion, where the estimated error dominates.*

(iv) `REFINE:` *Generate* $\mathcal{T}_{\ell+1} := \texttt{REFINE}(\mathcal{T}_\ell, \mathcal{M}_\ell)$ *so that all marked elements are refined.*

Output: *A sequence of conforming simplicial triangulations* $\mathcal{T}_\ell$, *discrete solutions* u_ℓ^*, *and error estimators* $\eta_\ell(u_\ell^*)$.

In the following, we will describe the setting of each module of the adaptive loop, as it is used in the remainder of this work.

2.4.1 Newest vertex bisection

The module `REFINE` uses newest vertex bisection (NVB). In the adaptive algorithm, a sequence of successively refined meshes $\{\mathcal{T}_\ell\}_{\ell=0}^L$ is generated from an initial conforming simplicial triangulation $\mathcal{T}_0$. It is useful to define the set $\mathbb{T} := \mathbb{T}(\mathcal{T}_0)$ of all refinements of $\mathcal{T}_0$ obtained by finitely many steps of NVB. We need to define the refinement strategy `REFINE` so that for a given triangulation $\mathcal{T}_{\ell-1}$, $\ell \in \{1, \dots, L\}$, and a set of marked elements $\mathcal{M}_{\ell-1} \subset \mathcal{T}_{\ell-1}$ the refined mesh can be obtained by $\mathcal{T}_\ell = \texttt{REFINE}(\mathcal{T}_{\ell-1}, \mathcal{M}_{\ell-1})$. Such a strategy should have the following properties:

(A) All marked elements are refined and

$$T = \bigcup \{T' \in \mathcal{T}_\ell \mid T' \subseteq T\} \quad \text{for all } T \in \mathcal{T}_{\ell-1}.$$

(B) The new triangulation is conforming.

(C) The created sequence is uniformly γ-shape regular, i.e.,

$$\max_{\ell=0,\dots,L} \max_{T\in\mathcal{T}_\ell} \frac{\operatorname{diam}(T)}{|T|^{1/d}} \leq \gamma < \infty, \tag{2.15}$$

where γ depends only on $\mathcal{T}_0$. For $d \geq 2$, Proposition 2.5 additionally implies

$$\max_{\ell=0,\dots,L} \max_{T\in\mathcal{T}_\ell} \max_{\substack{T'\in\mathcal{T}_\ell \\ T\cap T'\neq\emptyset}} \frac{\operatorname{diam}(T)}{\operatorname{diam}(T')} \leq \gamma^{n(d+1)} < \infty. \tag{2.16}$$

(D) The least amount of elements $T \in \mathcal{T}_{\ell-1}\backslash\mathcal{M}_{\ell-1}$ are refined to achieve (B) and (C).

One refinement strategy that satisfies these properties is NVB. We will first introduce newest vertex bisection in 2D and then give some remarks for $d \in \{1, 3\}$. The first step in the 2D algorithm is to assign a reference edge for every triangle in $\mathcal{T}_0$. For that, an arbitrary newest vertex is chosen in each triangle. The reference edge lies opposite to the newest vertex. An element is refined by halving the reference edge so that the midpoint becomes the newest vertex of the two new triangles. We can now formulate the algorithm:

(i) For every marked element $T \in \mathcal{M}_{\ell-1}$, we mark the reference edge.

(ii) Repeat recursively: If any non-reference edge of a triangle is marked, we additionally mark its reference edge.

The second step (ii) is repeated recursively to ensure that the resulting mesh will be conforming. Note that (ii) terminates as there are only finitely many edges in a triangulation. Following this procedure, we end up with four different cases for a triangle $T \in \mathcal{T}_{\ell-1}$ (see also Figure 2.1):

(iii) Apply the refinement pattern:

- If no edges are marked, the element remains unchanged i.e., $T \in \mathcal{T}_\ell$.

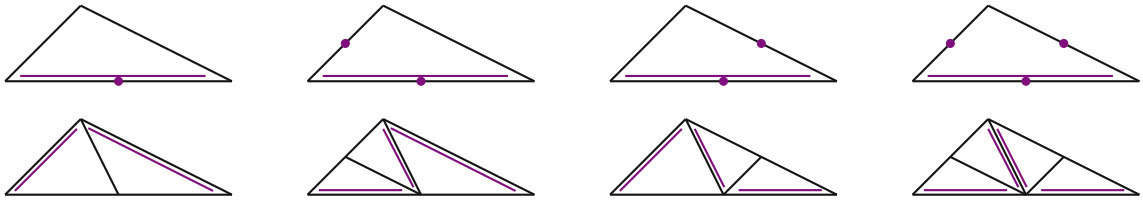

Figure 2.1: The four different cases of newest vertex bisection in 2D. Above: Edges with a violet dot are marked for refinement and the reference edge is always indicated with a violet line. Below: Refined element with new reference edges.

Figure 2.2: Refinement by NVB leads only to 4 similarity classes of triangles. We can see this by iterating NVB until no more new classes of triangles appear.

- If one edge is marked, it has to be the reference edge. Consequently, we halve the triangle as described above.
- If two edges are marked, one bisection is done for the reference edge. The other marked edge is the reference edge of one of the new triangles. We also bisect this triangle.
- If all edges are marked, the triangle is halved once as in the second case. Afterward, both reference edges of the new triangles are still marked. Hence, we also bisect these triangles.

When applying NVB repeatedly to a single element, we discover that just 4 similarity classes of triangles arise. Thus, in a sequence of meshes generated by NVB, only finitely many types of triangles appear; see Figure 2.2. Henceforth, such a sequence $\{\mathcal{T}_\ell\}_{\ell=0}^L$ is uniformly γ-shape regular. Because we solely mark necessary triangles $T \in \mathcal{T}_{\ell-1} \backslash \mathcal{M}_{\ell-1}$ in the recursive step and since all new nodes are edge midpoints, the described strategy also satisfies properties (B) and (D).

Generalizing NVB for $d \geq 3$ is not a trivial task. We will outline the algorithm given in [Ste08] and comment on the challenges that arise. Following the structure from the 2D algorithm, one needs to define a bisection rule. For a simplex T, denote the reference edge by E_T. Let $T = \operatorname{conv}(z_0, \dots, z_d)$ be a simplex and assume $E_T = \operatorname{conv}(z_0, z_d)$, then the children of T are given by $C_1(T) := \operatorname{conv}(z_0, \dots, z_{d-1}, y)$ and $C_2(T) := \operatorname{conv}(y, z_1, \dots, z_d)$, where $y = (z_0 + z_d)/2$. The last step of a bisection rule is the assignment of the reference edges of the children $C_1(T)$ and $C_2(T)$. A complete bisection rule can be found in [Ste08]. It is important to note that, if the assignment of reference edges is not well-thought, it is impossible to guarantee uniformly γ-shape regular triangulations using said bisection rule. However, the bisection rule proposed in [Ste08] only generates finitely many types of simplices, hence the created sequence of meshes is uniformly γ-shape regular, i.e., property (C) is fulfilled. This statement was proven in [Tra97]. We need to introduce some more notation, before we can formulate NVB for higher dimensions. Consider a simplicial mesh $\mathcal{T}$.

For a simplex $T = \operatorname{conv}(z_0, \dots, z_d) \in \mathcal{T}$, we define its edges $\mathcal{E}(T) := \{\operatorname{conv}(z_i, z_j) : i \neq j\}$. Furthermore, $\mathcal{E}(\mathcal{T}) := \bigcup_{T\in\mathcal{T}} \mathcal{E}(T)$ denotes the set of all edges of $\mathcal{T}$. Lastly, we define the refinement patch $\mathcal{R}(T) = \{T' \in \mathcal{T} : E_T \subset T'\}$ and say it is compatibly bisectable if and only if $\mathcal{R}(T) = \mathcal{R}^*(T) := \{T' \in \mathcal{T} : E_{T'} = E_T\}$. The following algorithm is a loop-based variation from Schön [Sch17] of the recursive algorithm proposed in [Ste08].

Algorithm 2.12 (Newest vertex bisection for $d \geq 3$)**.** ***Input:*** *A triangulation $\mathcal{T}$ and a set of marked elements $\mathcal{M} \subseteq \mathcal{T}$.*
Repeat the following steps (i)–(v)*, until $\mathcal{M} = \emptyset$:*

(i) *Define $\mathcal{E}^* := \{E_T \in \mathcal{E}(\mathcal{T}) : T \in \mathcal{M}\}$.*

(ii) *Repeat step* (a)–(b):

(a) *Define $\mathcal{U} := \{E_T \in \mathcal{E}(\mathcal{T})\backslash\mathcal{E}^* : T \in \mathcal{T}$ with $\mathcal{E}(T) \cap \mathcal{E}^* \neq \emptyset\}$.*

(b) *Update $\mathcal{E}^* \leftarrow\!\shortmid \mathcal{E}^* \cup \mathcal{U}$.*

until $\mathcal{U} = \emptyset$.

(iii) *Define the set of simplices to be bisected $\mathcal{R} := \{T \in \mathcal{T} : E_T \in \mathcal{E}^*$ and $\mathcal{R}(T) = \mathcal{R}^*(T)\}$.*

(iv) *Refine the triangulation by updating $\mathcal{T} \leftarrow\!\shortmid \mathcal{T}\backslash\mathcal{R} \cup \{C_1(T), C_2(T) : T \in \mathcal{R}\}$.*

(v) *Update the marked elements $\mathcal{M} \leftarrow\!\shortmid \mathcal{M}\backslash\mathcal{R}$.*

Output: *Refined triangulation $\mathcal{T}$, where all marked simplices have been bisected.*

So far, it is unclear whether Algorithm 2.12 terminates. Leaving this problem aside for now, the above algorithm only refines compatibly bisectable refinement patches, therefore maintaining the conformity of $\mathcal{T}$. In step (ii), we add reference edges $E_{T'}$ of elements T' to the set $\mathcal{E}^*$, if the reference edge of a marked element $T \in \mathcal{M}$ is an edge of T', i.e., $E_T \in \mathcal{E}(T')$. This process is repeated until no more new edges are added to $\mathcal{E}^*$. This recursion terminates since $\mathcal{T}$ consists only of finitely many simplices. Moreover, we add only reference edges of elements to $\mathcal{E}^*$ that need to be bisected for $\mathcal{T}$ to stay conforming. Hence, if the algorithm terminates, it satisfies properties (A), (B), and (D). Thus, it is only left to discuss if Algorithm 2.12 terminates. In [Ste08], a so-called *admissibility* condition for the initial triangulation $\mathcal{T}_0$ is given, which indeed ensures termination. This condition depends on a local numbering of the vertices. For $d = 3$ and a given triangulation $\mathcal{T}_0$, a local numbering that makes $\mathcal{T}_0$ an admissible mesh does not always exist. However, one can construct a finer triangulation from $\mathcal{T}_0$ that is conforming and fulfills an even stronger condition; see [Ste08]. The downside is that in 3D every tetrahedron is split into 12 new elements. Having said that, the recent work [DGS24] introduces a novel initialization algorithm such that newest vertex bisection terminates for arbitrary $\mathcal{T}_0$ in any dimension.

Remark 2.13 (NVB for $d = 1$)**.** *We can make some simple observations for $d = 1$. Starting with an initial conforming mesh $\mathcal{T}_0$, bisecting any subset of elements always results in a conforming triangulation. Since* $\operatorname{diam}(T) = |T|$*, every triangulation is γ-shape regular with $\gamma = 1$. As stated in Proposition 2.5, γ-shape regularity for $d \geq 2$ implies that the diameters of neighboring elements are comparable. This does not apply to $d = 1$. For that reason,*

newest vertex bisection in 1D has a new requirement, namely that the generated sequence of meshes $\{\mathcal{T}_\ell\}_{\ell=0}^L$ *satisfies* (2.16). *As for* $d = 2$, *the algorithm must bisect the least amount of extra elements* $T \in \mathcal{T}_{\ell-1}\backslash\mathcal{M}_{\ell-1}$ *to achieve this. An algorithm with this property is proposed and analyzed in [AFF+13].*

For any mesh $\mathcal{T}_H$ of Ω, we denote by $\texttt{REFINE}(\mathcal{T}_H)$ the set of all meshes that can be created by finitely many steps of refinement of $\mathcal{T}_H$.

Proposition 2.14. *Let* $\mathcal{T}_0$ *be an initial mesh. Then, newest vertex bisection satisfies:*

(R1) ***splitting property:*** *Each refined element is split into at least two and at most* $C_{\text{child}} \geq 2$ *new elements, i.e., for all* $\mathcal{T}_H \in \texttt{REFINE}(\mathcal{T}_0)$ *and* $\mathcal{M}_H \subseteq \mathcal{T}_H$, *the mesh* $\mathcal{T}_h = \texttt{REFINE}(\mathcal{T}_H, \mathcal{M}_H)$ *fulfills*

$$\#(\mathcal{T}_H\backslash\mathcal{T}_h) + \#\mathcal{T}_H \leq \#\mathcal{T}_h \leq C_{\text{child}}\,\#(\mathcal{T}_H\backslash\mathcal{T}_h) + \#(\mathcal{T}_H \cap \mathcal{T}_h).$$

(R2) ***overlay estimate:*** *For all meshes* $\mathcal{T}_H, \mathcal{T}_h \in \texttt{REFINE}(\mathcal{T}_0)$, *there exists a common refinement* $\mathcal{T}_H \oplus \mathcal{T}_h \in \texttt{REFINE}(\mathcal{T}_H) \cap \texttt{REFINE}(\mathcal{T}_h) \subseteq \texttt{REFINE}(\mathcal{T}_0)$ *such that*

$$\#(\mathcal{T}_H \oplus \mathcal{T}_h) \leq \#\mathcal{T}_H + \#\mathcal{T}_h - \#\mathcal{T}_0.$$

(R3) ***mesh-closure estimate:*** *For any sequence* $(\mathcal{T}_\ell)_{\ell\in\mathbb{N}_0}$ *with* $\mathcal{T}_{\ell+1} = \texttt{REFINE}(\mathcal{T}_\ell, \mathcal{M}_\ell)$ *and* $\mathcal{M}_\ell \subseteq \mathcal{T}_\ell$ *for all* $\ell \in \mathbb{N}_0$, *it holds*

$$\#\mathcal{T}_\ell - \#\mathcal{T}_0 \leq C_{\text{mesh}} \sum_{j=0}^{\ell-1} \#\mathcal{M}_j,$$

where C_{mesh} *depends only on* $\mathcal{T}_0$.

We refer to [BDD04; Ste07; Ste08; CKN+08; KPP13; GSS14] for proofs of the above statement. The properties (R1)–(R3) are crucial to show optimality of Algorithm 2.11; see [CFP+14].

2.4.2 Residual error estimator

The module `ESTIMATE` relies on the standard residual error estimator. First, let us introduce some useful notation. Let $\mathcal{T}_h$ be a conforming simplicial triangulation. The size of a triangle $T \in \mathcal{T}_h$ is given by $h_T := |T|^{1/d}$. If the intersection $E := T \cap T'$ of two elements $T, T' \in \mathcal{T}_h$ is a $(d-1)$-dimensional hyperface, we define the jump of a function $v \in C(\mathcal{T}) := \{v \in L^2(\Omega) : v|_T \in C(\overline{T}) \text{ for all } T \in \mathcal{T}\}$ on E by

$$[\![v]\!] := v|_T - v|_{T'}.$$

Let $v_h \in \mathcal{X}_h^p$ and consider $\eta_h(T, v_h)$ for $T \in \mathcal{T}_h$, the elementwise estimator. For the model problem (2.5), this is given by

$$\eta_h(T, v_h) := h_T^2 \|f + \operatorname{div}(\mathbf{K}\nabla v_h)\|_T^2 + h_T \|[\![\mathbf{K}\nabla v_h]\!] \cdot \mathbf{n}\|_{\partial T\cap\Omega}^2, \tag{2.17a}$$

where $\mathbf{n}$ is the outer normal vector of the element T. Define

$$\eta_h(\mathcal{U}_h, v_h) := \Big(\sum_{T \in \mathcal{U}_h} \eta_h(T, v_h)^2 \Big)^{1/2} \quad \text{for all } \mathcal{U}_h \subseteq \mathcal{T}_h \text{ and all } v_h \in \mathcal{X}_h^p. \tag{2.17b}$$

For $\mathcal{U}_h = \mathcal{T}_h$ we shall use the shorter notation $\eta_h(v_h) := \eta_h(\mathcal{T}_h, v_h)$. The standard residual error estimator (2.17) has some useful properties, that we summarize in the following proposition.

Proposition 2.15 (Axioms of adaptivity)**.** *Let $\mathcal{T}_0$ be an initial mesh, $\mathcal{T}_H \in \texttt{REFINE}(\mathcal{T}_0)$ and $\mathcal{T}_h \in \texttt{REFINE}(\mathcal{T}_H)$. Then, the standard residual error estimator fulfills:*

- **(A1)** ***stability:*** *$|\eta_h(\mathcal{U}_H, v_h) - \eta_H(\mathcal{U}_H, v_H)| \le C_{\mathrm{stab}} \, |\!|\!| v_h - v_H |\!|\!|$ for all $v_h \in \mathcal{X}_h^p, v_H \in \mathcal{X}_H^p$ and all $\mathcal{U}_H \subseteq \mathcal{T}_H \cap \mathcal{T}_h$.*
- **(A2)** ***reduction:*** *$\eta_h(\mathcal{T}_h \backslash \mathcal{T}_H, v_H) \le q_{\mathrm{red}} \, \eta_H(\mathcal{T}_H \backslash \mathcal{T}_h, v_H)$ for all $v_H \in \mathcal{X}_H^p$.*
- **(A3)** ***reliability:*** *$|\!|\!| u^* - u_H^* |\!|\!| \le C_{\mathrm{rel}} \, \eta_H(u_H^*)$ for the exact discrete solution.*
- **(A4)** ***discrete reliability:*** *$|\!|\!| u_h^* - u_H^* |\!|\!| \le C_{\mathrm{drel}} \, \eta_H(\mathcal{T}_H \backslash \mathcal{T}_h, u_H^*)$ for the exact discrete solutions.*

The constant C_{rel} depends only on γ-shape regularity, C_{stab} and C_{drel} depend additionally on the polynomial degree p, and, for NVB, it holds $q_{\mathrm{red}} = 2^{-1/(2d)}$.

The properties (A1)–(A4) are called axioms of adaptivity and were introduced in [CFP+14].

Remark 2.16. *Another assumption on the error estimator that can be found in the literature is quasi-monotonicity; see, e.g., [CFP+14]. An error estimator is quasi-monotone if there exists a constant $C_{\mathrm{mon}} > 0$ such that*

- **(QM)** ***quasi-monotonicity:*** *$\eta_h(u_h^*) \le C_{\mathrm{mon}} \, \eta_H(u_H^*)$ for all $\mathcal{T}_H \in \texttt{REFINE}(\mathcal{T}_0)$ and all $\mathcal{T}_h \in \texttt{REFINE}(\mathcal{T}_H)$.*

Moreover, the axioms (A1)–(A4) *already imply quasi-monotonicity* (QM) *as shown in the following corollary.*

Corollary 2.17. *Suppose the error estimator η_H satisfies stability* (A1)*, reduction* (A2)*, and discrete reliability* (A4)*. Then, the error estimator η_H is also quasi-monotone.*

Proof. Stability (A1), reduction (A2), and discrete reliability (A4) yield

$$\begin{aligned}
\eta_h(u_h^*)^2 &\overset{\text{(A1)}}{\le} 2\eta_h(u_H^*)^2 + 2C_{\mathrm{stab}}^2 |\!|\!| u_h^* - u_H^* |\!|\!|^2 \\
&= 2\eta_h(\mathcal{T}_h \backslash \mathcal{T}_H, u_H^*)^2 + 2\eta_h(\mathcal{T}_h \cap \mathcal{T}_H, u_H^*)^2 + 2C_{\mathrm{stab}}^2 |\!|\!| u_h^* - u_H^* |\!|\!|^2 \\
&\overset{\text{(A2)}}{\le} 2q_{\mathrm{red}}\eta_H(\mathcal{T}_H \backslash \mathcal{T}_h, u_H^*)^2 + 2\eta_H(\mathcal{T}_h \cap \mathcal{T}_H, u_H^*)^2 + 2C_{\mathrm{stab}}^2 |\!|\!| u_h^* - u_H^* |\!|\!|^2 \\
&\overset{\text{(A4)}}{\le} 2q_{\mathrm{red}}\eta_H(\mathcal{T}_H \backslash \mathcal{T}_h, u_H^*)^2 + 2\eta_H(\mathcal{T}_h \cap \mathcal{T}_H, u_H^*)^2 + 2C_{\mathrm{stab}}^2 C_{\mathrm{drel}}^2 \eta_H(\mathcal{T}_H \backslash \mathcal{T}_h, u_H^*)^2 \\
&\le (2 + 2C_{\mathrm{stab}}^2 C_{\mathrm{drel}}^2)\eta_H(u_H^*)^2.
\end{aligned}$$

This concludes the proof with $C_{\mathrm{mon}}^2 = 2 + 2C_{\mathrm{stab}}^2 C_{\mathrm{drel}}^2$. □

2.4.3 Dörfler marking

The module MARK in Algorithm 2.11 employs Dörfler marking [Dör96]. For a given parameter $0 < \theta \leq 1$, we say that a set $\mathcal{M}_\ell \subseteq \mathcal{T}_\ell$ fulfills the Dörfler criterion with respect to $\eta_\ell(u_\ell^*)$, if

$$\theta \eta_\ell(u_\ell^*)^2 \leq \sum_{T \in \mathcal{M}_\ell} \eta_\ell(T, u_\ell^*)^2 =: \eta_\ell(\mathcal{M}_\ell, u_\ell^*)^2. \tag{2.18}$$

This can be understood as selecting a set $\mathcal{M}_\ell$ of elements, whose associated estimator contribution is bigger than a θ-portion of the total error. To be able to have optimal convergence rates, we have to select a subset $\mathcal{M}_\ell$ with quasi-minimal cardinality. The set $\mathbb{M}(\mathcal{T}_\ell, \theta, u_\ell^*) := \{\mathcal{U}_\ell \subset \mathcal{T}_\ell \mid \theta \eta_\ell(u_\ell^*)^2 \leq \eta_\ell(\mathcal{U}_\ell, u_\ell^*)^2\}$ contains all subsets of $\mathcal{T}_\ell$ that satisfy the Dörfler criterion (2.18) for $\eta_\ell(u_\ell^*)$. Given a constant $C_{\mathrm{mark}} \geq 1$ we shall choose a set that fulfills

$$\mathcal{M}_\ell \in \mathbb{M}(\mathcal{T}_\ell, \theta, u_\ell^*) \quad \text{with} \quad \#\mathcal{M}_\ell \leq C_{\mathrm{mark}} \min_{\mathcal{U}_\ell \in \mathbb{M}(\mathcal{T}_\ell, \theta, u_\ell^*)} \#\mathcal{U}_\ell.$$

Furthermore, we want the MARK module to have linear cost. However, it is not immediately clear if this is possible, since the naive algorithm to obtain a set $\mathcal{M}_\ell$ with minimal cardinality includes sorting of the local contributions $\{\eta_\ell(T, u_\ell^*)\}_{T \in \mathcal{T}_\ell}$. An algorithm with linear cost guaranteeing $C_{\mathrm{mark}} = 2$ can be found in [Ste07]. Linear cost is even possible for $C_{\mathrm{mark}} = 1$ as shown in [PP20]. The choice of Dörfler marking is not arbitrary, as it is the optimal marking criterion, where optimality is to be understood in the following sense.

Proposition 2.18 (Optimality of Dörfler marking [CFP+14, Proposition 4.12])**.** *Suppose stability* (A1) *and discrete reliability* (A3)*. For all* $0 < \theta_0 < \theta_{\mathrm{opt}} := (1 + C_{\mathrm{rel}}^2 C_{\mathrm{stab}}^2)^{-1}$*, there exists* $0 < \kappa < 1$ *such that for all* $0 < \theta \leq \theta_0$*, all triangulations* $\mathcal{T}_H \in \texttt{REFINE}(\mathcal{T}_0)$*, and all refinements* $\mathcal{T}_h \in \texttt{REFINE}(\mathcal{T}_H)$*, it holds*

$$\eta_h(u_h^*)^2 \leq \kappa \eta_H(u_H^*)^2 \quad \Longrightarrow \quad \theta \eta_H(u_H^*)^2 \leq \eta_H(\mathcal{R}_{Hh}, u_H^*)^2.$$

The set $\mathcal{R}_{Hh} \subseteq \mathcal{T}_H$ *from* (A4) *satisfies* $\mathcal{T}_H \backslash \mathcal{T}_h \subseteq \mathcal{R}_{Hh}$ *and* $\#\mathcal{R}_{Hh} \leq C'_{\mathrm{rel}}(\#\mathcal{T}_h - \#\mathcal{T}_H)$*. Furthermore, discrete reliability* (A4) *yields* $|||u_h^* - u_H^*||| \leq C_{\mathrm{drel}}\, \eta_H(\mathcal{R}_{Hh}, u_H^*)$*.*

The proposition states that if the error estimator is reduced, then Dörfler marking holds on $\mathcal{R}_{Hh}$, which is essentially the set of refined elements. We refer to [CFP+14, Proposition 4.12] for a proof of this statement.

2.4.4 Iterative solver

The module SOLVE was already mentioned in Section 2.3.2. There, we stated that the discrete solution u_ℓ^* can be computed using an exact solver. This is not advisable if we want the module SOLVE to have cost proportional to $\mathcal{O}(\#\mathcal{T}_\ell)$ operations. Hence, the idea is to use a suitable iterative solver. In the next chapter, we will introduce such an iterative solver, namely a geometric multigrid method. Then, the exact FEM solution u_ℓ^* in Algorithm 2.11 will be replaced with an approximation u_ℓ^k obtained by k steps of the iterative algebraic solver.

3 Multigrid solver

The goal of this chapter is to formulate an iterative solver, that works well in the adaptive finite element algorithm. In our case, this will be a geometric multigrid solver. Therefore, we will first talk about the core ideas of multigrid methods.

3.1 Core properties

In this section, we give a brief introduction to geometric multigrid methods based on [BHM00; Gil07]. We will explain the algorithm and its motivation through an easy one-dimensional model problem discretized via finite differences.

3.1.1 Model problem and Jacobi method

We look at the second-order boundary value problem

$$\begin{aligned} -(u^*)'' &= f \quad \text{on } (0,1), \\ u^*(0) = u^*(1) &= 0. \end{aligned} \tag{3.1}$$

Then, the canonical finite difference discretization reads

$$\begin{aligned} -\frac{u_{j+1} - 2u_j + u_{j-1}}{h^2} &= f(x_j) \quad \text{for all } 1 \le j \le n-1, \\ u_0 = u_n &= 0, \end{aligned}$$

where $n \in 2\mathbb{N}$ is even and $n+1$ is the number of discretization points, $h = 1/n$ is the mesh size, $x_j = jh$ are the grid points in $[0,1]$, and the unkown $u_j \in \mathbb{R}$ is an approximation of $u^*(x_j)$ for all $j = 1, \dots, n-1$. We denote by $\mathcal{G}_h$ the grid with width h. The problem can be rewritten as a linear equation

$$\frac{1}{h^2} \begin{pmatrix} 2 & -1 & & & \\ -1 & 2 & -1 & & \\ & \ddots & \ddots & \ddots & \\ & & -1 & 2 & -1 \\ & & & -1 & 2 \end{pmatrix} \begin{pmatrix} u_1 \\ u_2 \\ \vdots \\ u_{n-2} \\ u_{n-1} \end{pmatrix} = \begin{pmatrix} f_1 \\ f_2 \\ \vdots \\ f_{n-2} \\ f_{n-1} \end{pmatrix}, \tag{3.2}$$

with $f_j := f(x_j)$. One can use direct methods such as Gaussian elimination to solve for the exact solution $u \in \mathbb{R}^{n-1}$. For such a particular 1D case, this may still yield linear performance (due to the band structure of the matrix in (3.2)) but becomes rather expensive in practical applications. A different approach is to use iterative methods, which start from an initial guess and try to improve it with every iteration. Such an iterative method is

the geometric multigrid method, developed to have certain interesting properties that we discuss subsequently.

Let us first discuss a simple iterative procedure, namely the Jacobi iteration. The equation (3.2) is of the form $Au = f$, i.e., a diagonally dominant and irreducible system of linear equations. Let $A = D + L + U$, where D is the diagonal of A, and L and U are the strictly lower and upper triangular parts of A. The equation can be transformed via

$$\begin{aligned} Au = f \quad &\Longleftrightarrow \quad (D + L + U)u = f \\ &\Longleftrightarrow \quad Du = -(L + U)u + f \\ &\Longleftrightarrow \quad u = -D^{-1}(L + U)u + D^{-1}f. \end{aligned}$$

One step of the so-called Jacobi method is defined by $u^{(i+1)} := -D^{-1}(L + U)u^{(i)} + D^{-1}f$. Let us examine the behavior of the Jacobi method. Consider the homogeneous problem $Au = 0$, thus $u = 0$, and for an approximation v, the error is $e = -v$. We apply the Jacobi method to different initial guesses

$$v_j^m := \sin\left(\frac{jm\pi}{n}\right), \quad 0 \le j \le n,\ 1 \le m \le n - 1,$$

where the vectors v^m are named Fourier modes, and the parameter m is called wavenumber or frequency. Small values of m give long and smooth waves, while large values correspond to highly oscillatory waves. Numerical experiments show that the Jacobi method eliminates oscillatory modes rather quickly as opposed to low-frequency modes, which are eliminated much slower. Therefore, applying such an iterative step is sometimes called smoothing, and the step itself can be called smoother. The limitations of the Jacobi method for low oscillatory modes stem from the smoothing only being able to treat error components associated with the fixed mesh size. Hence, a remedy is to introduce a mesh hierarchy as proposed by multigrid methods.

3.1.2 Multigrid algorithm in one dimension

One can observe that the projection of a smooth mode onto a coarser grid yields a more oscillatory mode. An example is shown in Figure 3.1. A natural question is how fine-grid vectors v^h are projected onto a coarser mesh $\mathcal{G}_{2h}$ with mesh size $2h$. The first choice would be to take the values from the finer grid directly, i.e., $v_j^{2h} := v_{2j}^h$. However, since loss of information occurs this way, another alternative is the weighting operator $I_h^{2h} : \mathbb{R}^{n-1} \to \mathbb{R}^{n/2-1}$, which is defined by

$$I_h^{2h} v^h = v^{2h} \quad \text{with} \quad v_j^{2h} := \frac{1}{4}\left(v_{2j-1}^h + 2v_j^h + v_{2j+1}^h\right).$$

We will also need a way to interpolate vectors v^{2h} from the coarse grid to the fine grid $\mathcal{G}_h$. To this end, we define the interpolation operator $I_{2h}^h : \mathbb{R}^{n/2-1} \to \mathbb{R}^{n-1}$, $I_{2h}^h v^{2h} = v^h$, where

$$\begin{aligned} v_{2j}^h &:= v_j^{2h}, \\ v_{2j+1}^h &:= \frac{1}{2}\left(v_j^{2h} + v_{j+1}^{2h}\right), \quad 0 \le j \le \frac{n}{2} - 1. \end{aligned}$$

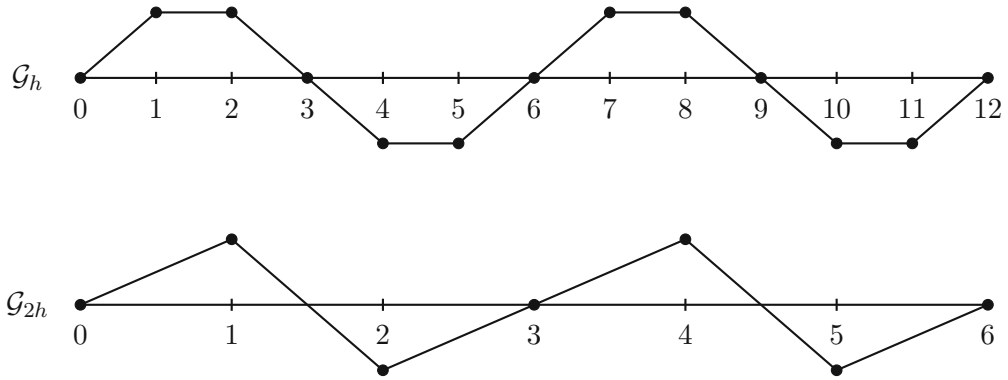

Figure 3.1: The low-frequency Fourier mode with wavenumber $m = 4$ on a grid of size $n = 12$ and its nodal projection onto a coarser grid with $n = 6$ grid points.

One idea of multigrid methods is to approximate the exact solution u of $Au = f$ on the fine grid using some iterations of a chosen iterative method (pre-smoothing), which provides an approximation v. Afterwards, the residual $r := f - Av$ is projected onto a coarser grid, where the leftover low-frequency components appear more oscillatory. On the coarse grid, we solve the residual equation $Ae = f - Av = r$ of reduced size exactly (coarse solve). Lastly, the solution e is interpolated back onto the fine grid, where we update our approximation to $v + I_{2h}^h e$ and may iterate again (post-smoothing). The described procedure is called the two-grid correction scheme. The algorithm for this scheme reads as follows:

Algorithm 3.1 (Two-grid correction scheme)**.** ***Input:*** *A matrix A^h, a vector f^h, an initial guess v^h, parameters α_1 and α_2, and an iterative method* (`SMOOTHER`)*.*

(i) *Pre-smoothing: Iterate the* `SMOOTHER` *α_1 times on $A^h u^h = f^h$ with initial guess v^h and compute the residual $r^h = f^h - A^h v^h$.*

(ii) *Restrict the residual to the coarse grid $r^{2h} = I_h^{2h} r^h$.*

(iii) *Coarse solve: Solve $A^{2h} e^{2h} = r^{2h}$ on $\mathcal{G}_{2h}$.*

(iv) *Interpolate the error back to $\mathcal{G}_h$, i.e., $e^h = I_{2h}^h e^{2h}$ and correct the approximation $v^h \leftarrow\!\shortmid v^h + e^h$.*

(v) *Post-smoothing: Iterate the* `SMOOTHER` *α_2 times on $A^h u^h = f^h$ with initial guess v^h.*

Output: *The improved approximation v^h.*

We overwrite the approximation v^h in the algorithm whenever we iterate on it. Note that the matrix A^{2h} is not yet defined. Looking at the initial idea, we find that A^{2h} should be the result of the discretization of the model problem (3.1) on the grid $\mathcal{G}_{2h}$. However, calculating this matrix is not practical, so instead we use our projection and interpolation operators and define $A^{2h} := I_h^{2h} A^h I_{2h}^h$. Since step (iii) is still expensive if $\mathcal{G}_{2h}$ is too fine, it is a good idea to iterate the two-step scheme until the coarsest grid yields a linear system small enough to be solved directly. This leads to the so-called V-cycle scheme. Let $\{\mathcal{G}_{2^\ell h}\}_{\ell=0}^L$ be a sequence of nested grids.

Algorithm 3.2 (V-cycle). ***Input:*** *A matrix A^h, a vector f^h, an initial guess v^h, parameters α_1 and α_2, and an iterative method* (`SMOOTHER`).

(i) *Pre-smoothing: Iterate the* `SMOOTHER` *α_1 times on $A^h u^h = f^h$ with initial guess v^h.*

(ii) *If $\mathcal{G}_h$ is the coarsest grid, then go to step* (iv).
Else, restrict to a coarser grid:

$$f^{2h} = I_h^{2h}(f^h - A^h v^h), \quad A^{2h} = I_h^{2h} A^h I_{2h}^h, \quad v^{2h} = \text{V-cycle}(A^{2h}, f^{2h}, 0).$$

(iii) *Correct the approximation $v^h \hookleftarrow v^h + I_{2h}^h v^{2h}$.*

(iv) *Post-smoothing: Iterate the* `SMOOTHER` *α_2 times on $A^h u^h = f^h$ with initial guess v^h.*

Output: *The improved approximation v^h.*

For simplicity, we denote the residual as just another right-hand side f^{2h} and the approximation of the solution of the residual equation as v^{2h}. Coarse grids can also be used to calculate a better initial guess. Moreover, smoothing steps on coarser levels are cheaper. This idea leads to the full multigrid (FMG) algorithm. We start on the coarsest grid, where we approximate the solution to $Au = f$. Then, we use the interpolation of this approximation as an initial vector for the next finer grid. Now we do a V-cycle between the two grids to improve the approximation. This gives a good initial guess for the next finer grid and a V-cycle on the three grids, we have already visited, improves the approximation again. The described process is repeated until a final V-cycle is performed on the finest grid. Let's summarize this procedure.

Algorithm 3.3 (FMG). ***Input:*** *A matrix A^h, a vector f^h, and a parameter α_0.*

(i) *If $\mathcal{G}_h$ is the coarsest grid, then set $v^h = 0$ and go to step* (iii).
Else, restrict to a coarser grid:

$$f^{2h} = I_h^{2h} f^h, \quad A^{2h} = I_h^{2h} A^h I_{2h}^h, \quad v^{2h} = \text{FMG}(A^{2h}, f^{2h}).$$

(ii) *Use the approximation as an initial guess on the finer grid $v^h = I_{2h}^h v^{2h}$.*

(iii) *Perform α_0 V-cycles, i.e., $v^h \hookleftarrow \text{V-cycle}(A^h, f^h, v^h)$*

Output: *The approximation v^h.*

It is not immediately clear how to choose the parameters α_1 and α_2 in Algorithm 3.2 and the parameter α_0 in Algorithm 3.3, since the user wants to balance accuracy with cost. An option to treat this problem for solvers designed for AFEM will be given in Chapter 6. For a better understanding, the scheme of grids for the V-cycle and full multigrid algorithm are shown in Figure 3.2.

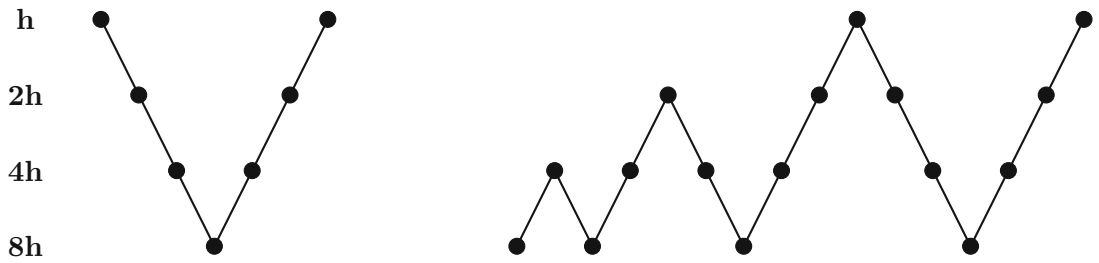

Figure 3.2: The structures of a V-cycle and full multigrid with $\alpha_0 = 1$.

Remark 3.4 (Cost of FMG)**.** *It may seem that the full multigrid would be far more expensive than a V-cycle on the same sequence of grids of L levels. However, the number of operations is multiplied by a constant depending only on α_0. We observe that the number of grid points and therefore the cost is divided by 2 whenever we move to a coarser grid. This yields the estimate*

$$\text{cost(FMG)}_L = \alpha_0 \Big(\sum_{j=0}^{L} \frac{1}{2^j} \Big) \text{ cost(V-cycle)}_L \leq 2\alpha_0 \text{ cost(V-cycle)}_L.$$

Lastly, convergence of standard multigrid algorithms has been proven in the literature. For completion, we present the following result from [Hac85, Theorem 7.2.5].

Theorem 3.5 (Convergence of V-cycle)**.** *Suppose the following properties:*

- *The matrix A^h is symmetric and positive definite (SPD).*
- *The projection and interpolation operators satisfy $I_h^{2h} = (I_{2h}^h)^T$ in the sense of matrices.*
- *For the coarse-grid matrix, it holds $A^{2h} = I_h^{2h} A^h I_{2h}^h$.*
- *The smoothing iterations $\{u^{(i)}\}_{i \in \mathbb{N}}$ are given by $u^{(i+1)} = S^h u^{(i)} + T^h f$ for matrices S^h and T^h associated to the grid of size h so that $S^h = I - (W^h)^{-1} A^h$, $W^h = (W^h)^T$ and $W^h - A^h$ is positive definite.*
- *There exists a constant $C_A > 0$ such that the approximation property*

$$\| (A^h)^{-1} - I_{2h}^h (A^{2h})^{-1} I_h^{2h} \| \leq C_A h^{2m}$$

holds, where $2m$ is the order of the differential operator.

If at least one smoothing step is done, i.e., $\alpha_1 + \alpha_2 > 0$, then the V-cycle yields convergence of the iterates to the true algebraic solution. □

After gaining the core understanding of geometric multigrid methods, we move on to discuss a multigrid method suitable as an iterative solver in Algorithm 2.11.

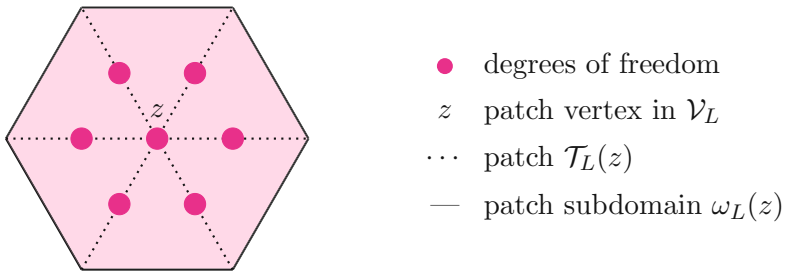

Figure 3.3: Degrees of freedom for the space $\mathcal{X}^2_{L,z}$ associated to the patch $\mathcal{T}_L(z)$.

3.2 Multigrid solver for adaptively refined meshes

The idea of using iterative methods for AFEM is rather natural since the `SOLVE` module in Algorithm 2.11 generates a linear equation. Furthermore, the adaptive loop provides a sequence of successively refined, and thus nested, meshes $\{\mathcal{T}_\ell\}_{\ell=0}^L$, which can be handled the same way as the grids $\{\mathcal{G}_{2^\ell h}\}_{\ell=0}^L$ in Algorithm 3.2 and 3.7. Since the discretization stems from a symmetric linear elliptic PDE, the arising matrix of the linear system is SPD and fits the previously discussed multigrid framework. Moreover, the interpolation operator is just the natural inclusion, because the finite element spaces associated to the triangulations $\mathcal{T}_\ell$ are nested

$$\mathcal{X}_0^1 \subseteq \mathcal{X}_1^1 \subseteq \cdots \subseteq \mathcal{X}_{L-1}^1 \subseteq \mathcal{X}_L^p,$$

where $p \geq 1$ is a fixed polynomial degree. In this section, we will use the functional description of the discrete problems (2.14) in order to avoid basis-dependent formulations induced by the matrices involved in solving these problems.

Let us introduce some useful notation. From now on, we consider $\{\mathcal{T}_\ell\}_{\ell=0}^L \subset \mathbb{T} = \mathbb{T}(\mathcal{T}_0)$ to be a sequence of successively refined simplicial triangulations, where NVB is used for the refinement. For a mesh $\mathcal{T}_\ell$, we recall that $\mathcal{V}_\ell$ denotes the set of vertices.

Definition 3.6. For all vertices $z \in \mathcal{V}_\ell$, we define the n-patch $\mathcal{T}_\ell^n(z)$ inductively by

$$\mathcal{T}_\ell(z) := \mathcal{T}_\ell^1(z) := \{T \in \mathcal{T}_\ell : z \in T\}, \quad \mathcal{T}_\ell^{n+1}(z) := \bigcup_{\substack{w \in T \cap \mathcal{V}_\ell \\ T \in \mathcal{T}_\ell^n(z)}} \mathcal{T}_\ell(w).$$

Moreover, we denote the corresponding n-patch subdomains by

$$\omega_\ell^n(z) := \operatorname{interior}\Big(\bigcup_{T \in \mathcal{T}_\ell^n(z)} T \Big).$$

Lastly, the size of a patch subdomain is given by $h_{\ell,z} := \max_{T \in \mathcal{T}_\ell(z)} h_T = \max_{T \in \mathcal{T}_\ell(z)} |T|^{1/d}$.

Furthermore, we define

$$\mathcal{V}_0^+ := \mathcal{V}_0 \text{ and } \mathcal{V}_\ell^+ := \mathcal{V}_\ell \backslash \mathcal{V}_{\ell-1} \cup \{\mathcal{V}_\ell \cap \mathcal{V}_{\ell-1} : \omega_\ell(z) \neq \omega_{\ell-1}(z)\} \text{ for } \ell \geq 1.$$

In other words, $\mathcal{V}_\ell^+$ is the set of new vertices in $\mathcal{T}_\ell$ as well as pre-existing vertices of $\mathcal{T}_{\ell-1}$, whose associated patch area was shrunk by the refinement. Lastly, we define the local spaces

$$\mathcal{X}_{\ell,z}^q := \mathbb{S}_0^q(\mathcal{T}_\ell(z)) \quad \text{for all } z \in \mathcal{V}_\ell \text{ and polynomial degrees } q \geq 1.$$

For $q = 1$ and $z \in \mathcal{V}_\ell \cap \partial\Omega$, we get $\mathcal{X}_{\ell,z}^1 = \emptyset$ by definition.

Recall from (2.14) that u_L^* is the exact FEM solution in the space $\mathcal{X}_L^p$. An iterative solver may be mathematically described by its iteration-step operator $\Phi_L : \mathcal{X}_L^p \to \mathcal{X}_L^p$, where $\Phi_L(u_L)$ is an improvement of the approximation $u_L \in \mathcal{X}_L^p$ to u_L^*. Then, the algebraic residual functional $R_L : \mathcal{X}_L^p \to \mathbb{R}$ is given by

$$v_L \in \mathcal{X}_L^p \mapsto R_L(v_L) := F(v_L) - \langle\!\langle u_L, v_L \rangle\!\rangle = \langle\!\langle u_L^* - u_L, v_L \rangle\!\rangle \in \mathbb{R}. \tag{3.3}$$

Another motivation for the construction of the solver is the levelwise orthogonal decomposition of the algebraic error $e_L^* := u_L^* - u_L$. We define $\rho_\ell^* \in \mathcal{X}_\ell^1$ for $\ell = 0, \dots, L-1$ to be the solution of

$$\langle\!\langle \rho_\ell^*, v_\ell \rangle\!\rangle = R_L(v_\ell) - \sum_{k=0}^{\ell-1} \langle\!\langle \rho_k^*, v_\ell \rangle\!\rangle \quad \text{for all } v_\ell \in \mathcal{X}_\ell^1.$$

Moreover, $\rho_L^* \in \mathcal{X}_L^p$ solves

$$\langle\!\langle \rho_L^*, v_L \rangle\!\rangle = R_L(v_L) - \sum_{k=0}^{L-1} \langle\!\langle \rho_k^*, v_L \rangle\!\rangle \quad \text{for all } v_L \in \mathcal{X}_L^p.$$

Hence, by construction, it follows

$$u_L^* = u_L + e_L^* = u_L + \sum_{\ell=0}^{L} \rho_\ell^*.$$

Furthermore, we observe $\langle\!\langle \rho_\ell^*, \rho_k^* \rangle\!\rangle = 0$ for all $0 \leq \ell, k \leq L$ with $\ell \neq k$, which follows from the Galerkin orthogonality by induction. Hence, we get

$$|\!|\!| u_L^* - u_L |\!|\!|^2 = |\!|\!| e_L^* |\!|\!|^2 = \sum_{\ell=0}^{L} |\!|\!| \rho_\ell^* |\!|\!|^2.$$

Since the components ρ_ℓ^* are pairwise orthogonal, it is a good idea to treat each error component on its respective level. We had a very similar observation in Section 3.1.2, where we saw that certain components of the error are more effectively eliminated on coarser grids. Although the described process constructs the exact algebraic error, it is not useful in practice since solving global problems on every level is very expensive. Therefore, the proposed multigrid method only solves one inexpensive global problem on the coarsest mesh. On the intermediate levels $\ell = 1, \dots, L-1$, local lowest-order problems on all patches $\mathcal{T}_\ell(z)$ for $z \in \mathcal{V}_\ell^+$ are solved. When $p = 1$, the same applies for $\ell = L$. If $p > 1$, then all patches of the finest mesh $\mathcal{T}_L$ are considered, i.e., the higher polynomial degree p is only taken into account on the final level $\ell = L$. The following algorithm calculates levelwise approximations of the algebraic error components/residual liftings ρ_ℓ^*. Furthermore, these approximations are also used to define an a-posteriori error estimator $\zeta_L(u_L)$ for the algebraic error.

Algorithm 3.7 (V-cycle of optimal local multigrid solver)**.** ***Input:*** *Current approximation* $u_L \in \mathcal{X}_L^p$*, triangulations* $\{\mathcal{T}_\ell\}_{\ell=0}^L$ *and polynomial degree* $p \geq 1$*.*
Solver step: *Follow the steps* (i)–(iii)*:*

(i) **Global residual problem on the coarsest mesh:**

- *Compute the lowest-order residual lifting* $\rho_0 \in \mathcal{X}_0^1$ *of*

$$\langle\!\langle \rho_0, v_0 \rangle\!\rangle = R_L(v_0) \quad \text{for all } v_0 \in \mathcal{X}_0^1. \tag{3.4}$$

- *Define the step-size* $\lambda_0 := 1$*.*
- *Initialize the error correction* $\sigma_0 := \lambda_0 \rho_0$ *and the a-posteriori estimator* $\zeta_0^2 := |\!|\!| \lambda_0 \rho_0 |\!|\!|^2$*.*

(ii) **Lowest-order local residual-updates:** *For* $\ell = 1, \dots, L-1$ *and also* $\ell = L$ *if* $p = 1$*, perform the following calculations:*

- *For all* $z \in \mathcal{V}_\ell^+$*, compute* $\rho_{\ell,z} \in \mathcal{X}_{\ell,z}^1$ *by solving*

$$\langle\!\langle \rho_{\ell,z}, v_{\ell,z} \rangle\!\rangle = R_L(v_{\ell,z}) - \langle\!\langle \sigma_{\ell-1}, v_{\ell,z} \rangle\!\rangle \quad \text{for all } v_{\ell,z} \in \mathcal{X}_{\ell,z}^1 \tag{3.5}$$

  and define the levelwise residual lifting $\rho_\ell := \sum_{z \in \mathcal{V}_\ell^+} \rho_{\ell,z}$*.*

- *Calculate*

$$s_\ell := \frac{R_L(\rho_\ell) - \langle\!\langle \sigma_{\ell-1}, \rho_\ell \rangle\!\rangle}{|\!|\!| \rho_\ell |\!|\!|^2} \tag{3.6}$$

  with the convention $0/0 := 0$ *in case of* $\rho_\ell = 0$*. Define the step-size*

$$\lambda_\ell := \begin{cases} s_\ell & \text{if } s_\ell \leq d+1 \\ (d+1)^{-1} & \text{otherwise.} \end{cases}$$

- *Define* $\sigma_\ell := \sigma_{\ell-1} + \lambda_\ell \rho_\ell$ *and* $\zeta_\ell^2 := \zeta_{\ell-1}^2 + \lambda_\ell \sum_{z \in \mathcal{V}_\ell^+} |\!|\!| \rho_{\ell,z} |\!|\!|^2$*.*

(iii) **High-order local residual-updates:** *If* $p > 1$*, do the following steps:*

- *For all* $z \in \mathcal{V}_L$*, compute* $\rho_{L,z} \in \mathcal{X}_{L,z}^p$ *by solving*

$$\langle\!\langle \rho_{L,z}, v_{L,z} \rangle\!\rangle = R_L(v_{L,z}) - \langle\!\langle \sigma_{L-1}, v_{L,z} \rangle\!\rangle \quad \text{for all } v_{L,z} \in \mathcal{X}_{L,z}^p \tag{3.7}$$

  and define $\rho_L := \sum_{z \in \mathcal{V}_L} \rho_{L,z}$*.*

- *Define the step-size*

$$\lambda_L := s_L := \frac{R_L(\rho_L) - \langle\!\langle \sigma_{L-1}, \rho_L \rangle\!\rangle}{|\!|\!| \rho_L |\!|\!|^2} \tag{3.8}$$

  with the convention $0/0 := 0$ *in case of* $\rho_L = 0$*.*

- *Define* $\sigma_L := \sigma_{L-1} + \lambda_L \rho_L$ *and* $\zeta_L^2 := \zeta_{L-1}^2 + \lambda_L \sum_{z \in \mathcal{V}_L} |\!|\!| \rho_{L,z} |\!|\!|^2$*.*

Output: *Improved approximation* $\Phi_L(u_L) := u_L + \sigma_L \in \mathcal{X}_L^p$ *and a-posteriori estimator* $\zeta_L(u_L) := \zeta_L$ *of the algebraic error.*

We note that the necessity of the case distinction of λ_ℓ will become more apparent later on in the analysis (see the proof of Lemma 4.2 on page 22), but in all practical applications we observed $s_\ell \leq d+1$ and hence $\lambda_\ell = s_\ell$ (see the experiments in Chapter 7). For now, we will just prove optimality of the choice of the step-size s_ℓ.

Lemma 3.8. *Let* $u_L + \sigma \in \mathcal{X}_L^p$ *be an approximation of* u_L^* *and* $\rho \in \mathcal{X}_L^p$ *a correction. Then, the optimal step-size is given by*

$$\arg\min_{\lambda\in\mathbb{R}} \|\!| u_L^* - (u_L + \sigma + \lambda\rho) |\!\| = \frac{\langle\!\langle u_L^* - (u_L+\sigma), \rho \rangle\!\rangle}{|\!\|\rho|\!\|^2}.$$

Proof. We want to determine the minimum of the function

$$G(\lambda) := |\!\| u_L^* - (u_L + \sigma + \lambda\rho) |\!\|^2 = |\!\| u_L^* - (u_L+\sigma) |\!\|^2 - 2\lambda \langle\!\langle u_L^* - (u_L+\sigma), \rho \rangle\!\rangle + \lambda^2 |\!\|\rho|\!\|^2.$$

The minimum translates to the best choice of the step-size λ in the error correction direction ρ so that after the update, the new iterate has the lowest algebraic error. Therefore, we calculate the derivative

$$G'(\lambda) = -2\langle\!\langle u_L^* - (u_L+\sigma), \rho \rangle\!\rangle + 2\lambda |\!\|\rho|\!\|^2$$

and note that $G'(\lambda) = 0$ if and only if

$$\lambda = \frac{\langle\!\langle u_L^* - (u_L+\sigma), \rho \rangle\!\rangle}{|\!\|\rho|\!\|^2} \overset{(3.3)}{=} \frac{R_L(\rho) - \langle\!\langle \sigma, \rho \rangle\!\rangle}{|\!\|\rho|\!\|^2}.$$

Since G is convex, it attains its global minimum at this point. □

In case of Algorithm 3.7, we have $\sigma = \sigma_{\ell-1}$ and $\rho = \rho_\ell$ on the levels $0 < \ell \leq L$. Thus, definitions (3.6) and (3.8) yield optimality of s_ℓ.

Remark 3.9. *Comparing Algorithm 3.7 to Algorithm 3.2, we see that the multigrid solver is just one iteration of a V-cycle with no pre- and one post-smoothing step. Furthermore, an optimal step-size is applied at the error correction stage. The solver uses additive Schwarz associated to patch subdomains as the smoother, which is equivalent to diagonal Jacobi smoothing for* $p = 1$ *and block-Jacobi smoothing for* $p > 1$*. For more details on this connection, we refer to [DJN15, Chapter 1].*

Remark 3.10 (Computational effort)**.** *We also want to comment on the computational effort of the proposed algorithm, since this was the initial motivation for using an iterative solver. The matrices for the local problems* (3.7) *have dimensions* $\mathcal{O}(p^d)$*, where the notationally hidden constant depends only on* γ*-shape regularity. In the implementation, the Cholesky factorization is applied to every patch on the finest level. Therefore, the computational effort on the finest mesh* $\mathcal{T}_L$ *is of order* $\mathcal{O}(p^{3d}\#\mathcal{T}_L)$*. The effort on the initial mesh depends only on* $\#\mathcal{T}_0$ *since lowest-order polynomials are employed. Moreover, let us discuss the effort on*

the intermediate levels. Because $\dim(\mathcal{X}^1_{\ell,z}) = 1$*, the effort for a patch solve associated to a vertex* $z \in \mathcal{V}_\ell^+$ *is constant and hence the combined effort on the levels* $\ell = 1, \dots, L-1$ *is*

$$\sum_{\ell=1}^{L-1} \sum_{z \in \mathcal{V}_\ell^+} \mathcal{O}(1).$$

By definition the set $\mathcal{V}_\ell^+$ *consists of new vertices and old vertices whose patch shrunk in the refinement step. Since in the second case the node patch changed, the vertex is contained in the patch of a new vertex. We already know that the number of vertices contained in a patch is uniformly bounded by* γ*-shape regularity. This implies*

$$\sum_{\ell=1}^{L-1} \#\mathcal{V}_\ell^+ \lesssim \sum_{\ell=1}^{L-1} \#(\mathcal{V}_\ell \backslash \mathcal{V}_{\ell-1}) = \sum_{\ell=1}^{L-1} (\#\mathcal{V}_\ell - \#\mathcal{V}_{\ell-1}) = \#\mathcal{V}_{L-1} - \#\mathcal{V}_0 \leq \#\mathcal{V}_L \simeq \#\mathcal{T}_L.$$

Hence, the overall effort is given by $\mathcal{O}(\#\mathcal{T}_L)$*, where the notationally hidden constant depends only on the initial mesh* $\mathcal{T}_0$*, the polynomial degree* p*, the dimension* d*, and* γ*-shape regularity. In particular, the overall effort does not depend on the number of triangulations* L*.*

4 Analysis of the multigrid solver

The objective of this chapter is to prove robust contraction of the algebraic error for the multigrid solver of Algorithm 3.7 which can be phrased as follows: for any $v_L \in \mathcal{X}_L^p$, let $\Phi_L(v_L)$ be the improved approximation of u_L^* from (2.14) via one step of multigrid (MG). Then, there exists a contraction constant $0 < q_{\mathrm{ctr}} < 1$ such that

$$|||u_L^* - \Phi_L(v_L)||| \leq q_{\mathrm{ctr}} \, |||u_L^* - v_L|||. \tag{4.1}$$

Furthermore, we will show efficiency and reliability of the built-in a-posteriori estimator

$$\zeta_L(v_L) \leq |||u_L^* - v_L||| \leq C'_{\mathrm{rel}} \, \zeta_L(v_L). \tag{4.2}$$

The constants q_{ctr} and C'_{rel} are independent of the number of levels L and the polynomial degree p. In this sense, we say that the solver is h- and p-robust.

In order to achieve this goal, we first prove some auxiliary results. Afterwards, we show the existence of a hp-robust local multilevel decomposition for functions $v_L \in \mathcal{X}_L^p$. This decomposition relies on the one-level p-robust decomposition from [SMP+08] and provides the p-robustness. The second building block is the strengthened Cauchy-Schwarz inequality, which together with a lower-order multilevel decomposition in the spirit of [WZ17] will give us h-robustness. Ultimately, we also prove equivalence of contraction (4.1) and reliability (4.2).

4.1 Auxiliary results

In this section, we first show that the number of overlapping patches is uniformly bounded, more precisely, each simplex in the mesh belongs to at most $d+1$ node patches.

Lemma 4.1. *For all simplices $T \in \mathcal{T}_\ell$, we have*

$$\#(\mathcal{V}_\ell \cap T) = d + 1. \tag{4.3}$$

This implies

$$\Big|\Big|\Big| \sum_{z \in \mathcal{V}_\ell} v_{\ell,z} \Big|\Big|\Big|^2 \leq (d+1) \sum_{z \in \mathcal{V}_\ell} |||v_{\ell,z}|||^2 \quad \text{for all } v_{\ell,z} \in \mathcal{X}_{\ell,z}^q \text{ and all } q \in \mathbb{N}. \tag{4.4}$$

Furthermore, it also holds that

$$\Big\| \nabla \Big(\sum_{z \in \mathcal{V}_\ell} v_{\ell,z} \Big) \Big\|^2 \leq (d+1) \sum_{z \in \mathcal{V}_\ell} \|\nabla v_{\ell,z}\|^2 \quad \text{for all } v_{\ell,z} \in \mathcal{X}_{\ell,z}^q \text{ and all } q \in \mathbb{N}. \tag{4.5}$$

Proof. The first statement follows directly from Definition 2.2 and Definition 2.3, since $T = \operatorname{conv}(z_0, \dots, z_d)$, where $\{z_0, \dots, z_d\} \subseteq \mathcal{V}_\ell$ with $\#\{z_0, \dots, z_d\} = d+1$, and there are no hanging nodes in conforming triangulations. Because the squared energy norm $\|\!|\cdot|\!\|^2$ is additive with respect to the simplex domains and $v_{\ell,z} \in \mathcal{X}^q_{\ell,z}$ are conforming with $\operatorname{supp} v_{\ell,z} \subseteq \overline{\omega_\ell(z)}$, we can rewrite the left-hand side of (4.4) as

$$\Big|\!\Big|\!\Big| \sum_{z\in\mathcal{V}_\ell} v_{\ell,z} \Big|\!\Big|\!\Big|^2 = \sum_{T\in\mathcal{T}_\ell} \Big|\!\Big|\!\Big| \sum_{z\in\mathcal{V}_\ell\cap T} v_{\ell,z} \Big|\!\Big|\!\Big|_T^2.$$

Applying the triangle inequality for $\|\!|\cdot|\!\|$ and the Cauchy-Schwarz inequality for $\mathbb{R}^{d+1}$ yields

$$\begin{aligned}\Big|\!\Big|\!\Big| \sum_{z\in\mathcal{V}_\ell} v_{\ell,z} \Big|\!\Big|\!\Big|^2 &\le \sum_{T\in\mathcal{T}_\ell} \Big(\sum_{z\in\mathcal{V}_\ell\cap T} |\!|\!| v_{\ell,z} |\!|\!|_T \Big)^2 \le \sum_{T\in\mathcal{T}_\ell} \#(\mathcal{V}_\ell \cap T) \sum_{z\in\mathcal{V}_\ell\cap T} |\!|\!| v_{\ell,z} |\!|\!|_T^2 \\ &\overset{(4.3)}{=} (d+1) \sum_{T\in\mathcal{T}_\ell} \sum_{z\in\mathcal{V}_\ell\cap T} |\!|\!| v_{\ell,z} |\!|\!|_T^2 = (d+1) \sum_{z\in\mathcal{V}_\ell} |\!|\!| v_{\ell,z} |\!|\!|^2.\end{aligned}$$

The estimate (4.5) follows analogously as the differential operator is linear, which concludes the proof. □

Other simple observations are the following bounds on the step-size and estimates for the levelwise solver updates.

Lemma 4.2. *Let $\ell \in \{1, \dots, L-1\}$ and also $\ell = L$ if $p = 1$. Then, it holds*

$$|\!|\!| \lambda_\ell \rho_\ell |\!|\!|^2 \le \lambda_\ell \sum_{z\in\mathcal{V}_\ell^+} |\!|\!| \rho_{\ell,z} |\!|\!|^2, \tag{4.6}$$

where λ_ℓ, ρ_ℓ and $\rho_{\ell,z}$ are defined in Algorithm 3.7. Whenever $p > 1$, we get

$$|\!|\!| \lambda_L \rho_L |\!|\!|^2 = \lambda_L \sum_{z\in\mathcal{V}_L} |\!|\!| \rho_{L,z} |\!|\!|^2. \tag{4.7}$$

Moreover, the step-size satisfies the upper and lower bounds

$$\lambda_\ell \le d+1 \quad \text{for } \ell = 1, \dots, L-1 \text{ in general and for } \ell = 1, \dots, L \text{ if } p = 1, \tag{4.8}$$

$$\frac{1}{d+1} \le \lambda_\ell \quad \text{for } \ell = 1, \dots, L. \tag{4.9}$$

Proof. We need to consider the case distinction in the construction of λ_ℓ in Algorithm 3.7.
Step 1: First, we prove (4.6) with equality if $s_\ell \le d+1$. Under this assumption, it holds that $\lambda_\ell = s_\ell = \big(R_L(\rho_\ell) - \langle\!\langle \sigma_{\ell-1}, \rho_\ell \rangle\!\rangle\big) / |\!|\!| \rho_\ell |\!|\!|^2$ and therefore

$$\begin{aligned}|\!|\!| \lambda_\ell \rho_\ell |\!|\!|^2 = \lambda_\ell^2 |\!|\!| \rho_\ell |\!|\!|^2 = \lambda_\ell \frac{R_L(\rho_\ell) - \langle\!\langle \sigma_{\ell-1}, \rho_\ell \rangle\!\rangle}{|\!|\!| \rho_\ell |\!|\!|^2} |\!|\!| \rho_\ell |\!|\!|^2 &= \lambda_\ell \sum_{z\in\mathcal{V}_\ell^+} \big(R_L(\rho_{\ell,z}) - \langle\!\langle \sigma_{\ell-1}, \rho_{\ell,z} \rangle\!\rangle \big) \\ &\overset{(3.5)}{=} \lambda_\ell \sum_{z\in\mathcal{V}_\ell^+} |\!|\!| \rho_{\ell,z} |\!|\!|^2.\end{aligned}$$

Step 2: Let us show (4.6) for the remaining cases, i.e., when $s_\ell > d+1$ and $\lambda_\ell = 1/(d+1)$. Using estimate (4.4) from Lemma 4.1, gives

$$\|\!|\lambda_\ell \rho_\ell|\!\|^2 = \frac{\lambda_\ell}{d+1}\|\!|\rho_\ell|\!\|^2 \overset{(4.4)}{\leq} \frac{\lambda_\ell}{d+1}(d+1)\sum_{z\in\mathcal{V}_\ell^+}\|\!|\rho_{\ell,z}|\!\|^2 = \lambda_\ell \sum_{z\in\mathcal{V}_\ell^+}\|\!|\rho_{\ell,z}|\!\|^2.$$

Step 3: The equality (4.7) follows analogously to step 1, if one exchanges $\mathcal{V}_L^+$ with $\mathcal{V}_L$.
Step 4: It remains to show the bounds for the step-size. The upper bound (4.8) follows by definition of λ_ℓ. Whenever $\lambda_\ell = 1/(d+1)$, the lower bound (4.9) holds with equality. In the other case, we apply Lemma 4.1 to obtain

$$\lambda_\ell = \frac{R_L(\rho_\ell) - \langle\!\langle \sigma_{\ell-1}, \rho_\ell\rangle\!\rangle}{\|\!|\rho_\ell|\!\|^2} \overset{(3.5)}{=} \frac{\sum_{z\in\mathcal{V}_\ell^+}\|\!|\rho_{\ell,z}|\!\|^2}{\|\!|\rho_\ell|\!\|^2} \overset{(4.4)}{\geq} \frac{1}{d+1}$$

and analogously, if $p > 1$,

$$\lambda_L = \frac{R_L(\rho_L) - \langle\!\langle \sigma_{L-1}, \rho_L\rangle\!\rangle}{\|\!|\rho_L|\!\|^2} \overset{(3.7)}{=} \frac{\sum_{z\in\mathcal{V}_L}\|\!|\rho_{L,z}|\!\|^2}{\|\!|\rho_L|\!\|^2} \overset{(4.4)}{\geq} \frac{1}{d+1}.$$

This concludes the proof. □

4.2 Multilevel hp-robust stable decomposition

This section aims to prove a multilevel hp-robust stable decomposition on NVB-generated simplicial triangulations. We will combine two known results: the one-level p-robust decomposition from [SMP+08] and the local multilevel decomposition for lowest-order functions from [WZ17]. We provide a proof of the second result, which requires the definition of certain averaging operators.

Definition 4.3. Let $\mathbb{S}^1_0(\mathcal{T}_\ell) = \mathcal{X}^1_\ell \subset \mathcal{X}$ be the lowest-order FEM space associated to the mesh $\mathcal{T}_\ell$. We denote by $\varphi_{\ell,z}$ the $\mathbb{S}^1(\mathcal{T}_\ell)$ hat-function associated with the vertex $z \in \mathcal{V}_\ell$. For every element $T \in \mathcal{T}_\ell$, we define the local L^2-projection $\mathcal{P}_{\ell,T} : L^2(\Omega) \to \mathcal{X}^1_\ell|_T = \mathbb{P}^1(T)$ by

$$\langle \mathcal{P}_{\ell,T} v, w\rangle_T = \langle v, w\rangle_T \quad \text{for all } w \in \mathcal{X}^1_\ell|_T \text{ and all } v \in L^2(\Omega).$$

Furthermore, the averaging operator $\Pi_\ell : L^2(\Omega) \to \mathcal{X}^1_\ell$ is defined through its values at the nodes

$$(\Pi_\ell v)(z) := \frac{\sum_{T\in\mathcal{T}_\ell(z)}|T|(\mathcal{P}_{\ell,T}v)(z)}{\sum_{T\in\mathcal{T}_\ell(z)}|T|} \quad \text{for all } z \in \mathcal{V}_\ell.$$

Lemma 4.4 (h-robust local multilevel decomposition for piecewise affine functions)**.** *For every function $v^1_L \in \mathcal{X}^1_L$, there exists a decomposition*

$$v^1_L = \sum_{\ell=0}^{L}\sum_{z\in\mathcal{V}_\ell^+} v^1_{\ell,z} \quad \textit{with } v^1_{\ell,z} \in \mathcal{X}^1_{\ell,z}, \tag{4.10}$$

which is stable in the sense of

$$\sum_{\ell=0}^{L} \sum_{z\in\mathcal{V}_\ell^+} \|\nabla v_{\ell,z}^1\|^2 \le C_{\mathrm{ML}}^2 \|\nabla v_L^1\|^2. \tag{4.11}$$

The constant C_{ML} depends only on the space dimension d, the γ-shape regularity (2.15)*, and* $\operatorname{diam}(\Omega)/h_0$.

Proof. Let $v_L^1 \in \mathcal{X}_L^1$. We define the levelwise contributions w_ℓ^1 of v_L^1 using the operators Π_ℓ from Definition 4.3

$$w_\ell^1 := (\Pi_\ell - \Pi_{\ell-1}) v_L^1 \quad \text{for } \ell = 0, \dots, L, \tag{4.12}$$

with the exception of $\Pi_{-1} := 0$. In [WZ17, Lemma 3.1], it is shown that $w_\ell^1 \in \operatorname{span}\{\varphi_{\ell,z} : z \in \mathcal{V}_\ell^+\}$. Hence, we get $w_\ell^1 = \sum_{z\in\mathcal{V}_\ell^+} v_{\ell,z}^1$ with $v_{\ell,z}^1 := w_\ell^1(z)\varphi_{\ell,z} \in \mathcal{X}_{\ell,z}^1$. With the telescoping sum and $\Pi_{-1} = 0$, we see

$$v_L^1 = \sum_{\ell=0}^{L} (\Pi_\ell - \Pi_{\ell-1}) v_L^1 \overset{(4.12)}{=} \sum_{\ell=0}^{L} w_\ell^1 = \sum_{\ell=0}^{L} \sum_{z\in\mathcal{V}_L^+} v_{\ell,z}^1. \tag{4.13}$$

Hence, we have shown the decomposition (4.10). It remains to prove its stability (4.11). Any two norms on a finite-dimensional space are equivalent. Thus, for the reference simplex T_{ref} we obtain

$$\|v\|_{L^\infty(T_{\mathrm{ref}})} \simeq \|v\|_{T_{\mathrm{ref}}} \quad \text{for all } v \in \mathbb{P}^1(T_{\mathrm{ref}}).$$

A scaling argument provides the estimate

$$|T|^{1/2}\|v\|_{L^\infty(T)} \lesssim \|v\|_T \le |T|^{1/2}\|v\|_{L^\infty(T)} \quad \text{for all } T \in \mathcal{T}_\ell \text{ and all } v \in \mathbb{P}^1(T), \tag{4.14}$$

where the hidden constant depends only on the dimension d. The hat functions satisfy $\|\varphi_{\ell,z}\|_{L^\infty(\Omega)} = 1$, which together with (4.14) applied to $w_\ell^1|_T \in \mathbb{P}^1(T)$ yields

$$\|v_{\ell,z}^1\|_{\omega_\ell(z)} \le \sum_{T\in\mathcal{T}_\ell(z)} \|w_\ell^1(z)\varphi_{\ell,z}\|_T \le \sum_{T\in\mathcal{T}_\ell(z)} \|w_\ell^1\|_{L^\infty(T)}|T|^{1/2} \overset{(4.14)}{\lesssim} \sum_{T\in\mathcal{T}_\ell(z)} \|w_\ell^1\|_T. \tag{4.15}$$

The discrete Cauchy-Schwarz inequality and γ-shape regularity guarantee

$$\Big(\sum_{T\in\mathcal{T}_\ell(z)} \|w_\ell^1\|_T\Big)^2 \le \#\mathcal{T}_\ell(z) \sum_{T\in\mathcal{T}_\ell(z)} \|w_\ell^1\|_T^2 \lesssim \|w_\ell^1\|_{\omega_\ell(z)}^2.$$

Along with (4.15), this implies

$$\|v_{\ell,z}^1\|_{\omega_\ell(z)} \lesssim \|w_\ell^1\|_{\omega_\ell(z)} \quad \text{for all } \ell = 0, \dots, L \text{ and } z \in \mathcal{V}_\ell^+. \tag{4.16}$$

We refer to [BS08, Lemma 4.5.3] for the inverse inequality

$$\|\nabla v_{\ell,z}\|_T \lesssim h_T^{-1}\|v_{\ell,z}\|_T \quad \text{for all } T \in \mathcal{T}_\ell(z) \text{ and all } v \in \mathcal{X}_{\ell,z}^1, \tag{4.17}$$

where the hidden constant depends only on γ-shape regularity. However, we can apply this inequality to patches, since the squared L^2-norm is additive and the sizes of elements in a patch are comparable via γ-shape regularity (2.16). Additionally, exploiting the stability of the operator Π_ℓ shown in [WZ17, Lemma 3.7], we are led to

$$\begin{aligned}\sum_{\ell=0}^{L}\sum_{z\in\mathcal{V}_\ell^+}\|\nabla v_{\ell,z}^1\|^2 &\overset{(4.17)}{\lesssim} \sum_{\ell=0}^{L}\sum_{z\in\mathcal{V}_\ell^+} h_{\ell,z}^{-2}\|v_{\ell,z}^1\|_{\omega_\ell(z)}^2 \overset{(4.16)}{\lesssim} \sum_{\ell=0}^{L}\sum_{z\in\mathcal{V}_\ell^+} h_{\ell,z}^{-2}\|w_\ell^1\|_{\omega_\ell(z)}^2 \\ &\overset{(4.12)}{=} \sum_{\ell=0}^{L}\sum_{z\in\mathcal{V}_\ell^+} h_{\ell,z}^{-2}\|(\Pi_\ell-\Pi_{\ell-1})v_L^1\|_{\omega_\ell(z)}^2 \overset{[WZ17]}{\lesssim} \sum_{z\in\mathcal{V}_0} h_{0,z}^{-2}\|\Pi_0 v_L^1\|_{\omega_0(z)}^2 + \|\nabla v_L^1\|^2.\end{aligned} \tag{4.18}$$

For the initial mesh, a different argument is needed. Using the local L^2-stability of Π_0 and that all elements in the initial mesh have comparable size, leads to

$$\sum_{z\in\mathcal{V}_0} h_{0,z}^{-2}\|\Pi_0 v_L^1\|_{\omega_0(z)}^2 \lesssim h_0^{-2}\sum_{z\in\mathcal{V}_0}\|v_L^1\|_{\omega_0^2(z)}^2.$$

With finite patch overlap and the Poincaré inequality we obtain

$$h_0^{-2}\sum_{z\in\mathcal{V}_0}\|v_L^1\|_{\omega_0^2(z)}^2 \lesssim h_0^{-2}\|v_L^1\|^2 \lesssim \|\nabla v_L^1\|^2.$$

This concludes the proof. □

Next, we formulate the p-robust decomposition from [SMP+08] but refer to the literature for the proof.

Lemma 4.5 (p-robust one-level decomposition)**.** *Let $v_L \in \mathcal{X}_L^p$. Then, there exist functions $v_L^1 \in \mathcal{X}_L^1$ and $\{v_{L,z}^p\}_{z\in\mathcal{V}_L} \in \mathcal{X}_{L,z}^p$ such that*

$$v_L = v_L^1 + \sum_{z\in\mathcal{V}_L} v_{L,z}^p. \tag{4.19}$$

The decomposition is stable in the sense of

$$\|\nabla v_L^1\|^2 + \sum_{z\in\mathcal{V}_L}\|\nabla v_{L,z}^p\|^2 \le C_{\mathrm{OL}}^2\|\nabla v_L\|^2, \tag{4.20}$$

where the constant $C_{\mathrm{OL}} \ge 1$ depends only on the space dimension d and the γ-shape regularity (2.15).

Ultimately, we can prove the desired *hp*-robust stable decomposition.

Proposition 4.6 (*hp*-robust local multilevel decomposition)**.** *Every $v_L \in \mathcal{X}_L^p$ can be decomposed into $v_0 \in \mathcal{X}_0^1$, $\{v_{\ell,z}\}_{z\in\mathcal{V}_\ell^+} \in \mathcal{X}_{\ell,z}^1$, and $\{v_{L,z}\}_{z\in\mathcal{V}_L} \in \mathcal{X}_{L,z}^p$ such that*

$$v_L = v_0 + \sum_{\ell=1}^{L-1}\sum_{z\in\mathcal{V}_\ell^+} v_{\ell,z} + \sum_{z\in\mathcal{V}_L} v_{L,z}. \tag{4.21}$$

The decomposition is stable in the sense of

$$\|\!|v_0|\!\|^2 + \sum_{\ell=1}^{L-1} \sum_{z\in\mathcal{V}_\ell^+} \|\!|v_{\ell,z}|\!\|^2 + \sum_{z\in\mathcal{V}_L} \|\!|v_{L,z}|\!\|^2 \leq C_{\mathrm{SD}}^2 \|\!|v_L|\!\|^2, \tag{4.22}$$

where the constant $C_{\mathrm{SD}} \geq 1$ *depends only on the space dimension* d, γ*-shape regularity* (2.15), $\operatorname{diam}(\Omega)/h_0$, *and* $\Lambda_{\max}/\Lambda_{\min}$.

Proof. Let $v_L \in \mathcal{X}_L^p$. We can apply Lemma 4.5 to obtain a decomposition on the finest level L. Furthermore, the lowest-order contribution v_L^1 from (4.19) can be decomposed as shown in Lemma 4.4. Thus, we get

$$\begin{aligned} v_L \overset{(4.19)}{=} v_L^1 + \sum_{z\in\mathcal{V}_L} v_{L,z}^p &\overset{(4.10)}{=} \sum_{\ell=0}^{L} \sum_{z\in\mathcal{V}_L^+} v_{\ell,z}^1 + \sum_{z\in\mathcal{V}_L} v_{L,z}^p \\ &= \sum_{z\in\mathcal{V}_0} v_{0,z}^1 + \sum_{\ell=1}^{L-1} \sum_{z\in\mathcal{V}_\ell^+} v_{\ell,z}^1 + \sum_{z\in\mathcal{V}_L^+} v_{L,z}^1 + \sum_{z\in\mathcal{V}_L} v_{L,z}^p. \end{aligned}$$

Defining the contributions $v_0 := \sum_{z\in\mathcal{V}_0} v_{0,z}^1$, $v_{\ell,z} := v_{\ell,z}^1 \in \mathcal{X}_{\ell,z}^1$ for $z \in \mathcal{V}_\ell^+$ and $\ell = 1,\dots,L-1$, and $v_{L,z} := v_{L,z}^1 + v_{L,z}^p \in \mathcal{X}_{L,z}^p$ for $z \in \mathcal{V}_L^+$ and $v_{L,z} := v_{L,z}^p \in \mathcal{X}_{L,z}^p$ for $z \in \mathcal{V}_L \backslash \mathcal{V}_L^+$ yields the decomposition (4.21). Next, we show stability of the decomposition. For $\ell = 0$, applying the estimate (4.5) leads to

$$\|\nabla v_0\|^2 \leq (d+1) \sum_{z\in\mathcal{V}_0} \|\nabla v_{0,z}^1\|^2.$$

The Young inequality establishes

$$\begin{aligned} \sum_{z\in\mathcal{V}_L} \|\nabla v_{L,z}\|^2 &\leq \sum_{z\in\mathcal{V}_L\backslash\mathcal{V}_L^+} \|\nabla v_{\ell,z}^p\|^2 + 2 \sum_{z\in\mathcal{V}_L^+} \left(\|\nabla v_{L,z}^1\|^2 + \|\nabla v_{L,z}^p\|^2\right) \\ &\leq 2 \left(\sum_{z\in\mathcal{V}_L^+} \|\nabla v_{L,z}^1\|^2 + \sum_{z\in\mathcal{V}_L} \|\nabla v_{L,z}^p\|^2 \right) \end{aligned}$$

on the finest level. We combine the last two estimates with $d \geq 1$ to obtain

$$\begin{aligned} &\|\nabla v_0\|^2 + \sum_{\ell=1}^{L-1} \sum_{z\in\mathcal{V}_\ell^+} \|\nabla v_{\ell,z}\|^2 + \sum_{z\in\mathcal{V}_L} \|\nabla v_{L,z}\|^2 \\ &\quad\leq (d+1)\Big(\sum_{z\in\mathcal{V}_0} \|\nabla v_{0,z}^1\|^2 + \sum_{\ell=1}^{L-1} \sum_{z\in\mathcal{V}_\ell^+} \|\nabla v_{\ell,z}^1\|^2 + \sum_{z\in\mathcal{V}_L^+} \|\nabla v_{L,z}^1\|^2 + \sum_{z\in\mathcal{V}_L} \|\nabla v_{L,z}^p\|^2 \Big) \\ &\quad= (d+1)\Big(\sum_{\ell=0}^{L} \sum_{z\in\mathcal{V}_\ell^+} \|\nabla v_{\ell,z}^1\|^2 + \sum_{z\in\mathcal{V}_L} \|\nabla v_{L,z}^p\|^2 \Big). \end{aligned}$$

Moreover, combining the results (4.11) and (4.20) yield stability in the $H^1(\Omega)$-seminorm

$$\|\nabla v_0\|^2 + \sum_{\ell=1}^{L-1} \sum_{z\in\mathcal{V}_\ell^+} \|\nabla v_{\ell,z}\|^2 + \sum_{z\in\mathcal{V}_L} \|\nabla v_{L,z}\|^2 \overset{(4.11)}{\leq} (d+1)\Big(C_{\mathrm{ML}}^2\|\nabla v_L^1\|^2 + \sum_{z\in\mathcal{V}_L} \|\nabla v_{L,z}^p\|^2\Big)$$
$$\overset{(4.20)}{\leq} \max\{1, C_{\mathrm{ML}}^2\} C_{\mathrm{OL}}^2 (d+1)\|\nabla v_L\|^2.$$

The norm equivalence (2.6) from Proposition 2.7 yields the estimate (4.22) with $C_{\mathrm{SD}}^2 := \max\{1, C_{\mathrm{ML}}^2\} C_{\mathrm{OL}}^2 (d+1)\Lambda_{\max}/\Lambda_{\min}$. □

4.3 Strengthened Cauchy–Schwarz inequality

The goal of this section is to prove a strengthened Cauchy–Schwarz inequality on NVB-generated adaptive meshes. To this end, we first show a strengthened Cauchy–Schwarz inequality on nested uniform meshes. Let us introduce some useful notation.

Definition 4.7. Let $\mathcal{T}_0$ be an initial triangulation of Ω, $\mathcal{T} \in \mathbb{T}$ a refinement of $\mathcal{T}_0$, and $T \in \mathcal{T}$. Furthermore, we consider the unique ancestor element $T_0 \in \mathcal{T}_0$ of T, i.e., $T \subseteq T_0$. We define the *element level* by

$$\operatorname{level}(T) := \log_2(|T_0|/|T|).$$

Since bisection halves the area of an element, the element level just denotes the number of times T_0 has been bisected to generate T, i.e., $|T| = 2^{-\operatorname{level}(T)}|T_0|$.

Lemma 4.8. *Let $\mathcal{T}_0$ be an initial triangulation and $\mathcal{T} \in \mathbb{T}$ a refinement of $\mathcal{T}_0$. For $T, T' \in \mathcal{T}$ with $T \cap T' \neq \emptyset$ it holds that*

$$|\operatorname{level}(T) - \operatorname{level}(T')| \leq C_{\mathrm{level}},$$

where the constant C_{level} depends only on the initial mesh $\mathcal{T}_0$ and γ-shape regularity (2.15).

Proof. Due to (2.16), the size of elements with non-empty intersection are comparable, in particular, $|T| \simeq |T'|$. Thus, we have $|T_0|/|T| \simeq |T_0'|/|T'|$ and the hidden constants $C \geq 1$ depend only on γ-shape regularity, the dimension d, and the initial triangulation $\mathcal{T}_0$. The monotonicity of the logarithm implies

$$\operatorname{level}(T) = \log_2\Big(\frac{|T_0|}{|T|}\Big) \leq \log_2\Big(C\frac{|T_0'|}{|T'|}\Big) = \log_2(C) + \operatorname{level}(T')$$

and the same holds with the roles of T and T' exchanged. Hence, we have the desired result with $C_{\mathrm{level}} = \log_2(C)$. □

Let $M = \max_{T\in\mathcal{T}_L} \operatorname{level}(T)$. We denote by $\{\widehat{\mathcal{T}}_j\}_{j=0}^M$ a sequence of uniformly refined triangulations that satisfy $\widehat{\mathcal{T}}_{j+1} := \texttt{REFINE}(\widehat{\mathcal{T}}_j, \widehat{\mathcal{T}}_j)$ and $\widehat{\mathcal{T}}_0 := \mathcal{T}_0$. From now on we assume $\mathcal{T}_0$ to be admissible since this ensures that every element $T \in \widehat{\mathcal{T}}_j$ satisfies $\operatorname{level}(T) = j$ and hence is only bisected once during uniform refinement; see [Ste08, Theorem 4.3]. For

$d = 2$ and an initial triangulation, a local numbering exists such that $\mathcal{T}_0$ is admissible. As mentioned in Section 2.4.1 this is not true for $d > 2$. However, instructions for constructing an admissible initial mesh $\mathcal{T}_0$ from any given triangulation are provided in [Ste08]. Moreover, denote by $\widehat{h}_j := \max_{T\in\widehat{\mathcal{T}}_j} |T|^{1/d}$ the mesh-size of the uniform triangulation $\widehat{\mathcal{T}}_j$. With the quasi-uniformity constant

$$C_{\mathrm{qu}} := \min\{h_T/h_{T'} : T, T' \in \widehat{\mathcal{T}}_0 = \mathcal{T}_0\} \in (0, 1], \tag{4.23}$$

it follows that $\widehat{h}_j \simeq h_T$ for all $T \in \widehat{\mathcal{T}}_j$ and all $j \in \mathbb{N}_0$ and the hidden constants depend only on C_{qu}. Every object associated with uniform meshes will be indicated with a hat, e.g., $\widehat{\mathcal{X}}_j^1$ is the lowest-order FEM space induced by $\widehat{\mathcal{T}}_j$. In order to facilitate working with adaptively refined meshes via properties of uniformly refined ones, we introduce the notion of local generations.

Definition 4.9. Let $\ell \in \{0, \dots, L\}$ and $z \in \mathcal{V}_\ell$. The *generation* $g_{\ell,z}$ of a patch $\mathcal{T}_\ell(z)$ is defined by

$$g_{\ell,z} := \max_{T\in\mathcal{T}_\ell(z)} \mathrm{level}(T) \in \mathbb{N}_0 \tag{4.24}$$

and gives the maximal element level in the patch $\mathcal{T}_\ell(z)$.

We can show that the patch subdomain of any vertex $z \in \mathcal{V}_\ell$ lies in an n-patch subdomain of the uniform mesh $\widehat{\mathcal{T}}_j$ with $g_{\ell,z} = j$.

Lemma 4.10. *There exists an index $n \in \mathbb{N}_0$ that depends only on the initial triangulation $\mathcal{T}_0$ and γ-shape regularity (2.15), such that $\omega_\ell(z) \subseteq \widehat{\omega}^n_{g_{\ell,z}}(z)$ for all $\ell \in \{0, \dots, L\}$ and all $z \in \mathcal{V}_\ell$.*

Proof. Let $\ell \in \{0, \dots, L\}$ and $z \in \mathcal{V}_\ell$. We define $r_{\ell,z} := \min_{T\in\mathcal{T}_\ell(z)} \mathrm{level}(T)$.
Step 1: We first show the existence of a constant $C_1 \in \mathbb{N}$ such that $g_{\ell,z} \le r_{\ell,z} + C_1$. By definition, there exists triangles $T, T' \in \mathcal{T}_\ell(z)$ that fulfill $g_{\ell,z} = \mathrm{level}(T)$ and $r_{\ell,z} = \mathrm{level}(T')$. From Lemma 4.8 we already know that $\mathrm{level}(T) \le \mathrm{level}(T') + C_{\mathrm{level}}$. This concludes the first step with $C_1 := \lceil C_{\mathrm{level}} \rceil$.
Step 2: Let $T \in \mathcal{T}_\ell(z)$. By definition, there exists an element $T' \in \widehat{\mathcal{T}}_{r_{\ell,z}}$ with $T \subseteq T'$ and $T' \subseteq \overline{\widehat{\omega}_{r_{\ell,z}}(z)}$. As the uniform meshes are obtained by bisecting every element once, we can decompose T' into elements $T'_k \in \widehat{\mathcal{T}}_{r_{\ell,z}+C_1}$ with $k = 1, \dots, 2^{C_1}$, i.e., $T' = \bigcup_{k=1}^{2^{C_1}} T'_k$. Thus, there exists an index $n \in \mathbb{N}$ with $n \le 2^{C_1}$ and $T' \subseteq \overline{\widehat{\omega}^n_{r_{\ell,z}+C_1}(z)}$. From the first step, we know $g_{\ell,z} \le r_{\ell,z} + C_1$ and consequently $\widehat{\omega}^n_{r_{\ell,z}+C_1}(z) \subseteq \widehat{\omega}^n_{g_{\ell,z}}(z)$. Hence, $T \subseteq T' \subseteq \overline{\widehat{\omega}^n_{g_{\ell,z}}(z)}$ which implies $\omega_\ell(z) \subseteq \widehat{\omega}^n_{g_{\ell,z}}(z)$ and therefore concludes the proof. □

We will need the last lemma to prove the strengthened Cauchy–Schwarz inequality on adaptive meshes. First, we prove a strengthened Cauchy–Schwarz inequality on uniform meshes in the following lemma.

Lemma 4.11 (Strengthened Cauchy–Schwarz inequality on nested uniform meshes)**.** *Let $0 \le i \le j$, $\widehat{u}_i \in \widehat{\mathcal{X}}_i^1$, and $\widehat{v}_j \in \widehat{\mathcal{X}}_j^1$. Consider a subset $\widehat{\mathcal{M}}_i \subseteq \widehat{\mathcal{T}}_i$ and denote $\widehat{\omega}_i := \mathrm{interior}\big(\bigcup_{T\in\widehat{\mathcal{M}}_i} T\big)$. Then, it holds that*

$$\langle\!\langle \widehat{u}_i, \widehat{v}_j \rangle\!\rangle_{\widehat{\omega}_i} \le \widehat{C}_{\mathrm{SCS}}\, \delta^{j-i} \widehat{h}_j^{-1} \|\nabla \widehat{u}_i\|_{\widehat{\omega}_i} \|\widehat{v}_j\|_{\widehat{\omega}_i}, \tag{4.25}$$

where $\delta = 2^{-1/d}$. *The constant* $\widehat{C}_{\mathrm{SCS}} > 0$ *depends only on the domain* Ω, *the space dimension* d, *the initial triangulation* $\mathcal{T}_0$, $\Lambda_{\max}$, $\max_{T\in\widehat{\mathcal{T}}_0} \|\operatorname{div}(\mathbf{K})\|_{L^\infty(T)}$, *the* γ*-shape regularity from* (2.15), *and the quasi-uniformity constant* C_{qu} *from* (4.23).

Proof. Let us start from the left-hand side of (4.25) and split the integral over $\widehat{\omega}_i$ into its elementwise components. Moreover, we apply integration by parts on every element $T \in \widehat{\mathcal{M}}_i$ to obtain

$$\begin{aligned}\langle\!\langle \widehat{u}_i, \widehat{v}_j\rangle\!\rangle_{\widehat{\omega}_i} &= \sum_{T\in\widehat{\mathcal{M}}_i} \int_T \mathbf{K}\nabla\widehat{u}_i \cdot \nabla\widehat{u}_j \, dx \\ &= \sum_{T\in\widehat{\mathcal{M}}_i} \Big(-\int_T \operatorname{div}(\mathbf{K}\nabla\widehat{u}_i)\widehat{v}_j \, dx + \int_{\partial T} \mathbf{K}\nabla\widehat{u}_i \cdot \mathbf{n}\, \widehat{v}_j \, dx \Big).\end{aligned}$$

Furthermore, the product rule implies $\operatorname{div}(\mathbf{A}\mathbf{u}) = \operatorname{div}(\mathbf{A})\cdot\mathbf{u} + \operatorname{tr}(\mathbf{A}\frac{\partial\mathbf{u}}{\partial x})$, where $\mathbf{A}$ is a matrix-valued function, $\mathbf{u}$ is a vector-valued function, and $\frac{\partial\mathbf{u}}{\partial x}$ denotes the Jacobian of $\mathbf{u}$. As $\widehat{u}_i|_T$ is an affine function on every element $T \in \widehat{\mathcal{M}}_i$, the second derivatives vanish and we get

$$\langle\!\langle \widehat{u}_i, \widehat{v}_j\rangle\!\rangle_{\widehat{\omega}_i} = \sum_{T\in\widehat{\mathcal{M}}_i} \Big(-\int_T \operatorname{div}(\mathbf{K})\cdot\nabla\widehat{u}_i \, \widehat{v}_j \, dx + \int_{\partial T} \mathbf{K}\nabla\widehat{u}_i \cdot \mathbf{n}\, \widehat{v}_j \, dx \Big).$$

Moreover, the Cauchy–Schwarz inequality and the assumption $\mathbf{K}|_T \in [W^{1,\infty}(T)]^{d\times d}_{\mathrm{sym}}$ for all $T \in \widehat{\mathcal{T}}_0$ yield

$$\begin{aligned}\langle\!\langle \widehat{u}_i, \widehat{v}_j\rangle\!\rangle_{\widehat{\omega}_i} &\le \sum_{T\in\widehat{\mathcal{M}}_i} \Big(\|\operatorname{div}(\mathbf{K})\cdot\nabla\widehat{u}_i\|_{L^2(T)}\|\widehat{v}_j\|_{L^2(T)} + \Lambda_{\max}\|\nabla\widehat{u}_i\|_{L^2(\partial T)}\|\widehat{v}_j\|_{L^2(\partial T)} \Big) \\ &\lesssim \sum_{T\in\widehat{\mathcal{M}}_i} \Big(\|\nabla\widehat{u}_i\|_{L^2(T)}\|\widehat{v}_j\|_{L^2(T)} + \|\nabla\widehat{u}_i\|_{L^2(\partial T)}\|\widehat{v}_j\|_{L^2(\partial T)} \Big),\end{aligned}$$

where the hidden constant is just the maximum of $\max_{T\in\widehat{\mathcal{T}}_0} \|\operatorname{div}(\mathbf{K})\|_{L^\infty(T)}$ and $\Lambda_{\max}$. For further calculations, we need a discrete trace inequality; see, e.g., [EG21a, Lemma 12.8]. Let $F = \operatorname{conv}(z_1, \dots, z_d)$ be a face of a simplex $T = \operatorname{conv}(z_0, \dots, z_d)$. Then, it holds that

$$\|v\|_{L^2(F)} \lesssim h_T^{-1/2}\|v\|_{L^2(T)} \quad \text{for all } v \in \mathbb{P}^1(T), \tag{4.26}$$

where the hidden constant depends only on γ-shape regularity. Since every simplex has $d+1$ faces we can extend this inequality to ∂T. The function $\widehat{v}_j$ is only piecewise linear on the finer mesh $\widehat{\mathcal{T}}_j$, however, we can decompose every element $T \in \widehat{\mathcal{T}}_i$ into elements of $\widehat{\mathcal{T}}_j$ as

$$\|\widehat{v}_j\|_{\partial T} = \sum_{\substack{T'\in\widehat{\mathcal{T}}_j \\ T'\subseteq T}} \|\widehat{v}_j\|_{\partial T\cap T'} \overset{(4.26)}{\lesssim} \sum_{\substack{T'\in\widehat{\mathcal{T}}_j \\ T'\subseteq T}} \widehat{h}_j^{-1/2}\|\widehat{v}_j\|_{T\cap T'} = \widehat{h}_j^{-1/2}\|\widehat{v}_j\|_T. \tag{4.27}$$

Ultimately, the uniform mesh size leads to

$$\begin{aligned}\langle\!\langle \widehat{u}_i, \widehat{v}_j\rangle\!\rangle_{\widehat{\omega}_i} &\overset{(4.27)}{\lesssim} \sum_{T\in\widehat{\mathcal{M}}_i} \Big(\|\nabla \widehat{u}_i\|_{L^2(T)} \|\widehat{v}_j\|_{L^2(T)} + \big(\widehat{h}_i^{-1/2} \|\nabla \widehat{u}_i\|_{L^2(T)}\big) \big(\widehat{h}_j^{-1/2} \|\widehat{v}_j\|_{L^2(T)}\big)\Big) \\ &= \sum_{T\in\widehat{\mathcal{M}}_i} (1 + \widehat{h}_i^{-1/2} \widehat{h}_j^{-1/2}) \|\nabla \widehat{u}_i\|_{L^2(T)} \|\widehat{v}_j\|_{L^2(T)}.\end{aligned}$$

Moreover, the identity $\widehat{h}_j, \widehat{h}_i \leq \operatorname{diam}(\Omega)$ implies $\widehat{h}_i^{-1/2} \widehat{h}_j^{-1/2} \gtrsim 1$. Since the volume of each element is halved by uniform refinement, it holds $\widehat{h}_j / \widehat{h}_i = 2^{-(j-i)/d}$ and hence $\delta^{j-i} = (2^{-1/(2d)})^{j-i} = (\widehat{h}_j / \widehat{h}_i)^{1/2}$. We thus obtain

$$\begin{aligned}\langle\!\langle \widehat{u}_i, \widehat{u}_j\rangle\!\rangle_{\widehat{\omega}_i} &\lesssim \sum_{T\in\widehat{\mathcal{M}}_i} \widehat{h}_i^{-1/2} \widehat{h}_j^{-1/2} \|\nabla \widehat{u}_i\|_{L^2(T)} \|\widehat{v}_j\|_{L^2(T)} \\ &= \sum_{T\in\widehat{\mathcal{M}}_i} \Big(\frac{\widehat{h}_j}{\widehat{h}_i}\Big)^{1/2} \widehat{h}_j^{-1} \|\nabla \widehat{u}_i\|_{L^2(T)} \|\widehat{v}_j\|_{L^2(T)} \\ &= \sum_{T\in\widehat{\mathcal{M}}_i} \delta^{j-i} \widehat{h}_j^{-1} \|\nabla \widehat{u}_i\|_{L^2(T)} \|\widehat{v}_j\|_{L^2(T)}.\end{aligned}$$

Lastly, we apply the discrete Cauchy–Schwarz inequality to see

$$\langle\!\langle \widehat{u}_i, \widehat{u}_j\rangle\!\rangle_{\widehat{\omega}_i} \lesssim \sum_{T\in\widehat{\mathcal{M}}_i} \delta^{j-i} \widehat{h}_j^{-1} \|\nabla \widehat{u}_i\|_{L^2(T)} \|\widehat{v}_j\|_{L^2(T)} \lesssim \delta^{j-i} \widehat{h}_j^{-1} \|\nabla \widehat{u}_i\|_{\widehat{\omega}_i} \|\widehat{v}_j\|_{\widehat{\omega}_i}.$$

This concludes the proof. □

We use the strengthened Cauchy–Schwarz inequality on uniform meshes to generalize the result for adaptive meshes.

Proposition 4.12 (Strengthened Cauchy–Schwarz inequality on nested adaptive meshes)**.** *For all $\ell \in \{1, \dots, L-1\}$ and $k \in \{1, \dots, \ell - 1\}$, consider levelwise functions $v_\ell = \sum_{z\in\mathcal{V}_\ell^+} v_{\ell,z}^1 \in \mathcal{X}_\ell^1$ and $u_k = \sum_{w\in\mathcal{V}_k^+} u_{k,w}^1 \in \mathcal{X}_k^1$ with $v_{\ell,z}^1 \in \mathcal{X}_{\ell,z}^1$ and $u_{k,w}^1 \in \mathcal{X}_{k,w}^1$. Then, it holds that*

$$\sum_{\ell=1}^{L-1} \sum_{k=1}^{\ell-1} \langle\!\langle u_k, v_\ell\rangle\!\rangle \leq C_{\mathrm{SCS}} \Big(\sum_{k=1}^{L-2} \sum_{w\in\mathcal{V}_k^+} |\!|\!| u_{k,w}^1 |\!|\!|^2 \Big)^{1/2} \Big(\sum_{\ell=1}^{L-1} \sum_{z\in\mathcal{V}_\ell^+} |\!|\!| v_{\ell,z}^1 |\!|\!|^2 \Big)^{1/2}, \tag{4.28}$$

where the constant $C_{\mathrm{SCS}} > 0$ depends only on Ω, the initial triangulation $\mathcal{T}_0$, $\Lambda_{\max}/\Lambda_{\min}$, $\max_{T\in\mathcal{T}_0} \|\operatorname{div}(\mathbf{K})\|_{L^\infty(T)}/\Lambda_{\min}$, γ-shape regularity (2.15), and the quasi-uniformity constant C_{qu} from (4.23).

Proof. Let $M = \max_{z\in\mathcal{V}_L} g_{L,z}$ be the maximal generation. We split the proof into seven steps.

Step 1: First, we show a general estimate not directly connected to the statement at

hand. However, it will turn out to be very useful. For all $0 < \delta < 1$ and $x_i, y_j \geq 0$ with $0 \leq i \leq j \leq M$, there holds

$$\sum_{i=0}^{M}\sum_{j=i}^{M} \delta^{j-i} x_i y_j \leq \frac{1}{1-\delta}\Big(\sum_{i=0}^{M} x_i^2\Big)^{1/2}\Big(\sum_{j=0}^{M} y_j^2\Big)^{1/2}. \tag{4.29}$$

We set $m := j - i$ and change the summation order of i and m to obtain

$$\sum_{i=0}^{M}\sum_{j=i}^{M} \delta^{j-i} x_i y_j = \sum_{i=0}^{M}\sum_{m=0}^{M-i} \delta^{m} x_i y_{m+i} = \sum_{m=0}^{M} \delta^m \sum_{i=0}^{M-m} x_i y_{m+i}.$$

The Cauchy–Schwarz inequality and the geometric series yield

$$\begin{aligned}\sum_{m=0}^{M} \delta^m \sum_{i=0}^{M-m} x_i y_{m+i} &\leq \sum_{m=0}^{M} \delta^m \Big[\Big(\sum_{i=0}^{M-m} x_i^2\Big)^{1/2}\Big(\sum_{i=0}^{M-m} y_{m+i}^2\Big)^{1/2}\Big] \\ &\leq \Big(\sum_{m=0}^{M}\delta^m\Big)\Big(\sum_{i=0}^{M} x_i^2\Big)^{1/2}\Big(\sum_{j=0}^{M} y_j^2\Big)^{1/2} \leq \frac{1}{1-\delta}\Big(\sum_{i=0}^{M} x_i^2\Big)^{1/2}\Big(\sum_{j=0}^{M} y_j^2\Big)^{1/2}.\end{aligned}$$

Hence, we proved the claim (4.29).

Step 2: For any $z \in \mathcal{V}_L$ and $0 \leq j \leq M$, we recall the patch generation $g_{\ell,z}$ from (4.24) and define

$$\mathscr{L}^{(1)}_{\underline{\ell},\overline{\ell}}(z,j) := \{\ell \in \{\underline{\ell},\dots,\overline{\ell}\} : z \in \mathcal{V}_\ell^+ \text{ and } g_{\ell,z} = j\} \quad \text{for all } 0 \leq \underline{\ell} \leq \overline{\ell} \leq L. \tag{4.30}$$

We recall that $\mathcal{V}_\ell^+$ contains the new vertices and their immediate neighbors. Hence, the set $\mathscr{L}^{(1)}_{\underline{\ell},\overline{\ell}}(z,j)$ keeps track of the levels, where the patch associated to the vertex z has been modified in the refinement and remains of generation j. For any $z \in \mathcal{V}_L$ and $0 \leq j \leq M$, we define a second set

$$\mathscr{L}^{(2)}_{\underline{\ell},\overline{\ell}}(z,j) := \{(\ell,w) : \ell \in \{\underline{\ell},\dots,\overline{\ell}\}, w \in \mathcal{V}_\ell^+, g_{\ell,w} = j \text{ and } z \in \overline{\omega_\ell(w)}\}. \tag{4.31}$$

In the set $\mathscr{L}^{(2)}_{\underline{\ell},\overline{\ell}}(z,j)$, we collect all levels and vertices whose patch is of generation j and contains the vertex z. Again the condition $w \in \mathcal{V}_\ell^+$ imposes to consider only new vertices or their immediate neighbors. Critically, there exist constants $C^{(1)}_{\mathrm{lev}}, C^{(2)}_{\mathrm{lev}} > 0$ depending only on γ-shape regularity such that the cardinalities of both types of sets are uniformly bounded, i.e.,

$$\max_{\substack{z\in\mathcal{V}_L\\ 0\leq j\leq M}} \#(\mathscr{L}^{(1)}_{0,L}(z,j)) \leq C^{(1)}_{\mathrm{lev}} < \infty \tag{4.32}$$

and

$$\max_{\substack{z\in\mathcal{V}_L\\ 0\leq j\leq M}} \#(\mathscr{L}^{(2)}_{0,L}(z,j)) \leq C^{(2)}_{\mathrm{lev}} < \infty. \tag{4.33}$$

The preceding statements are shown in [WC06, Lemma 3.1] for $d = 2$. However, the arguments can be transferred to three dimensions.

Step 3: In order to use the estimates from the last step, we reorder the contributions that fulfill a given patch constraint. To this end, we observe that for $0 \leq \underline{\ell} \leq \overline{\ell} \leq L$ and a fixed generation $j \in \{0, \dots, M\}$, it holds that

$$\begin{aligned}\big\{(\ell, z) \in \mathbb{N}_0 \times \mathcal{V}_L : \ell \in \{\underline{\ell}, \dots, \overline{\ell}\}, z \in \mathcal{V}_\ell^+ \text{ with } g_{\ell,z} = j\big\} \\ = \big\{(\ell, z) \in \mathbb{N}_0 \times \mathcal{V}_L : z \in \widehat{\mathcal{V}}_j, \ell \in \mathscr{L}^{(1)}_{\underline{\ell},\overline{\ell}}(z, j)\big\}\end{aligned} \tag{4.34}$$

The two sets represent different perspectives. Whenever we fix a generation j, we can either: sum over all levels and find associated new vertices or direct neighbors satisfying the generation constraint; or sum over all the uniform-mesh vertices $\widehat{\mathcal{V}}_j$ and find the levels where the generation constraint is satisfied.

Step 4: Consider $k \in \{0, \dots, L\}$, $w \in \mathcal{V}_k^+$, $i \in \{0, \dots, M\}$ such that $g_{k,w} = i$. This yields that there exists at least one element $T \in \mathcal{T}_k(w)$ that satisfies $T \in \widehat{\mathcal{T}}_i$. We recall $\widehat{h}_i \simeq h_T$ and that the sizes of any two elements contained in a patch are comparable via γ-shape regularity (2.15), i.e., $\widehat{h}_i \simeq h_T \simeq h_{k,w}$. Therefore, there exists a constant C_{eq} such that

$$\widehat{h}_i^{-1} \leq C_{\mathrm{eq}} h_{k,w}^{-1}. \tag{4.35}$$

Step 5: We can now prove the desired inequality (4.28). The main idea is to introduce new sums over the generations with generation constraints. For $\ell \in \{1, \dots, L-1\}$ and $k \in \{1, \dots, \ell - 1\}$, this leads to

$$\langle\!\langle u_k, v_\ell \rangle\!\rangle = \sum_{z \in \mathcal{V}_\ell^+} \sum_{w \in \mathcal{V}_k^+} \langle\!\langle u_{k,w}^1, v_{\ell,z}^1 \rangle\!\rangle = \sum_{i=0}^{M} \sum_{j=0}^{M} \sum_{\substack{z \in \mathcal{V}_\ell^+ \\ g_{\ell,z}=j}} \sum_{\substack{w \in \mathcal{V}_k^+ \\ g_{k,w}=i}} \langle\!\langle u_{k,w}^1, v_{\ell,z}^1 \rangle\!\rangle.$$

We aim to use the strengthened Cauchy–Schwarz inequality on uniform meshes (4.25) from Lemma 4.11. However, it can only be applied to piecewise affine functions on domains that can be decomposed into triangles of the coarser triangulation. Therefore, we split the inner sum over the generation at $j = i$ and obtain

$$\langle\!\langle u_k, v_\ell \rangle\!\rangle = \sum_{i=0}^{M} \sum_{j=0}^{i} \sum_{\substack{z \in \mathcal{V}_\ell^+ \\ g_{\ell,z}=j}} \sum_{\substack{w \in \mathcal{V}_k^+ \\ g_{k,w}=i}} \langle\!\langle u_{k,w}^1, v_{\ell,z}^1 \rangle\!\rangle + \sum_{i=0}^{M} \sum_{j=i+1}^{M} \sum_{\substack{z \in \mathcal{V}_\ell^+ \\ g_{\ell,z}=j}} \sum_{\substack{w \in \mathcal{V}_k^+ \\ g_{k,w}=i}} \langle\!\langle u_{k,w}^1, v_{\ell,z}^1 \rangle\!\rangle. \tag{4.36}$$

In the first term, we change the summation order of i and j. Moreover, we include the sums over ℓ and k like in (4.28), split the individual summands according to (4.36), and change

the order of summation of ℓ and k in the second term. This procedure warrants

$$\sum_{\ell=1}^{L-1}\sum_{k=1}^{\ell-1}\langle\!\langle u_k, v_\ell\rangle\!\rangle = \sum_{j=0}^{M}\sum_{i=j}^{M}\sum_{\ell=1}^{L-1}\sum_{k=1}^{\ell-1}\sum_{\substack{z\in\mathcal{V}_\ell^+\\ g_{\ell,z}=j}}\sum_{\substack{w\in\mathcal{V}_k^+\\ g_{k,w}=i}}\langle\!\langle u_{k,w}^1, v_{\ell,z}^1\rangle\!\rangle + \sum_{i=0}^{M}\sum_{j=i+1}^{M}\sum_{k=1}^{L-2}\sum_{\ell=k+1}^{L-1}\sum_{\substack{z\in\mathcal{V}_\ell^+\\ g_{\ell,z}=j}}\sum_{\substack{w\in\mathcal{V}_k^+\\ g_{k,w}=i}}\langle\!\langle u_{k,w}^1, v_{\ell,z}^1\rangle\!\rangle$$

We abbreviate the last two terms as S_1 and S_2 respectively. Since they are both treated in the same way, we proceed with the proof for S_1.

Step 6: Using (4.34) for the sums over k and w and recalling $\operatorname{supp} v_{\ell,z}^1 \subseteq \overline{w_\ell(z)}$ we get

$$\begin{aligned} S_1 &= \sum_{j=0}^{M}\sum_{i=j}^{M}\sum_{\ell=1}^{L-1}\sum_{\substack{z\in\mathcal{V}_\ell^+\\ g_{\ell,z}=j}}\Big\langle\!\Big\langle \sum_{w\in\widehat{\mathcal{V}}_i}\sum_{k\in\mathscr{L}_{1,\ell-1}^{(1)}(w,i)} u_{k,w}^1, v_{\ell,z}^1\Big\rangle\!\Big\rangle \\ &= \sum_{j=0}^{M}\sum_{i=j}^{M}\sum_{\ell=1}^{L-1}\sum_{\substack{z\in\mathcal{V}_\ell^+\\ g_{\ell,z}=j}}\Big\langle\!\Big\langle \sum_{w\in\widehat{\mathcal{V}}_i}\sum_{k\in\mathscr{L}_{1,\ell-1}^{(1)}(w,i)} u_{k,w}^1, v_{\ell,z}^1\Big\rangle\!\Big\rangle_{\omega_\ell(z)}. \end{aligned} \tag{4.37}$$

Note that the generation constraints yield $\sum_{w\in\widehat{\mathcal{V}}_i}\sum_{k\in\mathscr{L}_{1,\ell-1}^{(1)}(w,i)} u_{k,w}^1 \in \widehat{\mathcal{X}}_i^1$ and $v_{\ell,z}^1 \in \widehat{\mathcal{X}}_j^1$ for $g_{\ell,z}=j$. We observe that $g_{\ell,z}=j$ implies that the vertex patch $\mathcal{T}_\ell(z)$ can be decomposed into elements of the uniform mesh $\widehat{\mathcal{T}}_j$. Because $j\le i$, we can use the strengthened Cauchy–Schwarz inequality on uniform meshes (4.25) to obtain

$$S_1 \le \widehat{C}_{\mathrm{SCS}}\sum_{j=0}^{M}\sum_{i=j}^{M}\delta^{i-j}\sum_{\ell=1}^{L-1}\sum_{\substack{z\in\mathcal{V}_\ell^+\\ g_{\ell,z}=j}}\widehat{h}_i^{-1}\Big\|\sum_{w\in\widehat{\mathcal{V}}_i}\sum_{k\in\mathscr{L}_{1,\ell-1}^{(1)}(w,i)} u_{k,w}^1\Big\|_{\omega_\ell(z)}\|\nabla v_{\ell,z}^1\|_{\omega_\ell(z)}. \tag{4.38}$$

Before we can continue to estimate S_1, we focus on the term $\big\|\sum_{w\in\widehat{\mathcal{V}}_i}\sum_{k\in\mathscr{L}_{1,\ell-1}^{(1)}(w,i)} u_{k,w}^1\big\|_\omega^2$ for a given domain $\omega\subseteq\Omega$. We split the L^2-norm into its contributions on the triangles $T\in\widehat{\mathcal{T}}_i$. Note that for a given triangle $T\in\widehat{\mathcal{T}}_i$ only functions $u_{k,w}^1$, that satisfy $z\in\overline{\omega_k(w)}$ for all $z\in\widehat{\mathcal{V}}_i\cap T$, have support on T. Using the identity $\#(\widehat{\mathcal{V}}_i\cap T)=d+1$, the triangle

inequality, and the discrete Cauchy–Schwarz inequality leads to

$$\begin{aligned}\Big\| \sum_{w\in\widehat{\mathcal{V}}_i} \sum_{k\in\mathscr{L}^{(1)}_{1,\ell-1}(w,i)} u^1_{k,w}\Big\|^2_\omega &= \sum_{T\in\widehat{\mathcal{T}}_i} \Big\| \sum_{z\in\widehat{\mathcal{V}}_i\cap T} \sum_{(k,w)\in\mathscr{L}^{(2)}_{1,\ell-1}(z,i)} u^1_{k,w}\Big\|^2_{T\cap\omega} \\ &\le \sum_{T\in\widehat{\mathcal{T}}_i} \Big(\sum_{z\in\widehat{\mathcal{V}}_i\cap T} \sum_{(k,w)\in\mathscr{L}^{(2)}_{1,\ell-1}(z,i)} \|u^1_{k,w}\|_{T\cap\omega}\Big)^2 \\ &\overset{(4.33)}{\le} (d+1)C^{(2)}_{\mathrm{lev}} \sum_{T\in\widehat{\mathcal{T}}_i} \sum_{z\in\widehat{\mathcal{V}}_i\cap T} \sum_{(k,w)\in\mathscr{L}^{(2)}_{1,\ell-1}(z,i)} \|u^1_{k,w}\|^2_{T\cap\omega}\end{aligned}$$

Due to the generation constraint $g_{k,w} = i$, the support $\omega_k(w)$ of $u^1_{k,w}$ appearing in the above sum can be decomposed into elements of $\widehat{\mathcal{T}}_i$. For an element $T \in \widehat{\mathcal{T}}_i$ and vertex $z \in T \cap \widehat{V}_i$, we only need to consider $z \in \overline{\omega_k(w)}$, which exactly means $(k,w) \in \mathscr{L}^{(2)}_{1,\ell-1}(z,i)$. Let us fix a tuple (k,w), then we can collect the contributions $\|u^1_{k,w}\|^2_{T\cap\omega}$ over the triangulation $\widehat{\mathcal{T}}_i$ to obtain the full norm $\|u^1_{k,w}\|^2_\omega$. Since the generation constraint still holds, we get

$$\sum_{T\in\widehat{\mathcal{T}}_i} \sum_{z\in\widehat{\mathcal{V}}_i\cap T} \sum_{(k,w)\in\mathscr{L}^{(2)}_{1,\ell-1}(z,i)} \|u^1_{k,w}\|^2_{T\cap\omega} = \sum_{w\in\widehat{\mathcal{V}}_i} \sum_{k\in\mathscr{L}^{(1)}_{1,\ell-1}(w,i)} \|u^1_{k,w}\|^2_\omega.$$

Therefore, we have

$$\begin{aligned}\Big\| \sum_{w\in\widehat{\mathcal{V}}_i} \sum_{k\in\mathscr{L}^{(1)}_{1,\ell-1}(w,i)} u^1_{k,w}\Big\|^2_\omega &\le (d+1)C^{(2)}_{\mathrm{lev}} \sum_{w\in\widehat{\mathcal{V}}_i} \sum_{k\in\mathscr{L}^{(1)}_{1,\ell-1}(w,i)} \|u^1_{k,w}\|^2_\omega \\ &\overset{(4.34)}{=} (d+1)C^{(2)}_{\mathrm{lev}} \sum_{k=1}^{\ell-1} \sum_{\substack{w\in\mathcal{V}^+_k \\ g_{k,w}=i}} \|u^1_{k,w}\|^2_\omega \\ &\le (d+1)C^{(2)}_{\mathrm{lev}} \sum_{k=1}^{L-2} \sum_{\substack{w\in\mathcal{V}^+_k \\ g_{k,w}=i}} \|u^1_{k.w}\|^2_\omega. \qquad (4.39)\end{aligned}$$

By applying this estimate to (4.38) for $\omega = \omega_\ell(z)$ and employing the discrete Cauchy–Schwarz inequality, we get

$$\begin{aligned}S_1 &\lesssim \sum_{j=0}^{M}\sum_{i=j}^{M} \delta^{i-j} \sum_{\ell=1}^{L-1} \sum_{\substack{z\in\mathcal{V}^+_\ell \\ g_{\ell,z}=j}} \widehat{h}_i^{-1} \Big(\sum_{k=1}^{L-2} \sum_{\substack{w\in\mathcal{V}^+_k \\ g_{k,w}=i}} \|u^1_{k,w}\|^2_{\omega_\ell(z)}\Big)^{1/2} \|\nabla v^1_{\ell,z}\|_{\omega_\ell(z)} \\ &\lesssim \sum_{j=0}^{M}\sum_{i=j}^{M} \delta^{i-j} \Big(\sum_{\ell=1}^{L-1} \sum_{\substack{z\in\mathcal{V}^+_\ell \\ g_{\ell,z}=j}} \|\nabla v^1_{\ell,z}\|^2_{\omega_\ell(z)}\Big)^{1/2} \Big(\widehat{h}_i^{-2} \sum_{\ell=1}^{L-1} \sum_{\substack{z\in\mathcal{V}^+_\ell \\ g_{\ell,z}=j}} \sum_{k=1}^{L-2} \sum_{\substack{w\in\mathcal{V}^+_k \\ g_{k,w}=i}} \|u^1_{k,w}\|^2_{\omega_\ell(z)}\Big)^{1/2}.\end{aligned}$$

Note that $\|\nabla v^1_{\ell,z}\|_{\omega_\ell(z)} = \|\nabla v^1_{\ell,z}\|$. Let us simplify the term containing four sums. We recognize that we can change the order of summation such that the sums over ℓ and z are the inner two sums. From Lemma 4.10 we know that an index n exists such that $\omega_\ell(z) \subseteq \widehat{\omega}^n_j(z)$ for all $\ell = 1, \dots L-1$ and all $z \in \mathcal{V}^+_\ell$ with $g_{\ell,z} = j$. There exists a constant $C_{\mathrm{patch}} > 0$ depending only on γ-shape regularity (2.15), the dimension d and the patch layer n that gives an upper limit for the patch overlap of n-patches, i.e., for any $m \in \mathbb{N}$, $0 \le j \le M$ and $T \in \widehat{\mathcal{T}}_j$ there holds

$$\#\{z \in \widehat{\mathcal{V}}_j : T \subseteq \widehat{\omega}^n_j(z)\} \le C_{\mathrm{patch}}. \tag{4.40}$$

Thus, we have

$$\begin{aligned}\sum_{\ell=1}^{L-1} \sum_{\substack{z\in\mathcal{V}^+_\ell \\ g_{\ell,z}=j}} \|u^1_{k,w}\|^2_{\omega_\ell(z)} \le \sum_{\ell=1}^{L-1} \sum_{\substack{z\in\mathcal{V}^+_\ell \\ g_{\ell,z}=j}} \|u^1_{k,w}\|^2_{\widehat{\omega}^n_j(z)} &= \sum_{z\in\widehat{\mathcal{V}}_j} \sum_{\ell\in\mathscr{L}^{(1)}_{1,L-1}(z,j)} \|u^1_{k,w}\|^2_{\widehat{\omega}^n_j(z)} \\ &\overset{(4.32)}{\le} C^{(1)}_{\mathrm{lev}} \sum_{z\in\widehat{\mathcal{V}}_j} \|u^1_{k,w}\|^2_{\widehat{\omega}^n_j(z)} \overset{(4.40)}{\le} C_{\mathrm{patch}} C^{(1)}_{\mathrm{lev}} \|u^1_{k,w}\|^2.\end{aligned} \tag{4.41}$$

Moreover, we use the equivalence of mesh sizes from (4.35) and a Poincaré-inequality to prove

$$\sum_{k=1}^{L-2} \sum_{\substack{w\in\mathcal{V}^+_k \\ g_{k,w}=i}} \widehat{h}_i^{-2} \|u^1_{k,w}\|^2 \overset{(4.35)}{\le} C^2_{\mathrm{eq}} \sum_{k=1}^{L-2} \sum_{\substack{w\in\mathcal{V}^+_k \\ g_{k,w}=i}} h^{-2}_{k,w} \|u^1_{k,w}\|^2 \le C^2_{\mathrm{eq}} C^2_{\mathrm{P}} \sum_{k=1}^{L-2} \sum_{\substack{w\in\mathcal{V}^+_k \\ g_{k,w}=i}} \|\nabla u^1_{k,w}\|^2.$$

Combining the last estimates with the geometric series bound (4.29) finally yields

$$\begin{aligned} S_1 &\lesssim \sum_{j=0}^{M} \sum_{i=j}^{M} \delta^{i-j} \Big(\sum_{\ell=1}^{L-1} \sum_{\substack{z\in\mathcal{V}^+_\ell \\ g_{\ell,z}=j}} \|\nabla v^1_{\ell,z}\|^2 \Big)^{1/2} \Big(\sum_{k=1}^{L-2} \sum_{\substack{w\in\mathcal{V}^+_k \\ g_{k,w}=i}} \|\nabla u^1_{k,w}\|^2 \Big)^{1/2} \\ &\overset{(4.29)}{\lesssim} \Big(\sum_{j=1}^{M} \sum_{\ell=1}^{L-1} \sum_{\substack{z\in\mathcal{V}^+_\ell \\ g_{\ell,z}=j}} \|\nabla v^1_{\ell,z}\|^2 \Big)^{1/2} \Big(\sum_{i=1}^{M} \sum_{k=1}^{L-2} \sum_{\substack{w\in\mathcal{V}^+_k \\ g_{k,w}=i}} \|\nabla u^1_{k,w}\|^2 \Big)^{1/2} \\ &= \Big(\sum_{\ell=1}^{L-1} \sum_{z\in\mathcal{V}^+_\ell} \|\nabla v^1_{\ell,z}\|^2 \Big)^{1/2} \Big(\sum_{k=1}^{L-2} \sum_{w\in\mathcal{V}^+_k} \|\nabla u^1_{k,w}\|^2 \Big)^{1/2}. \end{aligned}$$

Ultimately, we use the norm equivalence (2.6) to bound S_1 by the right-hand side of (4.28). Tracking the constants in the above estimates, it follows that

$$S_1 \le \widetilde{C}_{\mathrm{SCS}} \Big(\sum_{\ell=1}^{L-1} \sum_{z\in\mathcal{V}^+_\ell} |\!|\!| v^1_{\ell,z} |\!|\!|^2 \Big)^{1/2} \Big(\sum_{k=1}^{L-2} \sum_{w\in\mathcal{V}^+_k} |\!|\!| u^1_{k,w} |\!|\!|^2 \Big)^{1/2},$$

where

$$\widetilde{C}_{\mathrm{SCS}} := \widehat{C}_{\mathrm{SCS}} C_{\mathrm{eq}} C_{\mathrm{P}} \Lambda_{\min}^{-1} (1-\delta)^{-1} \big[(d+1) C_{\mathrm{lev}}^{(2)} C_{\mathrm{patch}} C_{\mathrm{lev}}^{(1)}\big]^{1/2}.$$

Step 7: Checking the argument in Step 6, we reveal that the same argument bounds S_2 even with the same constant $\widetilde{C}_{\mathrm{SCS}}$. Overall, we thus prove (4.28) with $C_{\mathrm{SCS}} = 2\widetilde{C}_{\mathrm{SCS}}$. This concludes the proof. □

4.4 *hp*-robust contraction of the solver

Finally, we have gathered all the tools to prove the main result.

Theorem 4.13. *Consider the exact FEM solution $u_L^* \in \mathcal{X}_L^p$ of (2.14), an abitrary function $u_L \in \mathcal{X}_L^p$, and the solver iterate $\Phi_L(u_L) \in \mathcal{X}_L^p$ and the associated a-posteriori estimator $\zeta_L(u_L)$ as output of Algorithm 3.7. Then, there holds the following link between solver iterates and estimator*

$$|||u_L^* - \Phi_L(u_L)|||^2 \le |||u_L^* - u_L|||^2 - \zeta_L(u_L)^2. \tag{4.42}$$

Furthermore, the error estimator is efficient and reliable, i.e., there exists a constant $C'_{\mathrm{rel}} > 1$ such that

$$\zeta_L(u_L) \le |||u_L^* - u_L||| \le C'_{\mathrm{rel}} \zeta_L(u_L). \tag{4.43}$$

Finally, the reliability of the estimator is equivalent to the contraction of the algebraic error. Hence, there exists a constant $0 < q_{\mathrm{ctr}} < 1$ such that

$$|||u_L^* - \Phi_L(u_L)||| \le q_{\mathrm{ctr}} |||u_L^* - u_L|||. \tag{4.44}$$

This also yields that

$$|||u_L^* - \Phi_L(u_L)||| \le q_{\mathrm{ctr}} C'_{\mathrm{rel}} \zeta_L(u_L). \tag{4.45}$$

The constants q_{ctr} and C'_{rel} depend only on the space dimension d, the γ-shape regularity (2.15), the quasi-uniformity constant C_{qu} from (4.23), $\max_{T\in\mathcal{T}_0} \|\operatorname{div}(\mathbf{K})\|_{L^\infty(T)}/\Lambda_{\min}$, $\operatorname{diam}(\Omega)/h_0$, and $\Lambda_{\max}/\Lambda_{\min}$. Therefore, the constants are h- and p-robust.

Note that the efficiency of the a-posteriori estimator for the algebraic error, i.e., the lower bound in (4.43), is *guaranteed*. This means no constants arise in the estimate. To avoid a case distinction, we present the proof only for $p > 1$. Moreover, we split up the proof into the different statements from the above theorem.

Proof of the connection of the solver and estimator (4.42). The proof consists of two steps.
Step 1: First, we show the identity

$$\begin{aligned} \Big|\Big|\Big| \sum_{\ell=0}^{L-1} \lambda_\ell \rho_\ell \Big|\Big|\Big|^2 - 2\Big\langle\!\Big\langle u_L^* - u_L, \sum_{\ell=0}^{L-1} \lambda_\ell \rho_\ell \Big\rangle\!\Big\rangle \\ = -|||\rho_0|||^2 + \sum_{\ell=1}^{L-1} |||\lambda_\ell \rho_\ell|||^2 - 2 \sum_{\ell=1}^{L-1} \lambda_\ell \sum_{z\in\mathcal{V}_\ell^+} |||\rho_{\ell,z}|||^2. \end{aligned} \tag{4.46}$$

We recall $\sigma_\ell = \sum_{k=0}^{\ell} \lambda_k \rho_k$, $\rho_\ell = \sum_{z \in \mathcal{V}_\ell^+} \rho_{\ell,z}$, the definition of the residual (3.3), the global residual problem (3.4), and the local lowest-order problems (3.5) to develop

$$\begin{aligned}
\Big\langle\!\Big\langle u_L^* - u_L, \sum_{\ell=0}^{L-1} \lambda_\ell \rho_\ell \Big\rangle\!\Big\rangle &\overset{(3.3)}{=} R_L\Big(\sum_{\ell=0}^{L-1} \lambda_\ell \rho_\ell\Big) \overset{\lambda_0=1}{=} R_L(\rho_0) + \sum_{\ell=1}^{L-1} \lambda_\ell \sum_{z \in \mathcal{V}_\ell^+} R_L(\rho_{\ell,z}) \\
&\overset{(3.4)}{=} \|\rho_0\|^2 + \sum_{\ell=1}^{L-1} \lambda_\ell \sum_{z \in \mathcal{V}_\ell^+} R_L(\rho_{\ell,z}) \\
&\overset{(3.5)}{=} \|\rho_0\|^2 + \sum_{\ell=1}^{L-1} \lambda_\ell \sum_{z \in \mathcal{V}_\ell^+} \Big(\|\rho_{\ell,z}\|^2 + \langle\!\langle \sigma_{\ell-1}, \rho_{\ell,z} \rangle\!\rangle\Big) \\
&= \|\rho_0\|^2 + \sum_{\ell=1}^{L-1} \lambda_\ell \sum_{z \in \mathcal{V}_\ell^+} \Big(\|\rho_{\ell,z}\|^2 + \sum_{k=0}^{\ell-1} \langle\!\langle \lambda_k \rho_k, \rho_{\ell,z} \rangle\!\rangle\Big) \\
&= \|\rho_0\|^2 + \sum_{\ell=1}^{L-1} \lambda_\ell \sum_{z \in \mathcal{V}_\ell^+} \|\rho_{\ell,z}\|^2 + \sum_{\ell=1}^{L-1} \sum_{k=0}^{\ell-1} \langle\!\langle \lambda_k \rho_k, \lambda_\ell \rho_\ell \rangle\!\rangle.
\end{aligned}$$

Expanding the square and applying the last result yields the desired identity (4.46):

$$\begin{aligned}
&\Big\|\sum_{\ell=0}^{L-1} \lambda_\ell \rho_\ell\Big\|^2 - 2\Big\langle\!\Big\langle u_L^* - u_L, \sum_{\ell=0}^{L-1} \lambda_\ell \rho_\ell \Big\rangle\!\Big\rangle \\
&\qquad = \sum_{\ell=0}^{L-1} \|\lambda_\ell \rho_\ell\|^2 + 2 \sum_{\ell=1}^{L-1} \sum_{k=0}^{\ell-1} \langle\!\langle \lambda_k \rho_k, \lambda_\ell \rho_\ell \rangle\!\rangle - 2\Big\langle\!\Big\langle u_L^* - u_L, \sum_{\ell=0}^{L-1} \lambda_\ell \rho_\ell \Big\rangle\!\Big\rangle \\
&\qquad = -\|\rho_0\|^2 + \sum_{\ell=1}^{L-1} \|\lambda_\ell \rho_\ell\|^2 - 2 \sum_{\ell=1}^{L-1} \lambda_\ell \sum_{z \mathcal{V}_\ell^+} \|\rho_{\ell,z}\|^2.
\end{aligned}$$

Step 2: Recall that $\Phi(u_L) = u_L + \sigma_L = u_L + \sigma_{L-1} + \lambda_L \rho_L$. Moreover, from the definition of the residual (3.3), the identity (4.7), and the local problems (3.7), we get

$$\begin{aligned}
\|u_L^* - \Phi(u_L)\|^2 &= \|u_L^* - (u_L + \sigma_{L-1}) - \lambda_L \rho_L\|^2 \\
&= \|u_L^* - (u_L + \sigma_{L-1})\|^2 - 2\lambda_L \langle\!\langle u_L^* - (u_L + \sigma_{L-1}), \rho_L \rangle\!\rangle + \|\lambda_L \rho_L\|^2 \\
&\overset{(3.3)}{\overset{(4.7)}{=}} \|u_L^* - (u_L + \sigma_{L-1})\|^2 - 2\lambda_L \big(R_L(\rho_L) - \langle\!\langle \sigma_{L-1}, \rho_L \rangle\!\rangle\big) + \lambda_L \sum_{z \in \mathcal{V}_L} \|\rho_{L,z}\|^2 \qquad (4.47) \\
&\overset{(3.7)}{=} \Big\|u_L^* - \Big(u_L + \sum_{\ell=0}^{L-1} \lambda_\ell \rho_\ell\Big)\Big\|^2 - \lambda_L \sum_{z \in \mathcal{V}_L} \|\rho_{L,z}\|^2.
\end{aligned}$$

Focusing on the first term and expanding its square leads to

$$\begin{aligned}\Big|\!\Big|\!\Big|u_L^* - \Big(u_L + \sum_{\ell=0}^{L-1}\lambda_\ell\rho_\ell\Big)\Big|\!\Big|\!\Big|^2 &= |\!|\!|u_L^* - u_L|\!|\!|^2 + \Big|\!\Big|\!\Big|\sum_{\ell=0}^{L-1}\lambda_\ell\rho_\ell\Big|\!\Big|\!\Big|^2 - 2\Big\langle\!\Big\langle u_L^* - u_L, \sum_{\ell=0}^{L-1}\lambda_\ell\rho_\ell\Big\rangle\!\Big\rangle \\ &\overset{(4.46)}{=} |\!|\!|u_L^* - u_L|\!|\!|^2 - |\!|\!|\rho_0|\!|\!|^2 + \sum_{\ell=1}^{L-1}|\!|\!|\lambda_\ell\rho_\ell|\!|\!|^2 - 2\sum_{\ell=1}^{L-1}\lambda_\ell\sum_{z\in\mathcal{V}_\ell^+}|\!|\!|\rho_{\ell,z}|\!|\!|^2 \\ &\overset{(4.6)}{\le} |\!|\!|u_L^* - u_L|\!|\!|^2 - |\!|\!|\rho_0|\!|\!|^2 - \sum_{\ell=1}^{L-1}\lambda_\ell\sum_{z\in\mathcal{V}_\ell^+}|\!|\!|\rho_{\ell,z}|\!|\!|^2.\end{aligned}$$

We use this and the definition of the error estimator ζ_L in Algorithm 3.7 to obtain

$$\begin{aligned}|\!|\!|u_L^* - \Phi(u_L)|\!|\!|^2 &\le |\!|\!|u_L^* - u_L|\!|\!|^2 - |\!|\!|\rho_0|\!|\!|^2 - \sum_{\ell=1}^{L-1}\lambda_\ell\sum_{z\in\mathcal{V}_\ell^+}|\!|\!|\rho_{\ell,z}|\!|\!|^2 - \lambda_L\sum_{z\in\mathcal{V}_L}|\!|\!|\rho_{L,z}|\!|\!|^2 \\ &= |\!|\!|u_L^* - u_L|\!|\!|^2 - \zeta_L(u_L)^2\end{aligned}$$

This concludes the proof of (4.42). □

Proof of the equivalence of (4.43) *and* (4.44). Let us prove the equivalence of the upper bound in (4.43) and the error contraction (4.44).

Suppose reliability, i.e., the upper bound in (4.43) holds for a constant $C'_{\mathrm{rel}} > 1$. Then, it follows from (4.42) that

$$|\!|\!|u_L^* - \Phi(u_L)|\!|\!|^2 \overset{(4.42)}{\le} |\!|\!|u_L^* - u_L|\!|\!|^2 - \zeta_L(u_L)^2 \overset{(4.43)}{\le} |\!|\!|u_L^* - u_L|\!|\!|^2 - (C'_{\mathrm{rel}})^{-2}|\!|\!|u_L^* - u_L|\!|\!|^2.$$

Thus, we have proven contraction of the error (4.44) with $q_{\mathrm{ctr}}^2 := 1 - (C'_{\mathrm{rel}})^{-2} \in (0,1)$.

For the converse, suppose the error is contracted by some constant $0 < q_{\mathrm{ctr}} < 1$. With (4.47), we have

$$\begin{aligned}|\!|\!|u_L^* - \Phi(u_L)|\!|\!|^2 &= |\!|\!|u_L^* - (u_L + \sigma_{L-1} + \lambda_L\rho_L)|\!|\!|^2 \\ &\overset{(4.47)}{=} \Big|\!\Big|\!\Big|u_L^* - \Big(u_L + \sum_{\ell=0}^{L-1}\lambda_\ell\rho_\ell\Big)\Big|\!\Big|\!\Big|^2 - \lambda_L\sum_{z\in\mathcal{V}_L}|\!|\!|\rho_{L,z}|\!|\!|^2 \\ &= |\!|\!|u_L^* - u_L|\!|\!|^2 + \Big|\!\Big|\!\Big|\sum_{\ell=0}^{L-1}\lambda_\ell\rho_\ell\Big|\!\Big|\!\Big|^2 - 2\Big\langle\!\Big\langle u_L^* - u_L, \sum_{\ell=0}^{L-1}\lambda_\ell\rho_\ell\Big\rangle\!\Big\rangle - \lambda_L\sum_{z\in\mathcal{V}_L}|\!|\!|\rho_{L,z}|\!|\!|^2.\end{aligned}$$

This and the identity (4.46) yield

$$\begin{aligned}&|\!|\!|u_L^* - u_L|\!|\!|^2 \\ &= |\!|\!|u_L^* - \Phi(u_L)|\!|\!|^2 + |\!|\!|\rho_0|\!|\!|^2 - \sum_{\ell=1}^{L-1}|\!|\!|\lambda_\ell\rho_\ell|\!|\!|^2 + 2\sum_{\ell=1}^{L-1}\lambda_\ell\sum_{z\in\mathcal{V}_\ell^+}|\!|\!|\rho_{\ell,z}|\!|\!|^2 + \lambda_L\sum_{z\in\mathcal{V}_L}|\!|\!|\rho_{L,z}|\!|\!|^2 \\ &\le |\!|\!|u_L^* - \Phi(u_L)|\!|\!|^2 + 2|\!|\!|\rho_0|\!|\!|^2 + 2\sum_{\ell=1}^{L-1}\lambda_\ell\sum_{z\in\mathcal{V}_\ell^+}|\!|\!|\rho_{\ell,z}|\!|\!|^2 + 2\lambda_L\sum_{z\in\mathcal{V}_L}|\!|\!|\rho_{L,z}|\!|\!|^2.\end{aligned}$$

Hence, solver contraction (4.44) gives us

$$\begin{aligned}\|\!|u_L^* - u_L|\!\|^2 &\overset{(4.44)}{\leq} q_{\mathrm{ctr}}^2 \|\!|u_L^* - u_L|\!\|^2 + 2\Big(\|\!|\rho_0|\!\|^2 + \sum_{\ell=1}^{L-1} \lambda_\ell \sum_{z\in\mathcal{V}_\ell^+} \|\!|\rho_{\ell,z}|\!\|^2 + \lambda_L \sum_{z\in\mathcal{V}_L} \|\!|\rho_{L,z}|\!\|^2\Big) \\ &= q_{\mathrm{ctr}}^2 \|\!|u_L^* - u_L|\!\|^2 + 2\zeta_L(u_L)^2.\end{aligned}$$

Gathering the terms containing the algebraic error on the left-hand side and dividing by $1 - q_{\mathrm{ctr}}^2 > 0$ gives the upper bound in (4.43) with $(C'_{\mathrm{rel}})^2 = 2/(1 - q_{\mathrm{ctr}}^2) > 1$. □

Proof of efficiency and reliability (4.43). The efficiency, i.e., the lower bound of (4.43) follows directly from (4.42).

The reliability, i.e., the upper bound in (4.43) requires two main ingredients that were developed in Sections 4.2–4.3, namely a suitable stable decomposition and strengthened Cauchy–Schwarz estimate. Begin by applying the local multilevel decomposition from Proposition 4.6 to the algebraic error $u_L^* - u_L \in \mathcal{X}_L^p$. We obtain functions $v_0 \in \mathcal{X}_0^1$, $\{v_{\ell,z}\}_{z\in\mathcal{V}_\ell^+} \in \mathcal{X}_{\ell,z}^1$ and $\{v_{L,z}\}_{z\in\mathcal{V}_L} \in \mathcal{X}_{L,z}^p$ such that

$$u_L^* - u_L = v_0 + \sum_{\ell=1}^{L-1} \sum_{z\in\mathcal{V}_\ell^+} v_{\ell,z} + \sum_{z\in\mathcal{V}_L} v_{L,z} \quad \text{and} \tag{4.48}$$

$$\|\!|v_0|\!\|^2 + \sum_{\ell=1}^{L-1} \sum_{z\in\mathcal{V}_\ell^+} \|\!|v_{\ell,z}|\!\|^2 + \sum_{z\in\mathcal{V}_L} \|\!|v_{L,z}|\!\|^2 \leq C_{\mathrm{SD}}^2 \|\!|u_L^* - u_L|\!\|^2. \tag{4.49}$$

We use the definition of the residual (3.3), the global coarse residual problem (3.4), and the local problems (3.5) and (3.7) to obtain

$$\begin{aligned}\|\!|u_L^* - u_L|\!\|^2 &\overset{(4.48)}{=} \Big\langle\!\Big\langle u_L^* - u_L, v_0 + \sum_{\ell=1}^{L-1} \sum_{z\in\mathcal{V}_\ell^+} v_{\ell,z} + \sum_{z\in\mathcal{V}_L} v_{L,z} \Big\rangle\!\Big\rangle \\ &\overset{(3.3)}{\underset{(3.4)}{=}} \langle\!\langle \rho_0, v_0 \rangle\!\rangle + \sum_{\ell=1}^{L-1} \sum_{z\in\mathcal{V}_\ell^+} R_L(v_{\ell,z}) + \sum_{z\in\mathcal{V}_L} R_L(v_{L,z}) \\ &\overset{(3.5)}{\underset{(3.7)}{=}} \langle\!\langle \rho_0, v_0 \rangle\!\rangle + \sum_{\ell=1}^{L-1} \sum_{z\in\mathcal{V}_\ell^+} \Big(\langle\!\langle \rho_{\ell,z}, v_{\ell,z} \rangle\!\rangle + \langle\!\langle \sigma_{\ell-1}, v_{\ell,z} \rangle\!\rangle\Big) \\ &\qquad + \sum_{z\in\mathcal{V}_L} \Big(\langle\!\langle \rho_{L,z}, v_{L,z} \rangle\!\rangle + \langle\!\langle \sigma_{L-1}, v_{L,z} \rangle\!\rangle\Big).\end{aligned}$$

Plugging in $\sigma_\ell = \rho_0 + \sum_{k=1}^{\ell} \lambda_k \rho_k$ and gathering the terms containing ρ_0, we see

$$\begin{aligned}\|\!| u_L^* - u_L |\!\|^2 = \Big\langle\!\Big\langle \rho_0, v_0 + \sum_{\ell=1}^{L-1} \sum_{z\in\mathcal{V}_\ell^+} v_{\ell,z} + \sum_{z\in\mathcal{V}_L} v_{L,z} \Big\rangle\!\Big\rangle + \sum_{\ell=1}^{L-1} \sum_{z\in\mathcal{V}_\ell^+} \langle\!\langle \rho_{\ell,z}, v_{\ell,z} \rangle\!\rangle \\ + \sum_{z\in\mathcal{V}_L} \langle\!\langle \rho_{L,z}, v_{L,z} \rangle\!\rangle + \sum_{\ell=1}^{L-1} \sum_{k=1}^{\ell-1} \Big\langle\!\Big\langle \lambda_k \rho_k, \sum_{z\in\mathcal{V}_\ell^+} v_{\ell,z} \Big\rangle\!\Big\rangle + \sum_{k=1}^{L-1} \Big\langle\!\Big\langle \lambda_k \rho_k, \sum_{z\in\mathcal{V}_L} v_{L,z} \Big\rangle\!\Big\rangle.\end{aligned} \tag{4.50}$$

We estimate the five terms constituting the algebraic error separately. However, we will use the Young inequality

$$ab \le (\alpha/2)a^2 + (2\alpha)^{-1}b^2 \quad \text{for all } a, b \ge 0 \text{ and all } \alpha > 0 \tag{4.51}$$

multiple times. We recall the decomposition of the error (4.48) and use the Cauchy–Schwarz inequality for $\langle\!\langle \cdot, \cdot \rangle\!\rangle$ as well as the Young inequality (4.51) with $\alpha = 1$ to estimate the first term

$$\Big\langle\!\Big\langle \rho_0, v_0 + \sum_{\ell=1}^{L-1} \sum_{z\in\mathcal{V}_\ell^+} v_{\ell,z} + \sum_{z\in\mathcal{V}_L} v_{L,z} \Big\rangle\!\Big\rangle \overset{(4.48)}{=} \langle\!\langle \rho_0, u_L^* - u_L \rangle\!\rangle \le \frac{1}{2}\|\rho_0\|^2 + \frac{1}{2}\|\!| u_L^* - u_L |\!\|^2.$$

For the second term, the Cauchy–Schwarz inequality for $\langle\!\langle \cdot, \cdot \rangle\!\rangle$, the Young inequality (4.51) with $\alpha = 4C_{\mathrm{SD}}^2$ and the estimate (4.9) yield

$$\begin{aligned}\sum_{\ell=1}^{L-1} \sum_{z\in\mathcal{V}_\ell^+} \langle\!\langle \rho_{\ell,z}, v_{\ell,z} \rangle\!\rangle &\le 2C_{\mathrm{SD}}^2 \sum_{\ell=1}^{L-1} \sum_{z\in\mathcal{V}_\ell^+} \|\!| \rho_{\ell,z} |\!\|^2 + \frac{1}{8C_{\mathrm{SD}}^2} \sum_{\ell=1}^{L-1} \sum_{z\in\mathcal{V}_\ell^+} \|\!| v_{\ell,z} |\!\|^2 \\ &\overset{(4.9)}{\le} 2C_{\mathrm{SD}}^2 (d+1) \sum_{\ell=1}^{L-1} \lambda_\ell \sum_{z\in\mathcal{V}_\ell^+} \|\!| \rho_{\ell,z} |\!\|^2 + \frac{1}{8C_{\mathrm{SD}}^2} \sum_{\ell=1}^{L-1} \sum_{z\in\mathcal{V}_\ell^+} \|\!| v_{\ell,z} |\!\|^2.\end{aligned}$$

For the third term, the same arguments show

$$\sum_{z\in\mathcal{V}_L} \langle\!\langle \rho_{L,z}, v_{L,z} \rangle\!\rangle \le 2C_{\mathrm{SD}}^2 (d+1) \lambda_L \sum_{z\in\mathcal{V}_L} \|\!| \rho_{L,z} |\!\|^2 + \frac{1}{8C_{\mathrm{SD}}^2} \sum_{z\in\mathcal{V}_L} \|\!| v_{L,z} |\!\|^2.$$

Since $\rho_k = \sum_{w\in\mathcal{V}_k^+} \rho_{k,w}$, the strengthened Cauchy–Schwarz inequality (4.28) from Proposition 4.12 can be applied to the fourth term. Moreover, the Young inequality and the upper bound of the step-size (4.8) lead to

$$\begin{aligned}\sum_{\ell=1}^{L-1} \sum_{k=1}^{\ell-1} \Big\langle\!\Big\langle \lambda_k \rho_k, \sum_{z\in\mathcal{V}_\ell^+} v_{\ell,z} \Big\rangle\!\Big\rangle &\overset{(4.28)}{\le} C_{\mathrm{SCS}} \Big(\sum_{k=1}^{L-2} \sum_{w\in\mathcal{V}_k^+} \|\!| \lambda_k \rho_{k,w} |\!\|^2 \Big)^{1/2} \Big(\sum_{\ell=1}^{L-1} \sum_{z\in\mathcal{V}_\ell^+} \|\!| v_{\ell,z} |\!\|^2 \Big)^{1/2} \\ &\le 2C_{\mathrm{SCS}}^2 C_{\mathrm{SD}}^2 \sum_{k=1}^{L-2} \sum_{w\in\mathcal{V}_k^+} \|\!| \lambda_k \rho_{k,w} |\!\|^2 + \frac{1}{8C_{\mathrm{SD}}^2} \sum_{\ell=1}^{L-1} \sum_{z\in\mathcal{V}_\ell^+} \|\!| v_{\ell,z} |\!\|^2 \\ &\overset{(4.8)}{\le} 2C_{\mathrm{SCS}}^2 C_{\mathrm{SD}}^2 (d+1) \sum_{k=1}^{L-2} \lambda_k \sum_{w\in\mathcal{V}_k^+} \|\!| \rho_{k,w} |\!\|^2 + \frac{1}{8C_{\mathrm{SD}}^2} \sum_{\ell=1}^{L-1} \sum_{z\in\mathcal{V}_\ell^+} \|\!| v_{\ell,z} |\!\|^2.\end{aligned}$$

Ultimately, the last term consists of higher-order functions as well as a sum over the levels. Similar to [CNX12, Proof of Theorem 4.8], we want to exploit the finite overlap of patches. Therefore, we use the Cauchy–Schwarz and Young inequality to obtain

$$\begin{aligned}\sum_{k=1}^{L-1} \Big\langle\!\Big\langle \lambda_k \rho_k, \sum_{z\in\mathcal{V}_L} v_{L,z} \Big\rangle\!\Big\rangle &= \sum_{z\in\mathcal{V}_L} \Big\langle\!\Big\langle \sum_{k=1}^{L-1} \lambda_k \rho_k, v_{L,z} \Big\rangle\!\Big\rangle \\ &\le 2C_{\mathrm{SD}}^2 \sum_{z\in\mathcal{V}_L} \Big|\!\Big|\!\Big| \sum_{k=1}^{L-1} \lambda_k \rho_k \Big|\!\Big|\!\Big|_{\omega_L(z)}^2 + \frac{1}{8C_{\mathrm{SD}}^2} \sum_{z\in\mathcal{V}_L} |\!|\!| v_{L,z} |\!|\!|^2.\end{aligned}$$

As every simplex is contained in $d+1$ patches, the first term can be further estimated using the strengthened Cauchy–Schwarz inequality (4.28), the identity (4.6), and the upper bound of the step-size (4.8)

$$\begin{aligned}\sum_{z\in\mathcal{V}_L} \Big|\!\Big|\!\Big| \sum_{k=1}^{L-1} \lambda_k \rho_k \Big|\!\Big|\!\Big|_{\omega_L(z)}^2 &\le (d+1) \Big|\!\Big|\!\Big| \sum_{k=1}^{L-1} \lambda_k \rho_k \Big|\!\Big|\!\Big|^2 \\ &= (d+1)\Big[\sum_{k=1}^{L-1} |\!|\!| \lambda_k \rho_k |\!|\!|^2 + 2\sum_{\ell=1}^{L-1}\sum_{k=1}^{\ell-1} \langle\!\langle \lambda_k \rho_k, \lambda_\ell \rho_\ell \rangle\!\rangle\Big] \\ &\overset{(4.28)}{\le} (d+1)\Big[\sum_{k=1}^{L-1} |\!|\!| \lambda_k \rho_k |\!|\!|^2 + 2C_{\mathrm{SCS}} \Big(\sum_{k=1}^{L-2} \sum_{w\in\mathcal{V}_k^+} |\!|\!| \lambda_k \rho_{k,w} |\!|\!|^2\Big)^{1/2} \Big(\sum_{\ell=1}^{L-1} \sum_{z\in\mathcal{V}_\ell^+} |\!|\!| \lambda_\ell \rho_{\ell,z} |\!|\!|^2\Big)^{1/2}\Big] \\ &\overset{\substack{(4.6)\\(4.8)}}{\le} (d+1)[1+2C_{\mathrm{SCS}}(d+1)]\Big(\sum_{\ell=1}^{L-1} \lambda_\ell \sum_{z\in\mathcal{V}_\ell^+} |\!|\!| \rho_{\ell,z} |\!|\!|^2\Big).\end{aligned}$$

Altogether, we have that

$$\begin{aligned}&\sum_{k=1}^{L-1} \Big\langle\!\Big\langle \lambda_k \rho_k, \sum_{z\in\mathcal{V}_L} v_{L,z} \Big\rangle\!\Big\rangle \\ &\qquad \le 2C_{\mathrm{SD}}^2 (d+1)[1+2C_{\mathrm{SCS}}(d+1)]\Big(\sum_{\ell=1}^{L-1} \lambda_\ell \sum_{z\in\mathcal{V}_\ell^+} |\!|\!| \rho_{\ell,z} |\!|\!|^2\Big) + \frac{1}{8C_{\mathrm{SD}}^2} \sum_{z\in\mathcal{V}_L} |\!|\!| v_{L,z} |\!|\!|^2.\end{aligned}$$

Combining the bounds of the five terms that make up the algebraic error (4.50), defining the constant $(C'_{\mathrm{rel}})^2 := 4\max\{1/2, 2C_{\mathrm{SD}}^2(d+1)[2+2C_{\mathrm{SCS}}(d+1)+C_{\mathrm{SCS}}^2]\}$, and exploiting

the stability of the decomposition (4.49) gives the estimate

$$\begin{aligned}
|||u_L^* - u_L|||^2 &\le \frac{1}{2}|||\rho_0|||^2 + \frac{1}{2}|||u_L^* - u_L|||^2 + \frac{1}{4}(C'_{\mathrm{rel}})^2\Big(\sum_{\ell=1}^{L-1}\lambda_\ell \sum_{z\in\mathcal{V}_\ell^+}|||\rho_{\ell,z}|||^2 + \lambda_L\sum_{z\in\mathcal{V}_L}|||\rho_{L,z}|||^2\Big) \\
&\quad + \frac{1}{4C_{\mathrm{SD}}^2}\Big(\sum_{\ell=1}^{L-1}\sum_{z\in\mathcal{V}_\ell^+}|||v_{\ell,z}|||^2 + \sum_{z\in\mathcal{V}_L}|||v_{L,z}|||^2\Big) \\
&\overset{(4.49)}{\le} \frac{3}{4}|||u_L^* - u_L|||^2 + \frac{1}{4}(C'_{\mathrm{rel}})^2\Big(|||\rho_0|||^2 + \sum_{\ell=1}^{L-1}\lambda_\ell \sum_{z\in\mathcal{V}_\ell^+}|||\rho_{\ell,z}|||^2 + \lambda_L\sum_{z\in\mathcal{V}_L}|||\rho_{L,z}|||^2\Big) \\
&= \frac{3}{4}|||u_L^* - u_L|||^2 + \frac{1}{4}(C'_{\mathrm{rel}})^2\zeta_L(u_L)^2.
\end{aligned}$$

Rearranging the terms leads to the reliability of the error estimator

$$|||u_L^* - u_L|||^2 \le (C'_{\mathrm{rel}})^2\zeta_L(u_L)^2.$$

This concludes the proof of Theorem 4.13. □

5 Improved analysis of multigrid contraction: local dependence on the diffusion coefficient

In this chapter, we present new results improving the analysis of [IMP+24] by means of reworking the proofs of stable decompositions of Section 4.2 and strengthened Cauchy-Schwarz inequality of Section 4.3 in such a way that the inherent constants depend only on *local* variations of the diffusion coefficient. As a consequence, we can improve Theorem 4.13 so that the contraction factor and reliability constant depend only on the local diffusion-contrast.

The chapter is organized as follows: In Section 5.1, we state the main result in Theorem 5.1 and prove several auxiliary results. Section 5.2 then presents the strengthened Cauchy–Schwarz inequality with improved dependence on the diffusion-contrast. In Section 5.3, we establish an h-robust stable multilevel decomposition in the energy norm. For the case $d = 2$, Section 5.4 introduces a p-robust stable decomposition, which is then extended to an hp-robust stable decomposition in Section 5.5, where the stability constant depends only on local variations of the diffusion coefficient. Finally, the proof of Theorem 5.1 is provided in Section 5.6.

5.1 Main result

First, we present the improved version of Theorem 4.13 and provide explicit formulas for the new constants.

Theorem 5.1. *Let $d = 2$ and $p \geq 1$ or $d = 3$ and $p = 1$. Consider the exact FEM solution $u_L^* \in \mathcal{X}_L^p$ of (2.14), an abitrary function $u_L \in \mathcal{X}_L^p$, and the solver iterate $\Phi_L(u_L) \in \mathcal{X}_L^p$ and associated a-posteriori estimator $\zeta_L(u_L)$ as output from Algorithm 3.7. Then, there holds the following link between solver iterates and estimator*

$$|||u_L^* - \Phi_L(u_L)|||^2 \leq |||u_L^* - u_L|||^2 - \zeta_L(u_L)^2. \tag{5.1}$$

Furthermore, the error estimator is efficient and reliable, i.e., there exists a constant $\widetilde{C}_{\mathrm{rel}} > 1$ such that

$$\zeta_L(u_L) \leq |||u_L^* - u_L||| \leq \widetilde{C}_{\mathrm{rel}} \zeta_L(u_L). \tag{5.2}$$

Moreover, the reliability of the estimator is equivalent to the contraction of the algebraic error, i.e., there exists a constant $0 < q_{\mathrm{ctr}} < 1$ such that

$$|||u_L^* - \Phi_L(u_L)||| \leq q_{\mathrm{ctr}} |||u_L^* - u_L|||. \tag{5.3}$$

This also yields that

$$|||u_L^* - \Phi_L(u_L)||| \leq q_{\mathrm{ctr}} \widetilde{C}_{\mathrm{rel}} \zeta_L(u_L). \tag{5.4}$$

The constants q_{ctr} and $\widetilde{C}_{\mathrm{rel}}$ depend only on the space dimension d, the γ-shape regularity (2.15), the quasi-uniformity constant C_{qu} from (4.23), the initial mesh $\mathcal{T}_0$ and the local constants $C_{\mathrm{loc}}^{(1)}$ and $C_{\mathrm{loc}}^{(2)}$, which are defined as

$$C_{\mathrm{loc}}^{(1)} := \max\left\{ \sup_{z\in\mathcal{V}_0} \frac{\max_{T\subseteq\overline{\omega_0^2(z)}} \|\operatorname{div}(\mathbf{K})\|_{L^\infty(T)}}{\inf_{y\in\omega_0^2(z)} \lambda_{\min}(\mathbf{K}(y))}, \sup_{z\in\mathcal{V}_0} \frac{\sup_{y\in\omega_0^2(z)} \lambda_{\max}(\mathbf{K}(y))}{\inf_{y\in\omega_0^2(z)} \lambda_{\min}(\mathbf{K}(y))} \right\} \tag{5.5}$$

and

$$C_{\mathrm{loc}}^{(2)} := \sup_{z\in\mathcal{V}_0} \frac{\sup_{y\in\omega_0^3(z)} \lambda_{\max}(\mathbf{K}(y))}{\inf_{y\in\omega_0^3(z)} \lambda_{\min}(\mathbf{K}(y))}. \tag{5.6}$$

Therefore, the constants depend only on local variations of the diffusion coefficient. There exist constants $\widetilde{C}_{\mathrm{SD}}$, $\widetilde{C}_{\mathrm{ML}}$, and C'_{SCS} independent of the diffusion coefficient $\mathbf{K}$, explicitly given in Lemma 5.26, Proposition 5.19, and Proposition 5.9, respectively, such that the reliability constant $\widetilde{C}_{\mathrm{rel}}$ is given by

$$(\widetilde{C}_{\mathrm{rel}})^2 := 4\max\Big\{1/2, 2C_D(C_{\mathrm{loc}}^{(2)})^2(d+1)\big[2 + 2C'_{\mathrm{SCS}}C_{\mathrm{loc}}^{(1)}(d+1) + (C'_{\mathrm{SCS}}C_{\mathrm{loc}}^{(1)})^2\big]\Big\}, \tag{5.7}$$

where $C_{\mathrm{D}} = \widetilde{C}_{\mathrm{SD}}$ for $d = 2$ and $C_{\mathrm{D}} = \widetilde{C}_{\mathrm{ML}}$ for $d = 3$.

The proof is postponed to Section 5.6.

5.1.1 Auxiliary results

In this section, we present some useful properties of the interaction of patches of different levels. These will provide the technical geometric tools needed to prove the main results of this chapter. Our first goal is to show that patches, whose intersection has a positive measure, are contained in a two-layer patch of the initial mesh $\mathcal{T}_0$, recall Definition 3.6. For this, we need the following two lemmas.

Lemma 5.2 (Neighboring patches)**.** *Let $\ell \in \{0,\dots,L\}$, $z, w \in \mathcal{V}_\ell$ and consider vertices $z, w \in \mathcal{V}_\ell$ with $|\omega_\ell(z) \cap \omega_\ell(w)| > 0$. Then, it follows that $\omega_\ell(z) \cup \omega_\ell(w) \subseteq \omega_\ell^2(z) \cap \omega_\ell^2(w)$.*

Proof. The assumption $|\omega_\ell(z) \cap \omega_\ell(w)| > 0$ and the patch domains being open imply the existence of a simplex T such that $T \subseteq \overline{\omega_\ell(z)} \cap \overline{\omega_\ell(w)}$ and therefore $z, w \in \mathcal{V}_\ell \cap T$. The Definition 3.6 of n-patches yields $\omega_\ell(z) \subseteq \omega_\ell^2(w)$ and $\omega_\ell(w) \subseteq \omega_\ell^2(z)$, which concludes the proof. □

Lemma 5.3 (Patch ancestor)**.** *Let $\ell \in \{0,\dots,L\}$ and $z \in \mathcal{V}_\ell$. Then, there exists a vertex $z_0 \in \mathcal{V}_0$ such that $\omega_\ell(z) \subseteq \omega_0(z_0)$.*

Proof. We will treat $d = 2$ and $d = 3$ separately.
Step 1: Let $d = 2$. Every $T \in \mathcal{T}_\ell(z)$ has a unique ancestor $T' \in \mathcal{T}_0$ such that $T \subseteq T'$. We distinguish between three cases:
Case 1: All elements in the patch have the same ancestors, i.e., $\omega_\ell(z) \subseteq T'$. We can choose any vertex of T' as z_0.
Case 2: Suppose there are exactly two distinct ancestor simplices T'_1 and T'_2 such that

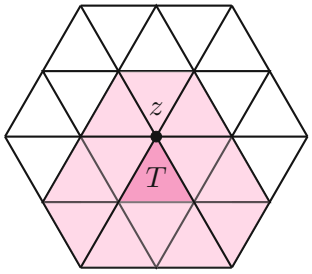

Figure 5.1: Illustration of the two-patch of z and the element-patch of T colored in pink.

$\omega_\ell(z) \subseteq T_1' \cup T_2'$. Then, there exists two elements $T_1, T_2 \in \mathcal{T}_\ell(z)$ with $T_1 \subseteq T_1'$ and $T_2 \subseteq T_2'$ such that $T_1 \cap T_2$ is an edge. Hence, T_1' and T_2' also share an edge. Both vertices of this coarse edge can be picked as z_0.
Case 3: Assume there are $n \geq 3$ ancestors $T_1', \dots, T_n'$ for the patch. Then, there exists $T_1, \dots, T_n \in \mathcal{T}_\ell(z)$ with $T_1 \subseteq T_1', \dots, T_n \subseteq T_n'$. Because a triangulation is a partition and $n \geq 3$, the intersection $T_1' \cap \dots \cap T_n'$ can at most contain one vertex. Thus, the observation

$$z \in T_1 \cap \dots \cap T_n \subseteq T_1' \cap \dots \cap T_n'$$

implies $z \in \mathcal{V}_0$ and $\omega_\ell(z) \subseteq \omega_0(z)$.
Step 2: Let us consider $d = 3$. The first two cases follow analogously if we exchange edges with faces. However, the third case needs to be treated differently. It can happen that $T_1' \cap \dots \cap T_n'$ is an edge. In that case, we can choose any of the two vertices contained in the edges as z_0. Lastly, if $T_1' \cap \dots \cap T_n'$ is not an edge, we continue as in Case 3 of Step 1. This concludes the proof. □

Combining Lemma 5.2 and Lemma 5.3 gives us the desired result.

Corollary 5.4 (Ancestor of level-overlapping patches)**.** *Let $\ell, k \in \{0, \dots, L\}$, $z \in \mathcal{V}_\ell$ and $w \in \mathcal{V}_k$ with $|\omega_\ell(z) \cap \omega_k(w)| > 0$. Then, there exists a vertex $w_0 \in \mathcal{T}_0$ such that $\omega_\ell(z) \cup \omega_k(w) \subseteq \omega_0^2(w_0)$.*

Proof. From Lemma 5.3 we get $z_0, w_0 \in \mathcal{V}_0$ such that $\omega_\ell(z) \subseteq \omega_0(z_0)$ and $\omega_k(w) \subseteq \omega_0(w_0)$. Since $|\omega_0(z_0) \cap \omega_0(w_0)| > 0$ according to $\omega_\ell(z) \cap \omega_\ell(w) \subseteq \omega_0(z_0) \cap \omega_0(w_0)$, Lemma 5.2 yields $\omega_\ell(z) \cup \omega_k(w) \subseteq \omega_0^2(z_0) \cap \omega_0^2(w_0)$. This concludes the proof. □

Moreover, we introduce the so-called element-patches.

Definition 5.5. Let $\ell \in \mathbb{N}$ and $T \in \mathcal{T}_\ell$. Then, we define the *element-patch* by

$$\omega_\ell(T) := \operatorname{interior}\Big(\bigcup_{\substack{T' \in \mathcal{T}_\ell(z) \\ z \in T \cap \mathcal{V}_\ell}} T' \Big).$$

For $z \in T$, it follows directly from the definition that $\omega_\ell(T) \subseteq \omega_\ell^2(z)$. In the next lemma, we show that any vertex patch is contained in a vertex patch of the previous level.

Lemma 5.6. *Let $\ell \in \{1, \dots, L\}$. For every $z \in \mathcal{V}_\ell$, there exists a vertex $z' \in \mathcal{V}_{\ell-1}$ such that $\omega_\ell(z) \subseteq \omega_{\ell-1}(z')$ and consequently $\omega_\ell^2(z) \subseteq \omega_{\ell-1}^2(z')$. Furthermore, there exists an element $T \in \mathcal{T}_{\ell-1}$ such that $z, z' \in T$.*

Proof. We need to distinguish between two cases.
Case 1: Suppose $z \in \mathcal{V}_{\ell-1}$. Then, it immediately follows that $\omega_\ell(z) \subseteq \omega_{\ell-1}(z)$ and $z \in T$ for all $T \in \mathcal{T}_{\ell-1}(z)$.
Case 2: Assume $z \notin \mathcal{V}_{\ell-1}$. Due to the used NVB refinement, z has to be the midpoint of an edge of the mesh $\mathcal{T}_{\ell-1}$, i.e., $z \in E := \operatorname{conv}\{z_1, z_2\}$ with $z_1, z_2 \in \mathcal{T}_{\ell-1}$. We can choose z' as either vertex z_1 or z_2. Moreover, there is at least one element $T \in \mathcal{T}_{\ell-1}$ with $E \subset T$ and hence $z, z' \in T$. This concludes the proof. □

For the following result, we define $\widetilde{r}_{\ell,z} := \min_{T \in \mathcal{T}_\ell^2(z)} \operatorname{level}(T)$.

Lemma 5.7. *Let $\ell \in \{1, \dots, L\}$, $z \in \mathcal{V}_\ell$, and $z' \in \mathcal{V}_{\ell-1}$ given by Lemma 5.6 yielding $\omega_\ell^2(z) \subseteq \omega_{\ell-1}^2(z')$. Then, there exists $C_1, k \in \mathbb{N}$ depending only on the initial mesh $\mathcal{T}_0$ and uniform γ-shape regularity such that $g_{\ell,z} \leq \widetilde{r}_{\ell-1,z'} + C_1$ and $\omega_{\ell-1}^2(z') \subseteq \widehat{\omega}_{g_{\ell,z}}^k(z)$, with $g_{\ell,z}$ defined in* (4.24).

Proof. **Step 1:** Let $z \in \mathcal{V}_\ell$ and the associated $z' \in \mathcal{V}_{\ell-1}$. Then, there exists an element $T \in \mathcal{T}_\ell(z)$ such that $g_{\ell,z} = \operatorname{level}(T)$. Furthermore, there is an element $T' \in \mathcal{T}_{\ell-1}^2(z')$ so that $\widetilde{r}_{\ell-1,z'} = \operatorname{level}(T')$. Since we can find a triangle $T'' \in \mathcal{T}_{\ell-1}(z')$ with $T \subseteq T''$ and $|T| \simeq |T''|$ and since all triangles in $\mathcal{T}_{\ell-1}^2(z')$ have comparable size, we have $|T| \simeq |T'|$ with hidden constants that depend only on γ-shape regularity. Let $T_0, T_0' \in \mathcal{T}_0$ denote the ancestors of T and T' respectively. Then, there exists a constant $C > 0$ that depends only on the initial mesh and γ-shape regularity such that

$$\operatorname{level}(T) = \log_2\Big(\frac{|T_0|}{|T|}\Big) \leq \log_2\Big(C\frac{|T_0'|}{|T'|}\Big) = \log_2(C) + \operatorname{level}(T').$$

For $C_1 := \lceil \log_2(C) \rceil$, we get $g_{\ell,z} \leq \widetilde{r}_{\ell-1,z'} + C_1$.
Step 2: From Lemma 5.6, we know that z and z' lie in a shared element $T \in \mathcal{T}_{\ell-1}(z')$, i.e., $z, z' \in T$. Moreover, there is a triangle $\widetilde{T} \in \widehat{\mathcal{T}}_{\widetilde{r}_{\ell-1,z'}}$ with $z, z' \in T \subseteq \widetilde{T}$. Thus, it holds that $z' \in \widetilde{T}$ and by the definition of $\widetilde{r}_{\ell-1,z'}$ also $\omega_{\ell-1}^2(z') \subseteq \widehat{\omega}_{\widetilde{r}_{\ell-1,z'}}^2(\widetilde{T})$. Furthermore, we can decompose any element $T' \in \widehat{\mathcal{T}}_{\widetilde{r}_{\ell-1,z'}}$ into elements $T_j' \in \widehat{\mathcal{T}}_{\widetilde{r}_{\ell-1,z'}+C_1}$ with $j = 1, \dots, 2^{C_1}$, i.e., $T' = \bigcup_{j=1}^{2^{C_1}} T_j'$. In particular, this holds for $\widetilde{T}$. Since $z \in \widetilde{T}$, we get $\widetilde{T} \subseteq \widehat{\omega}^{2^{C_1}}_{\widetilde{r}_{\ell-1,z'}+C_1}(z)$. Hence, there exists an integer $k \in \mathbb{N}$ with $k \leq 2^{C_1+2}$ such that $\widehat{\omega}^2_{\widetilde{r}_{\ell-1,z'}}(\widetilde{T}) \subseteq \widehat{\omega}^k_{\widetilde{r}_{\ell-1,z'}+C_1}(z)$. Finally, Step 1 yields

$$\omega_{\ell-1}^2(z') \subseteq \widehat{\omega}^2_{\widetilde{r}_{\ell-1,z'}}(\widetilde{T}) \subseteq \widehat{\omega}^k_{\widetilde{r}_{\ell-1,z'}+C_1}(z) \subseteq \widehat{\omega}^k_{g_{\ell,z}}(z).$$

This concludes the proof. □

5.2 Strengthened Cauchy–Schwarz inequality

With the results from the previous section, we can improve the constant $\widehat{C}_{\mathrm{SCS}}$ in Lemma 4.11 and subsequently also the constant C_{SCS} in Proposition 4.12. Let $\mathcal{T} \in \mathbb{T}$ be a refinement of the initial mesh $\mathcal{T}_0$ and $\mathcal{M} \subseteq \mathcal{T}$. For $\omega := \operatorname{interior}\big(\bigcup_{T\in\mathcal{M}} T\big)$, we define

$$C[\omega] := \max\{\max_{T\in\mathcal{M}} \|\operatorname{div}(\mathbf{K})\|_{L^\infty(T)}, \sup_{y\in\omega} \lambda_{\max}(\mathbf{K}(y))\}. \tag{5.8}$$

Lemma 5.8 (Strengthened Cauchy–Schwarz inequality on nested uniform meshes with a local diffusion-contrast dependence)**.** *Let $0 \le i \le j$, $\widehat{u}_i \in \widehat{\mathcal{X}}^1_i$, and $\widehat{v}_j \in \widehat{\mathcal{X}}^1_j$. Consider a subset $\widehat{\mathcal{M}}_i \subseteq \widehat{\mathcal{T}}_i$ and denote $\widehat{\omega}_i := \operatorname{interior}\big(\bigcup_{T\in\widehat{\mathcal{M}}_i} T\big)$. Then, it holds that*

$$\langle\!\langle \widehat{u}_i, \widehat{v}_j \rangle\!\rangle_{\widehat{\omega}_i} \le \widehat{C}'_{\mathrm{SCS}} C[\widehat{\omega}_i]\, \delta^{j-i} \widehat{h}_j^{-1} \|\nabla \widehat{u}_i\|_{\widehat{\omega}_i} \|\widehat{v}_j\|_{\widehat{\omega}_i}, \tag{5.9}$$

where $\delta = 2^{-1/(2d)}$. The constant $\widehat{C}'_{\mathrm{SCS}} > 0$ depends only on the domain Ω, the space dimension d, the initial triangulation $\mathcal{T}_0$, the γ-shape regularity from (2.15), and the quasi-uniformity constant C_{qu} from (4.23).

Proof. Let us start from the left-hand side of (5.9) and split the integral over $\widehat{\omega}_i$ into its elementwise components. Moreover, we use integration by parts, the product rule, and that $\widehat{u}_i|_T$ is an affine function on every element $T \in \widehat{\mathcal{M}}_i$ to obtain

$$\langle\!\langle \widehat{u}_i, \widehat{v}_j \rangle\!\rangle_{\widehat{\omega}_i} = \sum_{T\in\widehat{\mathcal{M}}_i} \Big(-\int_T \operatorname{div}(\mathbf{K}) \cdot \nabla \widehat{u}_i\, \widehat{v}_j\, dx + \int_{\partial T} \mathbf{K} \nabla \widehat{u}_i \cdot \mathbf{n}\, \widehat{v}_j\, dx \Big).$$

We use the eigenvalue identity (2.7) to estimate the boundary integral. Moreover, the Cauchy–Schwarz inequality and the assumption $\mathbf{K}|_T \in [W^{1,\infty}(T)]^{d\times d}$ for all $T \in \widehat{\mathcal{T}}_0$ yield

$$\begin{aligned}
\langle\!\langle \widehat{u}_i, \widehat{v}_j \rangle\!\rangle_{\widehat{\omega}_i} &\le \sum_{T\in\widehat{\mathcal{M}}_i} \max_{T\subseteq\overline{\widehat{\omega}_i}} \|\operatorname{div}\mathbf{K}\|_{L^\infty(T)} \|\nabla\widehat{u}_i\|_{L^2(T)} \|\widehat{v}_j\|_{L^2(T)} \\
&\quad + \sum_{T\in\widehat{\mathcal{M}}_i} \sup_{y\in\widehat{\omega}_i} \lambda_{\max}(\mathbf{K}(y)) \|\nabla\widehat{u}_i\|_{L^2(\partial T)} \|\widehat{v}_j\|_{L^2(\partial T)} \\
&\le C[\widehat{\omega}_i] \sum_{T\in\widehat{\mathcal{M}}_i} \Big(\|\nabla\widehat{u}_i\|_{L^2(T)} \|\widehat{v}_j\|_{L^2(T)} + \|\nabla\widehat{u}_i\|_{L^2(\partial T)} \|\widehat{v}_j\|_{L^2(\partial T)} \Big).
\end{aligned}$$

Following the steps from the proof of Lemma 4.11, we conclude the proof. □

Proposition 5.9 (Strengthened Cauchy–Schwarz inequality on nested adaptive meshes with a local diffusion-contrast dependence)**.** *For all $\ell \in \{1,\dots,L-1\}$ and $k \in \{1,\dots,\ell-1\}$, consider levelwise functions $v_\ell = \sum_{z\in\mathcal{V}^+_\ell} v^1_{\ell,z} \in \mathcal{X}^1_\ell$ and $u_k = \sum_{w\in\mathcal{V}^+_k} u^1_{k,w} \in \mathcal{X}^1_k$ with $v^1_{\ell,z} \in \mathcal{X}^1_{\ell,z}$ and $u^1_{k,w} \in \mathcal{X}^1_{k,w}$. Then, it holds that*

$$\sum_{\ell=1}^{L-1} \sum_{k=1}^{\ell-1} \langle\!\langle u_k, v_\ell \rangle\!\rangle \le C'_{\mathrm{SCS}} C^{(1)}_{\mathrm{loc}} \Big(\sum_{k=1}^{L-2} \sum_{w\in\mathcal{V}^+_k} |\!|\!| u^1_{k,w} |\!|\!|^2 \Big)^{1/2} \Big(\sum_{\ell=1}^{L-1} \sum_{z\in\mathcal{V}^+_\ell} |\!|\!| v^1_{\ell,z} |\!|\!|^2 \Big)^{1/2}, \tag{5.10}$$

where the constant $C_{\mathrm{loc}}^{(1)}$ *is defined in* (5.5) *and the constant* $C'_{\mathrm{SCS}} > 0$ *depends only on* Ω, *the initial triangulation* $\mathcal{T}_0$, γ*-shape regularity* (2.15), *and the quasi-uniformity constant* C_{qu} *from* (4.23).

Proof. Let $M = \max_{z\in\mathcal{V}_L} g_{L,z}$ be the maximal generation. We recall the representation (4.37) of S_1 in Step 5 of the proof of Proposition 4.12, namely

$$S_1 = \sum_{j=0}^{M}\sum_{i=j}^{M}\sum_{\ell=1}^{L-1}\sum_{\substack{z\in\mathcal{V}_\ell^+\\ g_{\ell,z}=j}} \Big\langle\!\Big\langle \sum_{w\in\widehat{\mathcal{V}}_i}\sum_{k\in\mathscr{L}_{1,\ell-1}^{(1)}(w,i)} u_{k,w}^1, v_{\ell,z}^1\Big\rangle\!\Big\rangle_{\omega_\ell(z)}.$$

Because $j \le i$, we can use the strengthened Cauchy–Schwarz inequality on uniform meshes (5.9) to obtain

$$S_1 \le \widehat{C}_{\mathrm{SCS}} \sum_{j=0}^{M}\sum_{i=j}^{M}\delta^{i-j}\sum_{\ell=1}^{L-1}\sum_{\substack{z\in\mathcal{V}_\ell^+\\ g_{\ell,z}=j}} C[\omega_\ell(z)]\,\widehat{h}_i^{-1}\Big\| \sum_{w\in\widehat{\mathcal{V}}_i}\sum_{k\in\mathscr{L}_{1,\ell-1}^{(1)}(w,i)} u_{k,w}^1\Big\|_{\omega_\ell(z)} \|\nabla v_{\ell,z}^1\|_{\omega_\ell(z)}.$$

By applying (4.39) for $\omega = \omega_\ell(z)$ and employing the discrete Cauchy–Schwarz inequality, we get

$$\begin{aligned}
S_1 &\lesssim \sum_{j=0}^{M}\sum_{i=j}^{M}\delta^{i-j}\sum_{\ell=1}^{L-1}\sum_{\substack{z\in\mathcal{V}_\ell^+\\ g_{\ell,z}=j}} \widehat{h}_i^{-1} C[\omega_\ell(z)]^{1/2}\Big(\sum_{k=1}^{L-2}\sum_{\substack{w\in\mathcal{V}_k^+\\ g_{k,w}=i}} \|u_{k,w}^1\|_{\omega_\ell(z)}^2\Big)^{1/2} C[\omega_\ell(z)]^{1/2}\|\nabla v_{\ell,z}^1\|_{\omega_\ell(z)}\\
&\lesssim \sum_{j=0}^{M}\sum_{i=j}^{M}\delta^{i-j}\Big(\sum_{\ell=1}^{L-1}\sum_{\substack{z\in\mathcal{V}_\ell^+\\ g_{\ell,z}=j}} C[\omega_\ell(z)]\|\nabla v_{\ell,z}^1\|_{\omega_\ell(z)}^2\Big)^{1/2}\\
&\qquad\qquad \times\Big(\widehat{h}_i^{-2}\sum_{\ell=1}^{L-1}\sum_{\substack{z\in\mathcal{V}_\ell^+\\ g_{\ell,z}=j}}\sum_{k=1}^{L-2}\sum_{\substack{w\in\mathcal{V}_k^+\\ g_{k,w}=i}} C[\omega_\ell(z)]\|u_{k,w}^1\|_{\omega_\ell(z)}^2\Big)^{1/2}.
\end{aligned}$$

Let us focus on the term $C[\omega_\ell(z)]\|u_{k,w}^1\|_{\omega_\ell(z)}^2$. Since $u_{k,w}^1 \in \mathcal{X}_{k,w}^1$, the norm $\|u_{k,w}^1\|_{\omega_\ell(z)}^2$ only has a positive value if $|\omega_\ell(z)\cap\omega_k(w)| > 0$. Therefore, Corollary 5.4 yields the existence of a vertex $w_0 \in \mathcal{V}_0$ independent of ℓ and z such that $\omega_\ell(z)\cup\omega_k(w) \subseteq \omega_0^2(w_0)$. Thus, we have

$$C[\omega_\ell(z)]\|u_{k,w}^1\|_{\omega_\ell(z)}^2 \le \max\Big\{\max_{T\subseteq\overline{\omega_0^2(w_0)}}\|\operatorname{div}\mathbf{K}\|_{L^\infty(T)}, \sup_{y\in\omega_0^2(w_0)}\lambda_{\max}(\mathbf{K}(y))\Big\}\|u_{k,w}^1\|_{\omega_\ell(z)}^2.$$

As previously established in (4.41), there holds

$$\begin{aligned}
&\sum_{\ell=1}^{L-1}\sum_{\substack{z\in\mathcal{V}_\ell^+\\ g_{\ell,z}=j}} C[\omega_\ell(z)]\|u_{k,w}^1\|_{\omega_\ell(z)}^2\\
&\qquad \le C_{\mathrm{patch}}C_{\mathrm{lev}}^{(1)}\max\Big\{\max_{T\subseteq\overline{\omega_0^2(w_0)}}\|\operatorname{div}\mathbf{K}\|_{L^\infty(T)}, \sup_{y\in\omega_0^2(w_0)}\lambda_{\max}(\mathbf{K}(y))\Big\}\|u_{k,w}^1\|^2.
\end{aligned}$$

Moreover, we use the equivalence of mesh sizes from (4.35), a Poincaré inequality on the patch $\omega_k(w)$, and the norm equivalence (2.6) to prove

$$\begin{aligned}
C[\omega_0^2(w_0)]\widehat{h}_i^{-2}\|u_{k,w}^1\|^2 &\overset{(4.35)}{\leq} C[\omega_0^2(w_0)]C_{\mathrm{eq}}^2 h_{k,w}^{-2}\|u_{k,w}^1\|^2 \leq C[\omega_0^2(w_0)]C_{\mathrm{eq}}^2 C_{\mathrm{P}}^2\|\nabla u_{k,w}^1\|^2 \\
&\overset{(2.6)}{\leq} C[\omega_0^2(w_0)]C_{\mathrm{eq}}^2 C_{\mathrm{P}}^2 \frac{1}{\inf_{y\in\omega_k(w)}\lambda_{\min}(\mathbf{K}(y))}\|\!|u_{k,w}^1|\!\|^2 \\
&\leq C[\omega_0^2(w_0)]C_{\mathrm{eq}}^2 C_{\mathrm{P}}^2 \frac{1}{\inf_{y\in\omega_0^2(w_0)}\lambda_{\min}(\mathbf{K}(y))}\|\!|u_{k,w}^1|\!\|^2 \\
&= C_{\mathrm{eq}}^2 C_{\mathrm{P}}^2 \max\left\{\frac{\max_{T\subseteq\overline{\omega_0^2(w_0)}}\|\operatorname{div}\mathbf{K}\|_{L^\infty(T)}}{\inf_{y\in\omega_0^2(w_0)}\lambda_{\min}(\mathbf{K}(y))}, \frac{\sup_{y\in\omega_0^2(w_0)}\lambda_{\max}(\mathbf{K}(y))}{\inf_{y\in\omega_0^2(w_0)}\lambda_{\min}(\mathbf{K}(y))}\right\}\|\!|u_{k,w}^1|\!\|^2
\end{aligned}$$

For every $\ell\in\{1,\dots,L-1\}$ and $z\in\mathcal{V}_\ell$, Lemma 5.3 yields a vertex $z_0\in\mathcal{V}_0$ such that $\omega_\ell(z)\subseteq\omega_0(z_0)\subseteq\omega_0^2(z_0)$. We use this and the norm equivalence (2.6) to obtain

$$\begin{aligned}
C[\omega_\ell(z)]\|\nabla v_{\ell,z}^1\|_{\omega_\ell(z)}^2 &\overset{(2.6)}{\leq} C[\omega_\ell(z)]\frac{1}{\inf_{y\in\omega_\ell(z)}\lambda_{\min}(\mathbf{K}(y))}\|\!|v_{\ell,z}^1|\!\|^2 \\
&\leq \max\left\{\frac{\max_{T\subseteq\overline{\omega_0^2(z_0)}}\|\operatorname{div}\mathbf{K}\|_{L^\infty(T)}}{\inf_{y\in\omega_0^2(z_0)}\lambda_{\min}(\mathbf{K}(y))}, \frac{\sup_{y\in\omega_0^2(z_0)}\lambda_{\max}(\mathbf{K}(y))}{\inf_{y\in\omega_0^2(z_0)}\lambda_{\min}(\mathbf{K}(y))}\right\}\|\!|v_{\ell,z}^1|\!\|^2.
\end{aligned}$$

Taking the supremum over all vertices of the initial mesh and applying the geometric series bound (4.29) finally yields

$$\begin{aligned}
S_1 &\lesssim C_{\mathrm{loc}}^{(1)}\sum_{j=0}^{M}\sum_{i=j}^{M}\delta^{i-j}\Big(\sum_{\ell=1}^{L-1}\sum_{\substack{z\in\mathcal{V}_\ell^+\\ g_{\ell,z}=j}}\|\!|v_{\ell,z}^1|\!\|^2\Big)^{1/2}\Big(\sum_{k=1}^{L-2}\sum_{\substack{w\in\mathcal{V}_k^+\\ g_{k,w}=i}}\|\!|u_{k,w}^1|\!\|^2\Big)^{1/2} \\
&\overset{(4.29)}{\lesssim} C_{\mathrm{loc}}^{(1)}\Big(\sum_{j=1}^{M}\sum_{\ell=1}^{L-1}\sum_{\substack{z\in\mathcal{V}_\ell^+\\ g_{\ell,z}=j}}\|\!|v_{\ell,z}^1|\!\|^2\Big)^{1/2}\Big(\sum_{i=1}^{M}\sum_{k=1}^{L-2}\sum_{\substack{w\in\mathcal{V}_k^+\\ g_{k,w}=i}}\|\!|u_{k,w}^1|\!\|^2\Big)^{1/2} \\
&= C_{\mathrm{SCS}}C_{\mathrm{loc}}^{(1)}\Big(\sum_{\ell=1}^{L-1}\sum_{z\in\mathcal{V}_\ell^+}\|\!|v_{\ell,z}^1|\!\|^2\Big)^{1/2}\Big(\sum_{k=1}^{L-2}\sum_{w\in\mathcal{V}_k^+}\|\!|u_{k,w}^1|\!\|^2\Big)^{1/2}.
\end{aligned}$$

This concludes the proof with

$$C_{\mathrm{SCS}} := \widehat{C}'_{\mathrm{SCS}}C_{\mathrm{eq}}C_{\mathrm{P}}(1-\delta)^{-1}\big((d+1)C_{\mathrm{lev}}^{(2)}C_{\mathrm{patch}}C_{\mathrm{lev}}^{(1)}\big)^{1/2}.$$

□

5.3 Multilevel h-robust decomposition

The goal of this section is to show stability of the decomposition (4.10) from Lemma 4.4 in the energy norm such that the constant C_{ML} in (4.11) with $\|\nabla\cdot\|$ being replaced by $\|\!|\cdot|\!\|$ depends only locally on the contrast factor of the diffusion coefficient.

5.3.1 Challenges

The proof of Lemma 4.4 relies on [WZ17, Lemma 3.7] which in turn uses H^1-stability of the L^2-projection. Therefore, we present the proof of [WZ17, Lemma 3.7] to explain the challenges of extending the result to the energy norm with only local dependence on the diffusion coefficient.

Proposition 5.10 ([WZ17, Lemma 3.7])**.** *Let Π_ℓ be the averaging operator from Definition 4.3. Then, it holds that*

$$\sum_{\ell=1}^{L} \sum_{z\in\mathcal{V}_\ell^+} h_{\ell,z}^{-2} \|(\Pi_\ell - \Pi_{\ell-1})v\|_{\omega_\ell(z)}^2 \leq C_{\mathrm{SA}}^2 \|\nabla v\|^2 \quad \text{for all } v \in H_0^1(\Omega), \tag{5.11}$$

where the constant $C_{\mathrm{SA}} > 0$ depends only on the space dimension d and γ-shape regularity (2.15)*.*

In [WZ17, Lemma 3.4], local L^2-stability of Π_ℓ is shown. However, note that (5.11) leads us to estimate terms of the type $\|\Pi_{\ell-1}v\|_T^2$ for triangles $T \in \mathcal{T}_\ell$ and any function $v \in H_0^1(\Omega)$. Thus, we first introduce an auxiliary result.

Lemma 5.11 (Estimates on different levels)**.** *For $\ell \in \{1,\dots,L\}$ and $z \in \mathcal{V}_\ell$ let $z' \in \mathcal{V}_{\ell-1}$ be the vertex provided by Lemma 5.6. Then, it holds that*

$$\|\Pi_{\ell-1}v\|_{\omega_\ell(z)}^2 \lesssim \|v\|_{\omega_{\ell-1}^2(z')}^2. \tag{5.12}$$

Proof. Let $T \in \mathcal{T}_{\ell,z}$ and let $T' \in \mathcal{T}_{\ell-1}$ denote its ancestor. We get

$$\|\Pi_{\ell-1}v\|_T^2 \leq \|\Pi_{\ell-1}v\|_{T'}^2 \lesssim \|v\|_{\omega_{\ell-1}(T')}^2.$$

The vertex $z' \in \mathcal{V}_{\ell-1}$ allows to satisfy $\omega_\ell(z) \subseteq \omega_{\ell-1}(z')$. Thus, we can use finite patch overlap to obtain

$$\begin{aligned}\|\Pi_{\ell-1}v\|_{\omega_\ell(z)}^2 &= \sum_{T\in\mathcal{T}_\ell(z)} \|\Pi_{\ell-1}v\|_T^2 \leq \sum_{T'\in\mathcal{T}_{\ell-1}(z')} \|\Pi_{\ell-1}v\|_{T'}^2 \\ &\lesssim \sum_{T'\in\mathcal{T}_{\ell-1}(z')} \|v\|_{\omega_{\ell-1}(T')} \lesssim \|v\|_{\omega_{\ell-1}^2(z')}^2\end{aligned}$$

This concludes the proof. □

Proof of Proposition 5.10. We present the proof for completeness. Let $v \in H_0^1(\Omega)$. For $m \in \mathbb{N}$, we denote by $\widehat{Q}_m$ the $L^2(\Omega)$-projection onto $\widehat{\mathcal{X}}_m^1$. Let $\widehat{Q}_m := \widehat{Q}_0$ for $m < 0$. Let $\ell \in \{1,\dots,L\}$, $z \in \mathcal{V}_\ell^+$, and $z' = z'[z]$ from Lemma 5.6. From Lemma 5.7, we get

$$\widehat{Q}_{g_{\ell,z}-C_1}v \in \widehat{\mathcal{X}}_{r_{\ell-1,z'}}^1$$

and therefore that $(\widehat{Q}_{g_{\ell,z}-C_1}v)|_T$ is linear for every $T \in \mathcal{T}_{\ell-1}^2(z')$. Moreover, Lemma 5.6 also yields that $(\widehat{Q}_{g_{\ell,z}-C_1}v)|_T$ is linear for every $T \in \mathcal{T}_\ell^2(z)$. This implies

$$(\widehat{Q}_{g_{\ell,z}-C_1}v)|_{\omega_\ell(z)} = (\Pi_\ell\widehat{Q}_{g_{\ell,z}-C_1}v)|_{\omega_\ell(z)} = (\Pi_{\ell-1}\widehat{Q}_{g_{\ell,z}-C_1}v)|_{\omega_\ell(z)}. \tag{5.13}$$

We use Lemma 5.11 to obtain

$$\begin{aligned}
&\sum_{\ell=1}^{L}\sum_{z\in\mathcal{V}_\ell^+} h_{\ell,z}^{-2}\|(\Pi_\ell-\Pi_{\ell-1})v\|^2_{\omega_\ell(z)}\\
&\quad\overset{(5.13)}{=}\sum_{\ell=1}^{L}\sum_{z\in\mathcal{V}_\ell^+} h_{\ell,z}^{-2}\|\Pi_\ell(v-\widehat{Q}_{g_{\ell,z}-C_1}v)-\Pi_{\ell-1}(v-\widehat{Q}_{g_{\ell,z}-C_1}v)\|^2_{\omega_\ell(z)}\\
&\quad\lesssim\sum_{\ell=1}^{L}\sum_{z\in\mathcal{V}_\ell^+} h_{\ell,z}^{-2}\big(\|\Pi_\ell(v-\widehat{Q}_{g_{\ell,z}-C_1}v)\|^2_{\omega_\ell(z)}+\|\Pi_{\ell-1}(v-\widehat{Q}_{g_{\ell,z}-C_1}v)\|^2_{\omega_\ell(z)}\big)\\
&\quad\overset{(5.12)}{\lesssim}\sum_{\ell=1}^{L}\sum_{z\in\mathcal{V}_\ell^+} h_{\ell,z}^{-2}\|v-\widehat{Q}_{g_{\ell,z}-C_1}v\|^2_{\omega^2_{\ell-1}(z'[z])}.
\end{aligned}$$

Changing the summation order using the generations and applying Lemma 5.7, we see

$$\begin{aligned}
\sum_{\ell=1}^{L}\sum_{z\in\mathcal{V}_\ell^+} h_{\ell,z}^{-2}\|(\Pi_\ell-\Pi_{\ell-1})v\|^2_{\omega_\ell(z)} &\lesssim \sum_{\ell=1}^{L}\sum_{z\in\mathcal{V}_\ell^+} h_{\ell,z}^{-2}\|v-\widehat{Q}_{g_{\ell,z}-C_1}v\|^2_{\omega^2_{\ell-1}(z'[z])}\\
&\overset{\widehat{h}_m\simeq h_{\ell,z}}{\simeq}\sum_{m=0}^{\infty}\sum_{\ell=1}^{L}\sum_{\substack{z\in\mathcal{V}_\ell^+\\ g_{\ell,z}=m}}\widehat{h}_m^{-2}\|v-\widehat{Q}_{m-C_1}v\|^2_{\omega^2_{\ell-1}(z'[z])}\\
&\le\sum_{m=0}^{\infty}\sum_{\ell=1}^{L}\sum_{\substack{z\in\mathcal{V}_\ell^+\\ g_{\ell,z}=m}}\widehat{h}_m^{-2}\|v-\widehat{Q}_{m-C_1}v\|^2_{\widehat{\omega}^k_m(z)}.
\end{aligned}$$

We rewrite the sums using (4.30), exploit the uniform bound (4.32), and apply finite patch overlap to establish

$$\begin{aligned}
\sum_{\ell=1}^{L}\sum_{z\in\mathcal{V}_\ell^+} h_{\ell,z}^{-2}\|(\Pi_\ell-\Pi_{\ell-1})v\|^2_{\omega_\ell(z)} &\lesssim \sum_{m=0}^{\infty}\sum_{z\in\widehat{\mathcal{V}}_m}\sum_{\ell\in\mathscr{L}^{(1)}_{1,L}(z,m)}\widehat{h}_m^{-2}\|v-\widehat{Q}_{m-C_1}v\|^2_{\widehat{\omega}^k_m(z)}\\
&\overset{(4.32)}{\lesssim}\sum_{m=0}^{\infty}\sum_{z\in\widehat{\mathcal{V}}_m}\widehat{h}_m^{-2}\|v-\widehat{Q}_{m-C_1}v\|^2_{\widehat{\omega}^k_m(z)}\\
&\lesssim\sum_{m=0}^{\infty}\widehat{h}_m^{-2}\|v-\widehat{Q}_{m-C_1}v\|^2.
\end{aligned}$$

Recalling $2^{N/d}\widehat{h}_{m+N} = \widehat{h}_m$ for any $N \geq 0$ and $\widehat{Q}_m = \widehat{Q}_0$ for $m < 0$ leads to

$$\begin{aligned}\sum_{m=0}^{\infty} \widehat{h}_m^{-2}\|v - \widehat{Q}_{m-C_1}v\|^2 &= \|v - \widehat{Q}_0 v\|^2 \sum_{m=0}^{C_1-1} \widehat{h}_m^{-2} + \sum_{m=0}^{\infty} \widehat{h}_{m+C_1}^{-2}\|v - \widehat{Q}_m v\|^2 \\ &\leq \widehat{h}_0^{-2}\|v - \widehat{Q}_0 v\|^2 \sum_{m=0}^{\infty} 2^{-2m/d} + 4^{C_1/d} \sum_{m=0}^{\infty} \widehat{h}_m^{-2}\|v - \widehat{Q}_m v\|^2 \qquad (5.14) \\ &\leq \left((1 - 4^{-1/d})^{-1} + 4^{C_1/d}\right) \sum_{m=0}^{\infty} \widehat{h}_m^{-2}\|v - \widehat{Q}_m v\|^2.\end{aligned}$$

Finally, the stability of the multilevel decomposition for the L^2-projection gives

$$\sum_{\ell=1}^{L} \sum_{z \in \mathcal{V}_\ell^+} h_{\ell,z}^{-2}\|(\Pi_\ell - \Pi_{\ell-1})v\|_{\omega_\ell(z)}^2 \lesssim \sum_{m=0}^{\infty} \widehat{h}_m^{-2}\|v - \widehat{Q}_m v\|^2 \lesssim \|\nabla u\|^2$$

A proof for the last estimate can be found in [Xu97, Theorem 4.31]. □

Remark 5.12 (Energy norm estimates)**.** *The challenge with the approach of Proposition 5.10 is that the result does not transfer immediately to the energy norm. To keep local dependencies on the diffusion coefficient, we need to change to the energy norm while the estimates are still local (on patches). Doing so would result in the sought stability*

$$\sum_{\ell=0}^{L} \sum_{z \in \mathcal{V}_\ell^+} |\!|\!| v_{\ell,z} |\!|\!|^2 \lesssim \sum_{m=0}^{\infty} |\!|\!| v_L^1 - \widehat{Q}_m v_L^1 |\!|\!|^2, \qquad (5.15)$$

with a constant that depends only locally on the diffusion. Moreover, we have not been able to estimate the right-hand side of (5.15) *(given in the energy norm) with* $|\!|\!| v_L^1 |\!|\!|^2$.

Remark 5.13 (Different choices of averaging operators)**.** *In [FFP+17] the same strategy as in the proof of Proposition 5.10 is used to show stability of a multilevel decomposition. The biggest difference is that the Scott–Zhang projection* J_ℓ *is utilized instead of the operator* Π_ℓ*. We want to underline that the estimate*

$$\sum_{m=0}^{\infty} \widehat{h}_m^{-2}\|v - \widehat{Q}_m v\|^2 \lesssim \|\nabla v\|^2 \quad \text{for all } v \in H_0^1(\Omega) \qquad (5.16)$$

is the crucial step in both [WZ17] and [FFP+17]. Furthermore, a similar estimate

$$\sum_{m=0}^{\infty} \widehat{h}_m^{-2}\|(\widehat{Q}_m - \widehat{Q}_{m-1})v\|^2 \lesssim \|\nabla v\|^2 \quad \text{for all } v \in H_0^1(\Omega)$$

is used in [CNX12] to show a localized stable lowest-order multilevel decomposition.

5.3.2 Useful concepts

To overcome the challenges mentioned in the previous section, we introduce some useful concepts, namely the so-called K-functional, a weighted $L^2(\Omega)$-scalar product, and extension operators on Sobolev spaces.

Definition 5.14 (K-functional)**.** For any Lipschitz domain $\omega \subseteq \mathbb{R}^d$, $u \in L^2(\omega)$ and $t > 0$ we define the K-functional by

$$K(t, u, \omega) := \inf_{v \in H^2(\omega)} \big(\|u - v\|_\omega^2 + t^2 |v|_{H^2(\omega)}^2 \big)^{1/2}.$$

Definition 5.15 (Weighted L^2-norm)**.** Let the diffusion coefficient $\mathbf{K}$ be given. For every $T_0 \in \mathcal{T}_0$, we define the *weights*

$$\mathbf{k}_{T_0} := \min_{y \in \omega_0(T_0)} \lambda_{\min}(\mathbf{K}(y)). \tag{5.17}$$

The *weighted $L^2(\Omega)$-scalar product* is given by

$$\langle u, v \rangle_{\mathbf{K}} := \sum_{T_0 \in \mathcal{T}_0} \mathbf{k}_{T_0} \int_{T_0} uv \, dx \quad \text{for all } u, v \in L^2(\Omega).$$

Furthermore, the corresponding norm is

$$\|u\|_{\mathbf{K}}^2 := \sum_{T_0 \in \mathcal{T}_0} \mathbf{k}_{T_0} \, \|u\|_{T_0}^2 \quad \text{for all } u \in L^2(\Omega). \tag{5.18}$$

For $m \geq 0$, let us denote by $\widehat{Q}_{m,\mathbf{K}} : L^2(\Omega) \to \widehat{\mathcal{X}}_m^1$ the projections for the weighted scalar product, i.e., it holds that

$$\langle \widehat{Q}_{m,\mathbf{K}} u, v \rangle_{\mathbf{K}} = \langle u, v \rangle_{\mathbf{K}} \quad \text{for all } v \in \widehat{\mathcal{X}}_m^1. \tag{5.19}$$

The following observations will be useful for the main theorem.

Lemma 5.16 (K-functional for extended functions)**.** *Let $\omega_2 \subseteq \omega_1 \subseteq \mathbb{R}^d$ be two nested and bounded Lipschitz domains. Then, it holds that*

$$\inf_{v \in H^2(\omega_1)} \big(\|u - v\|_{\omega_2}^2 + t^2 |v|_{H^2(\omega_2)}^2 \big) = K(t, u, \omega_2)^2. \tag{5.20}$$

Moreover, for a Lipschitz domain $\omega \subseteq \mathbb{R}^d$ and any extension operator $R : L^2(\omega) \to L^2(\mathbb{R}^d)$ we have

$$K(t, u, \omega) \leq K(t, Ru, \mathbb{R}^d). \tag{5.21}$$

Proof. **Step 1:** Since $H^2(\omega_1) \subseteq H^2(\omega_2)$, the first inequality follows directly

$$\inf_{v \in H^2(\omega_1)} \big(\|u - v\|_{\omega_2}^2 + t^2 |v|_{H^2(\omega_2)}^2 \big) \geq K(t, u, \omega_2)^2.$$

To show equality, we introduce an extension operator $\widetilde{R} : H^2(\omega_2) \to H^2(\mathbb{R}^d)$, see, e.g., [AF03, Theorem 5.24]. Thus, for every $v \in H^2(\omega_2)$ there exists a function $\widetilde{R}v =: \widetilde{v} \in H^2(\mathbb{R}^d)$, and

in particular $\widetilde{v} \in H^2(\omega_1)$ such that $\widetilde{v}|_{\omega_2} = v$. Hence, we obtain the equality (5.20).
Step 2: The restriction $v|_\omega$ of a function $v \in H^2(\mathbb{R}^2)$ lies in $H^2(\omega)$ and it holds

$$\|u - v|_\omega\|_\omega^2 + t^2|v|_\omega|_{H^2(\omega)}^2 \leq \|Ru - v\|_{\mathbb{R}^2}^2 + t^2|v|_{H^2(\mathbb{R}^2)}^2.$$

Therefore, we get

$$\inf_{v \in H^2(\omega)} \big(\|u - v\|_\omega^2 + t^2|v|_{H^2(\omega)}^2\big) \leq \inf_{v \in H^2(\mathbb{R}^2)} \big(\|Ru - v\|_{\mathbb{R}^2}^2 + t^2|v|_{H^2(\mathbb{R}^2)}^2\big).$$

This concludes the proof. □

Lemma 5.17. *Let $\omega \subseteq \mathbb{R}^d$ be a bounded Lipschitz domain. Then, there exists an extension operator $E_\omega : H^1(\omega) \to H^1(\mathbb{R}^d)$ and a constant $C_\omega \geq 1$ depending only on ω that fulfill*

$$(E_\omega v)|_\omega = v \quad \text{and} \quad \|\nabla E_\omega v\|_{\mathbb{R}^d} \leq C_\omega \|\nabla v\|_\omega \quad \text{for all } v \in H^1(\omega). \tag{5.22}$$

We refer to [Bur99, Theorem 2.2] and [Leo09, Theorem 12.3] for further details.

5.3.3 Improved proofs

We can now present our improved result. With the tools from the last section, stability of the multilevel decomposition for the weighted L^2-projection in the energy norm is shown. Lastly, to obtain the desired stability of the decomposition, we follow the structure of the proof of Proposition 5.10 while keeping the dependency on the diffusion coefficient local.

Proposition 5.18. *For all $u \in H_0^1(\Omega)$, it holds that*

$$\sum_{m=0}^{\infty} \widehat{h}_m^{-2} \|u - \widehat{Q}_{m,\mathbf{K}} u\|_{\mathbf{K}}^2 \leq C_{\mathrm{WP}}^2 |\!|\!| u |\!|\!|^2, \tag{5.23}$$

where the constant constant $C_{\mathrm{WP}} > 0$ depends only on the initial mesh $\mathcal{T}_0$, the space dimension d, and the γ-shape regularity (2.15)

Proof. **Step 1 (Elementwise stability estimates):** Let $u \in H_0^1(\Omega)$. By the definition of $\widehat{Q}_{m,\mathbf{K}}$ (5.19), it follows that

$$\begin{aligned} \|u - \widehat{Q}_{m,\mathbf{K}} u\|_{\mathbf{K}}^2 &= \langle u - \widehat{Q}_{m,\mathbf{K}} u, u - \widehat{Q}_{m,\mathbf{K}} u\rangle_{\mathbf{K}} \overset{(5.19)}{=} \langle u - \widehat{Q}_{m,\mathbf{K}} u, u - v_m\rangle_{\mathbf{K}} \\ &\leq \|u - \widehat{Q}_{m,\mathbf{K}} u\|_{\mathbf{K}} \|u - v_m\|_{\mathbf{K}} \quad \text{for all } v_m \in \widehat{\mathcal{X}}_m^1. \end{aligned} \tag{5.24}$$

Let us denote by $\widehat{P}_m : L^2(\Omega) \to \widehat{\mathcal{X}}_m^1$ the Scott–Zhang projection, which among others possesses the following property: There exists a constant $C > 0$ depending only on the γ-shape regularity such that

$$\|v - \widehat{P}_m v\|_T \leq C h_T^2 |v|_{H^2(\widehat{\omega}_m(T))} \quad \text{for all } T \in \widehat{\mathcal{T}}_m \text{ and all } v \in H^2(\Omega). \tag{5.25}$$

Further details can be found in [BS08, Section 4.8]. We apply (5.24) to $v_m = \widehat{P}_m v$ for any $v \in H^2(\Omega)$. This leads to

$$\|u - \widehat{Q}_{m,\mathbf{K}} u\|_{\mathbf{K}}^2 \leq \|u - \widehat{P}_m v\|_{\mathbf{K}}^2 \lesssim \|u - v\|_{\mathbf{K}}^2 + \|v - \widehat{P}_m v\|_{\mathbf{K}}^2.$$

We use (5.25) and finite patch overlap to obtain

$$\begin{aligned}\|u-\widehat{Q}_{m,\mathbf{K}}u\|_{\mathbf{K}}^2 &\lesssim \sum_{T_0\in\mathcal{T}_0}\mathbf{k}_{T_0}\sum_{\substack{T\in\widehat{\mathcal{T}}_m\\ T\subseteq T_0}}\big(\|u-v\|_T^2+\|v-\widehat{P}_m v\|_T^2\big)\\ &\overset{(5.25)}{\lesssim}\sum_{T_0\in\mathcal{T}_0}\mathbf{k}_{T_0}\sum_{\substack{T\in\widehat{\mathcal{T}}_m\\ T\subseteq T_0}}\Big(\|u-v\|_{\widehat{\omega}_m(T)}^2+\widehat{h}_m^4|v|_{H^2(\widehat{\omega}_m(T))}^2\Big)\\ &\lesssim\sum_{T_0\in\mathcal{T}_0}\mathbf{k}_{T_0}\Big(\|u-v\|_{\omega_0(T_0)}^2+\widehat{h}_m^4|v|_{H^2(\omega_0(T_0))}^2\Big).\end{aligned}$$

Step 2 (Weighted, extended estimates): Since $v\in H^2(\Omega)$ was arbitrary, Lemma 5.16 yields

$$\|u-\widehat{Q}_{m,\mathbf{K}}u\|_{\mathbf{K}}^2\overset{(5.20)}{\lesssim}\sum_{T_0\in\mathcal{T}_0}\mathbf{k}_{T_0}K(\widehat{h}_m^2,u,\omega_0(T_0))^2.$$

Summing over the generations, utilizing the extension operators $E_{\omega_0(T_0)}$, and applying Lemma 5.16 gives us

$$\begin{aligned}\sum_{m=0}^{\infty}\widehat{h}_m^{-2}\|u-\widehat{Q}_{m,\mathbf{K}}u\|_{\mathbf{K}}^2&\lesssim\sum_{m=0}^{\infty}\widehat{h}_m^{-2}\sum_{T_0\in\mathcal{T}_0}\mathbf{k}_{T_0}K(\widehat{h}_m^2,u,\omega_0(T_0))^2\\ &\overset{(5.21)}{\leq}\sum_{m=0}^{\infty}\widehat{h}_m^{-2}\sum_{T_0\in\mathcal{T}_0}\mathbf{k}_{T_0}K(\widehat{h}_m^2,E_{\omega_0(T_0)}u,\mathbb{R}^d)^2\\ &=\sum_{T_0\in\mathcal{T}_0}\mathbf{k}_{T_0}\sum_{m=0}^{\infty}\widehat{h}_m^{-2}K(\widehat{h}_m^2,E_{\omega_0(T_0)}u,\mathbb{R}^d)^2.\end{aligned}\tag{5.26}$$

Step 3 (Summability of K-functional): For $d=2$ and $d=3$, it is shown in [BY93, Lemma 7.3] and [HWZ12, Lemma 4.3] respectively that

$$\sum_{m=0}^{\infty}\widehat{h}_m^{-2}K(\widehat{h}_m^2,v,\mathbb{R}^d)^2\lesssim\|\nabla v\|_{\mathbb{R}^d}^2\quad\text{for all } v\in H^1(\mathbb{R}^d).\tag{5.27}$$

Step 4 (Stability of the extensions): Applying (5.27) to $E_{\omega_0(T_0)}u$, using the stability of the extension (5.22) and exploiting the norm equivalence (2.6) and the definition (5.17) of $\mathbf{k}_{T_0}$, we are led to

$$\begin{aligned}\sum_{m=0}^{\infty}\widehat{h}_m^{-2}\|u-\widehat{Q}_{m,\mathbf{K}}u\|_{\mathbf{K}}^2&\overset{(5.26)\,(5.27)}{\lesssim}\sum_{T_0\in\mathcal{T}_0}\mathbf{k}_{T_0}\|\nabla E_{\omega_0(T_0)}u\|_{\mathbb{R}^d}^2\overset{(5.22)}{\leq}\sum_{T_0\in\mathcal{T}_0}\mathbf{k}_{T_0}C_{\omega_0(T_0)}\|\nabla u\|_{\omega_0(T_0)}^2\\ &\overset{(2.6)}{\leq}\big(\max_{T_0\in\mathcal{T}_0}C_{\omega_0(T_0)}\big)\sum_{T_0\in\mathcal{T}_0}\mathbf{k}_{T_0}\frac{1}{\inf_{y\in\omega_0(T_0)}\lambda_{\min}(\mathbf{K}(y))}|\!|\!|u|\!|\!|_{\omega_0(T_0)}^2\\ &\overset{(5.18)}{=}\big(\max_{T_0\in\mathcal{T}_0}C_{\omega_0(T_0)}\big)\sum_{T_0\in\mathcal{T}_0}|\!|\!|u|\!|\!|_{\omega_0(T_0)}^2.\end{aligned}$$

Due to finite patch overlap, we finally obtain

$$\sum_{m=0}^{\infty} \widehat{h}_m^{-2} \|u - \widehat{Q}_{m,\mathbf{K}} u\|_{\mathbf{K}}^2 \lesssim \max_{T_0 \in \mathcal{T}_0} C_{\omega_0(T_0)} \sum_{T_0 \in \mathcal{T}_0} \|\!|u|\!\|_{\omega_0(T_0)}^2 \lesssim \max_{T_0 \in \mathcal{T}_0} C_{\omega_0(T_0)} \|\!|u|\!\|^2.$$

This concludes the proof. □

Proposition 5.19. *Let $v_L^1 \in \mathcal{X}_L^1$. Then, there exists functions $v_0^1 \in \mathcal{X}_0^1$ and $\{v_{\ell,z}^1\}_{z \in \mathcal{V}_\ell^+} \in \mathcal{X}_{\ell,z}^1$ for $\ell = 1, \dots, L$ such that*

$$v_L^1 = v_0^1 + \sum_{\ell=1}^{L} \sum_{z \in \mathcal{V}_\ell^+} v_{\ell,z}^1. \tag{5.28}$$

Furthermore, it holds that

$$\|\!|v_0^1|\!\|^2 + \sum_{\ell=1}^{L} \sum_{z \in \mathcal{V}_\ell^+} \|\!|v_{\ell,z}^1|\!\|^2 \leq \widetilde{C}_{\mathrm{ML}} C_{\mathrm{loc}}^{(2)} \|\!|v_L^1|\!\|^2, \tag{5.29}$$

where the constant $C_{\mathrm{loc}}^{(2)} > 0$ is defined in (5.6) and the constant $\widetilde{C}_{\mathrm{ML}} > 0$ depends only on the initial mesh $\mathcal{T}_0$, the space dimension d, and γ-shape regularity (2.15).

Remark 5.20. *Compared to the decomposition in Lemma 4.4 the component v_0^1 for the initial mesh is global now. This eliminates the dependency on* $\operatorname{diam}(\Omega)/h_0$.

Proof of Proposition 5.19. We use the same decomposition as in the proof of Lemma 4.4. With $v_0^1 := \Pi_0 v_L^1$ it follows that

$$v_L^1 = \sum_{\ell=0}^{L} (\Pi_\ell - \Pi_{\ell-1}) v_L^1 = v_0^1 + \sum_{\ell=1}^{L} \sum_{z \in \mathcal{V}_\ell^+} v_{\ell,z}^1.$$

We want to show that this decomposition is stable.
Step 1 ($\ell = 0$): First, we show stability of v_0^1. For this we use the local stability of Π_0 in the H^1-seminorm as shown in [WZ17, Lemma 3.4]. With the norm equivalence (2.6) it follows that

$$\begin{aligned}
\|\!|v_0^1|\!\|^2 = \sum_{T \in \mathcal{T}_0} \|\!|v_0^1|\!\|_T^2 &\leq \sum_{T \in \mathcal{T}_0} \sup_{y \in T} \lambda_{\max}(\mathbf{K}(y)) \|\nabla v_0^1\|_T^2 \overset{[\mathrm{WZ17}]}{\lesssim} \sum_{T \in \mathcal{T}_0} \sup_{y \in T} \lambda_{\max}(\mathbf{K}(y)) \|\nabla v_L^1\|_{\omega_0(T)}^2 \\
&\leq \sum_{T \in \mathcal{T}_0} \frac{\sup_{y \in T} \lambda_{\max}(\mathbf{K}(y))}{\inf_{y \in \omega_0(T)} \lambda_{\min}(\mathbf{K}(y))} \|\!|v_L^1|\!\|_{\omega_0(T)}^2 \leq C_{\mathrm{loc}}^{(2)} \sum_{T \in \mathcal{T}_0} \|\!|v_L^1|\!\|_{\omega_0(T)}^2.
\end{aligned}$$

Using finite patch overlap, we obtain the desired estimate

$$\|\!|v_0^1|\!\|^2 \lesssim C_{\mathrm{loc}}^{(2)} \|\!|v_L^1|\!\|^2.$$

Step 2 (L^2-projections estimates): It is left to estimate the sum in (5.28). The norm equivalence (2.6) leads to

$$\sum_{\ell=1}^{L}\sum_{z\in\mathcal{V}_\ell^+}\|\!|v_{\ell,z}^1|\!\|_{\omega_\ell(z)}^2 \le \sum_{\ell=1}^{L}\sum_{z\in\mathcal{V}_\ell^+}\sup_{y\in\omega_\ell(z)}\lambda_{\max}(\mathbf{K}(y))\|\nabla v_{\ell,z}^1\|_{\omega_\ell(z)}^2.$$

Analogously to Lemma 4.4, the inverse inequality (4.17), and the estimate (4.16) establish

$$\sum_{\ell=1}^{L}\sum_{z\in\mathcal{V}_\ell^+}\|\!|v_{\ell,z}^1|\!\|_{\omega_\ell(z)}^2 \lesssim \sum_{\ell=1}^{L}\sum_{z\in\mathcal{V}_\ell^+}\sup_{y\in\omega_\ell(z)}\lambda_{\max}(\mathbf{K}(y))h_{\ell,z}^{-2}\,\|(\Pi_\ell-\Pi_{\ell-1})v_L^1\|_{\omega_\ell(z)}^2.$$

For $\ell\in\{1,\dots,L\}$ and $z\in\mathcal{V}_\ell^+$, Lemma 5.6 yields a vertex $z'=z'[z]\in\mathcal{V}_{\ell-1}$ such that $\omega_\ell^2(z)\subseteq\omega_{\ell-1}^2(z')$. Let $\widehat{Q}_{m,\mathbf{K}}:=\widehat{Q}_{0,\mathbf{K}}$ for $m<0$. Then, Lemma 5.7 implies

$$\widehat{Q}_{g_{\ell,z}-C_1,\mathbf{K}}v_L^1\in\widehat{\mathcal{X}}^1_{\widetilde{r}_{\ell-1,z'}}$$

and hence that $(\widehat{Q}_{g_{\ell,z}-C_1,\mathbf{K}}v_L^1)|_T$ is linear for every $T\in\mathcal{T}_{\ell-1}^2(z')$ and hence also for every $T\in\mathcal{T}_\ell^2(z)$. Thus, we have

$$(\widehat{Q}_{g_{\ell,z}-C_1,\mathbf{K}}v_L^1)|_{\omega_\ell(z)}=(\Pi_\ell\widehat{Q}_{g_{\ell,z}-C_1,\mathbf{K}}v_L^1)|_{\omega_\ell(z)}=(\Pi_{\ell-1}\widehat{Q}_{g_{\ell,z}-C_1,\mathbf{K}}v_L^1)|_{\omega_\ell(z)}. \tag{5.30}$$

With Lemma 5.11 we can estimate the local L^2-norms for $\ell\in\{1,\dots,L\}$

$$\begin{aligned}
\|(\Pi_\ell-\Pi_{\ell-1})v_L^1\|_{\omega_\ell(z)}^2 &\overset{(5.30)}{=} \|\Pi_\ell(v_L^1-\widehat{Q}_{g_{\ell,z}-C_1,\mathbf{K}}v_L^1)-\Pi_{\ell-1}(v_L^1-\widehat{Q}_{g_{\ell,z}-C_1,\mathbf{K}}v_L^1)\|_{\omega_\ell(z)}^2\\
&\lesssim \|\Pi_\ell(v_L^1-\widehat{Q}_{g_{\ell,z}-C_1,\mathbf{K}}v_L^1)\|_{\omega_\ell(z)}^2+\|\Pi_{\ell-1}(v_L^1-\widehat{Q}_{g_{\ell,z}-C_1,\mathbf{K}}v_L^1)\|_{\omega_\ell(z)}^2\\
&\overset{(5.12)}{\lesssim} \|v_L^1-\widehat{Q}_{g_{\ell,z}-C_1,\mathbf{K}}v_L^1\|_{\omega_\ell^2(z)}^2+\|v_L^1-\widehat{Q}_{g_{\ell,z}-C_1,\mathbf{K}}v_L^1\|_{\omega_{\ell-1}^2(z')}^2\\
&\lesssim \|v_L^1-\widehat{Q}_{g_{\ell,z}-C_1,\mathbf{K}}v_L^1\|_{\omega_{\ell-1}^2(z')}^2.
\end{aligned}$$

Step 3 (Weighted estimates): Let $\ell\in\{1,\dots,L\}$, $T\in\mathcal{T}_\ell$, and $T_0\in\mathcal{T}_0$ be the unique ancestor of T. For a more concise notation, we define

$$\mathbf{k}_T:=\inf_{y\in\omega_0(T_0)}\lambda_{\min}(\mathbf{K}(y)).$$

We use this to obtain

$$\begin{aligned}
\sum_{\ell=1}^{L}\sum_{z\in\mathcal{V}_\ell^+}\|\!|v_{\ell,z}^1|\!\|^2 &\lesssim \sum_{\ell=1}^{L}\sum_{z\in\mathcal{V}_\ell^+}\sup_{y\in\omega_\ell(z)}\lambda_{\max}(\mathbf{K}(y))\,h_{\ell,z}^{-2}\sum_{T\in\mathcal{T}_{\ell-1}^2(z'[z])}\|v_L^1-\widehat{Q}_{g_{\ell,z}-C_1,\mathbf{K}}v_L^1\|_T^2\\
&\le \sum_{\ell=1}^{L}\sum_{z\in\mathcal{V}_\ell^+}\frac{\sup_{y\in\omega_\ell(z)}\lambda_{\max}(\mathbf{K}(y))}{\inf_{T\in\mathcal{T}_{\ell-1}^2(z'[z])}\mathbf{k}_T}\,h_{\ell,z}^{-2}\sum_{T\in\mathcal{T}_{\ell-1}^2(z'[z])}\mathbf{k}_T\|v_L^1-\widehat{Q}_{g_{\ell,z}-C_1,\mathbf{K}}v_L^1\|_T^2.
\end{aligned}$$

From Lemma 5.3, we know that there exists a vertex $z_0 = z_0[z] \in \mathcal{V}_0$ with $\omega_{\ell-1}(z'[z]) \subseteq \omega_0(z_0[z])$. Thus, it also holds that $\omega_\ell^2(z) \subseteq \omega_{\ell-1}^2(z'[z]) \subseteq \omega_0^2(z_0[z])$. This implies

$$\begin{aligned}\inf_{T\in\mathcal{T}_{\ell-1}^2(z'[z])} \mathbf{k}_T &= \inf_{T\in\mathcal{T}_{\ell-1}^2(z'[z])} \inf_{y\in\omega_0(T_0)} \lambda_{\min}(\mathbf{K}(y)) \geq \inf_{T_0\in\mathcal{T}_0^2(z_0[z])} \inf_{y\in\omega_0(T_0)} \lambda_{\min}(\mathbf{K}(y)) \\ &= \inf_{y\in\omega_0^3(z_0[z])} \lambda_{\min}(\mathbf{K}(y))\end{aligned}$$

and $\sup_{y\in\omega_\ell(z)} \lambda_{\max}(\mathbf{K}(y)) \leq \sup_{y\in\omega_0^3(z_0[z])} \lambda_{\max}(\mathbf{K}(y))$. Therefore, we have shown that

$$\sum_{\ell=1}^{L} \sum_{z\in\mathcal{V}_\ell^+} |\!|\!| v_{\ell,z}^1 |\!|\!|^2 \lesssim C_{\mathrm{loc}}^{(2)} \sum_{\ell=1}^{L} \sum_{z\in\mathcal{V}_\ell^+} h_{\ell,z}^{-2} \sum_{T\in\mathcal{T}_{\ell-1}^2(z'[z])} \mathbf{k}_T \|v_L^1 - \widehat{Q}_{g_{\ell,z}-C_1,\mathbf{K}} v_L^1\|_T^2 \tag{5.31}$$

Step 4 (Level-generation estimates): We want to change from a patch of level $\ell-1$ to a patch of the generation $g_{\ell,z}$. Recall that there exists an index $k \in \mathbb{N}$ such that $\omega_{\ell-1}^2(z') \subseteq \widehat{\omega}_{g_{\ell,z}}^k(z)$. We distinguish two cases: First, we assume that $T_1, \dots, T_j \in \widehat{\mathcal{T}}_{g_{\ell,z}}^k(z)$ with $T = \bigcup_{i=1}^j T_i$ and $T \in \mathcal{T}_{\ell-1}^2(z')$. Then, the ancestor $T_0 \in \mathcal{T}_0$ of T is also the ancestor of $T_1, \dots, T_j$ and we can rewrite

$$\mathbf{k}_T \|v_L^1 - \widehat{Q}_{g_{\ell,z}-C_1,\mathbf{K}} v_L^1\|_T^2 = \sum_{i=1}^{j} \mathbf{k}_{T_i} \|v_L^1 - \widehat{Q}_{g_{\ell,z}-C_1,\mathbf{K}} v_L^1\|_{T_i}^2.$$

Second, we assume that $T_1, \dots, T_j \in \mathcal{T}_{\ell-1}^2(z')$ with $T = \bigcup_{i=1}^j T_i$ and $T \in \widehat{\mathcal{T}}_{g_{\ell,z}}^k(z)$. This implies that all $T_1, \dots, T_j$ and T have the same ancestor $T_0 \in \mathcal{T}_0$. Hence, it holds that

$$\sum_{i=1}^{j} \mathbf{k}_{T_i} \|v_L^1 - \widehat{Q}_{g_{\ell,z}-C_1,\mathbf{K}} v_L^1\|_{T_i}^2 = \mathbf{k}_T \|v_L^1 - \widehat{Q}_{g_{\ell,z}-C_1,\mathbf{K}} v_L^1\|_T^2.$$

Using these observations we obtain

$$\sum_{T\in\mathcal{T}_{\ell-1}^2(z'[z])} \mathbf{k}_T \|v_L^1 - \widehat{Q}_{g_{\ell,z}-C_1,\mathbf{K}} v_L^1\|_T^2 \leq \sum_{T\in\widehat{\mathcal{T}}_{g_{\ell,z}}^k(z)} \mathbf{k}_T \|v_L^1 - \widehat{Q}_{g_{\ell,z}-C_1,\mathbf{K}} v_L^1\|_T^2. \tag{5.32}$$

Step 5 (Sum over generations estimates): With (5.32), we can estimate the right-hand side of (5.31). Afterwards, we rewrite the expression by introducing a sum over the generations

$$\begin{aligned}&\sum_{\ell=1}^{L} \sum_{z\in\mathcal{V}_\ell^+} h_{\ell,z}^{-2} \sum_{T\in\widehat{\mathcal{T}}_{g_{\ell,z}}^k(z)} \mathbf{k}_T \|v_L^1 - \widehat{Q}_{g_{\ell,z}-C_1,\mathbf{K}} v_L^1\|_T^2 \\ &\quad\simeq \sum_{m=0}^{\infty} \widehat{h}_m^{-2} \sum_{\ell=1}^{L} \sum_{\substack{z\in\mathcal{V}_\ell^+ \\ g_{\ell,z}=m}} \sum_{T\in\widehat{\mathcal{T}}_m^k(z)} \mathbf{k}_T \|v_L^1 - \widehat{Q}_{m-C_1,\mathbf{K}} v_L^1\|_T^2 \\ &\quad\overset{(4.34)}{=} \sum_{m=0}^{\infty} \widehat{h}_m^{-2} \sum_{z\in\widehat{\mathcal{V}}_m} \sum_{\ell\in\mathscr{L}_{1,L}^{(1)}(z,m)} \sum_{T\in\widehat{\mathcal{T}}_m^k(z)} \mathbf{k}_T \|v_L^1 - \widehat{Q}_{m-C_1,\mathbf{K}} v_L^1\|_T^2.\end{aligned}$$

From (4.32) we know that the set $\mathscr{L}^{(1)}_{1,L}(z,m)$ is uniformly bounded. Thus, we obtain

$$\begin{aligned}
&\sum_{\ell=1}^{L}\sum_{z\in\mathcal{V}_\ell^+} h_{\ell,z}^{-2}\sum_{T\in\widehat{\mathcal{T}}^k_{g_{\ell,z}}(z)} \mathbf{k}_T\|v_L^1-\widehat{Q}_{g_{\ell,z}-C_1,\mathbf{K}}v_L^1\|_T^2\\
&\quad\lesssim \sum_{m=0}^{\infty}\widehat{h}_m^{-2}\sum_{z\in\widehat{\mathcal{V}}_m}\sum_{T\in\widehat{\mathcal{T}}^k_m(z)}\mathbf{k}_T\|v_L^1-\widehat{Q}_{m-C_1,\mathbf{K}}v_L^1\|_T^2 \qquad (5.33)\\
&\quad\simeq \sum_{m=0}^{\infty}\widehat{h}_m^{-2}\sum_{T\in\mathcal{T}_0}\mathbf{k}_T\|v_L^1-\widehat{Q}_{m-C_1,\mathbf{K}}v_L^1\|_T^2.
\end{aligned}$$

Step 6 (Stability of the decomposition): We combine (5.31) and (5.33) to derive

$$\begin{aligned}
\sum_{\ell=1}^{L}\sum_{z\in\mathcal{V}_\ell^+}\|v_{\ell,z}^1\|^2_{\omega_\ell(z)} &\lesssim C^{(2)}_{\mathrm{loc}}\sum_{m=0}^{\infty}\widehat{h}_m^{-2}\sum_{T\in\mathcal{T}_0}\mathbf{k}_T\|v_L^1-\widehat{Q}_{m-C_1,\mathbf{K}}v_L^1\|_T^2\\
&= C^{(2)}_{\mathrm{loc}}\sum_{m=0}^{\infty}\widehat{h}_m^{-2}\|v_L^1-\widehat{Q}_{m-C_1,\mathbf{K}}v_L^1\|^2_{\mathbf{K}}.
\end{aligned}$$

Furthermore, analogously to (5.14) we get for $M=\max_{z\in\mathcal{V}_L} g_{L,z}$

$$\sum_{m=0}^{\infty}\widehat{h}_m^{-2}\|v_L^1-\widehat{Q}_{m-C_1,\mathbf{K}}v_L^1\|^2_{\mathbf{K}}\le\Big((1-4^{-1/d})^{-1}+4^{C_1/d}\Big)\sum_{m=0}^{M}\widehat{h}_m^{-2}\|v_L^1-\widehat{Q}_{m,\mathbf{K}}v_L^1\|^2_{\mathbf{K}}.$$

Finally, we can use Proposition 5.18 and Step 1 to obtain the desired result

$$|\!|\!|v_0|\!|\!|^2+\sum_{\ell=1}^{L}\sum_{z\in\mathcal{V}_\ell^+}|\!|\!|v_{\ell,z}^1|\!|\!|^2\lesssim C^{(2)}_{\mathrm{loc}}\Big(|\!|\!|v_L^1|\!|\!|^2+\sum_{m=0}^{M}\widehat{h}_m^{-2}|\!|\!|v_L^1-\widehat{Q}_{m,\mathbf{K}}v_L^1|\!|\!|^2_{\mathbf{K}}\Big)\overset{(5.23)}{\lesssim} C^{(2)}_{\mathrm{loc}}|\!|\!|v_L^1|\!|\!|^2$$

This concludes the proof. □

Remark 5.21 (Alternative constant of stability)**.** *It is possible to obtain the following estimate*

$$\sum_{\ell=1}^{L}\sum_{z\in\mathcal{V}_\ell^+}|\!|\!|v_{\ell,z}^1|\!|\!|^2\lesssim\left(\sup_{z\in\mathcal{V}_0}\frac{\sup_{y\in\omega_0^2(z)}\lambda_{\max}(\mathbf{K}(y))}{\inf_{y\in\omega_0^2(z)}\lambda_{\min}(\mathbf{K}(y))}\right)^2|\!|\!|v_L^1|\!|\!|^2,$$

where the hidden constant depends only on the initial mesh $\mathcal{T}_0$, the space dimension d, and the γ-shape regularity (2.15)*. Note that, in this case, the local diffusion-contrast appears on the smaller patch $\omega_0^2(z)$ but with a power of two. Depending on the diffusion coefficient this estimate could be more useful than the estimate* (5.29) *in Proposition 5.19.*

Remark 5.22 (Choice of initial mesh)**.** *In order to exploit the local constant $C^{(2)}_{\mathrm{loc}}$, the initial mesh $\mathcal{T}_0$ should be chosen such that the patches $\omega_0^3(z)$ for all $z\in\mathcal{V}_0$ only lie across at most two regions, where the diffusion is changing rapidly.*

5.4 Extension to p-robustness for $d = 2$

The goal of this section is to construct a p-robust one-level decomposition that is stable in the energy norm with a constant that depends only locally on the contrast of the diffusion coefficient. To this end, we will use the decomposition from [SMP+08]. Since most of the estimates in [SMP+08] are already local, we only need to change the norm in the proofs of [SMP+08]. However, we first define the edge patch.

Definition 5.23. Let $\ell \in \mathbb{N}$, $z_1, z_2 \in \mathcal{V}_\ell$, and $E = \operatorname{conv}\{z_1, z_2\}$. Then, we define the *edge patch* by

$$\omega_\ell(E) := \omega_\ell(z_1) \cup \omega_\ell(z_2).$$

Lemma 5.24. *Let $d = 2$ and $v_L \in \mathcal{X}_L^p$. Then, there exists functions $v_L^1 \in \mathcal{X}_L^1$ and $\{v_{L,z}^p\}_{z\in\mathcal{V}_L} \in \mathcal{X}_{L,z}^p$ such that*

$$v_L = v_L^1 + \sum_{z\in\mathcal{V}_L} v_{L,z}^p \quad \text{with } v_L^1 \in \mathcal{X}_L^1 \text{ and } v_{L,z}^p \in \mathcal{X}_{L,z}^p \text{ for all } z \in \mathcal{V}_L. \tag{5.34}$$

Moreover, the decomposition is stable in the sense of

$$|\!|\!| v_L^1 |\!|\!|^2 + \sum_{z\in\mathcal{V}_L} |\!|\!| v_{L,z}^p |\!|\!|^2 \le \widetilde{C}_{\mathrm{OL}} C_{\mathrm{loc}}^{(2)} |\!|\!| v_L |\!|\!|^2, \tag{5.35}$$

where $C_{\mathrm{loc}}^{(2)} > 0$ is defined in (5.6) and the constant $\widetilde{C}_{\mathrm{OL}} > 0$ depends only on the space dimension d and the γ-shape regularity (2.15).

Proof. **Step 1 (Lowest-order component):** For the construction of the decomposition, the lowest-order Scott–Zhang projection $P_L : L^2(\Omega) \to \mathcal{X}_L^1$ is utilized. We will use the following properties: Let $T \in \mathcal{T}_L$ and $v \in H_0^1(\Omega)$. Then, it holds that

$$\|\nabla P_L v\|_T \lesssim \|\nabla v\|_{\omega_L(T)} \tag{5.36}$$

and

$$\|v - P_L v\|_T \lesssim h_T \|\nabla v\|_{\omega_L(T)} \tag{5.37}$$

where the hidden constants depend only on γ-shape regularity. Let us define $v_L^1 := P_L v_L$ and hence $v_L = v_L^1 + v_1$ for some $v_1 = (1 - P_L)v_L \in \mathcal{X}_L^p$. First, we show that $|\!|\!| v_L^1 |\!|\!|^2 \lesssim C_{\mathrm{loc}}^{(2)} |\!|\!| v_L |\!|\!|^2$. The norm equivalence (2.6) and the local H^1-stability of the Scott–Zhang projection (5.36) prove

$$\begin{aligned} |\!|\!| v_L^1 |\!|\!|^2 &\lesssim \sum_{z\in\mathcal{V}_L} |\!|\!| P_L v_L |\!|\!|_{\omega_L(z)}^2 \overset{(2.6)}{\le} \sum_{z\in\mathcal{V}_L} \sup_{y\in\omega_L(z)} \lambda_{\max}(\mathbf{K}(y)) \|\nabla P_L v_L\|_{\omega_L(z)}^2 \\ &\overset{(5.36)}{\lesssim} \sum_{z\in\mathcal{V}_L} \sup_{y\in\omega_L(z)} \lambda_{\max}(\mathbf{K}(y)) \|\nabla v_L\|_{\omega_L^2(z)}^2 \overset{(2.6)}{\le} \sum_{z\in\mathcal{V}_L} \frac{\sup_{y\in\omega_L(z)} \lambda_{\max}(\mathbf{K}(y))}{\inf_{y\in\omega_L^2(z)} \lambda_{\min}(\mathbf{K}(y))} |\!|\!| v_L |\!|\!|_{\omega_L^2(z)}^2. \end{aligned}$$

From Lemma 5.3 we know there exists a vertex $z_0 \in \mathcal{V}_0$ such that $\omega_L(z) \subseteq \omega_0(z_0)$. Using finite patch overlap, we obtain

$$|\!|\!| v_L^1 |\!|\!|^2 \lesssim C_{\mathrm{loc}}^{(2)} |\!|\!| v_L |\!|\!|^2.$$

Step 2 (Vertex contributions): We denote by Π_0^z the averaging operator introduced in [SMP+08] corresponding to an interior vertex $z \in \mathcal{V}_L^\Omega := \mathcal{V}_L \cap \Omega$. In [SMP+08, Lemma 3.2] it is shown that $\Pi_0^z v \in \mathcal{X}_{L,z}^p$ for any $v \in \mathcal{X}_L^p$. Furthermore, the proof of [SMP+08, Theorem 3.4] contains the local estimate

$$\|\nabla \Pi_0^z v\|^2 = \|\nabla \Pi_0^z v\|_{\omega_L(z)} \lesssim \|\nabla v\|^2_{\omega_L(z)} + h_{L,z}^{-2}\|v\|^2_{\omega_L(z)} \quad \text{for all } v \in \mathcal{X}_L^p, \tag{5.38}$$

where the hidden constant depends only on γ-shape regularity. We further decompose v_1 using these averaging operators such that

$$v_1 = (1 - P_L)v_L = \sum_{z \in \mathcal{V}_L^\Omega} \Pi_0^z v_1 + v_2$$

for some $v_2 \in \mathcal{X}_L^p$. Recall that $v_1 = v_L - P_L v_L$. Applying the norm estimate (2.6) and the local H^1-stability and first-order approximation property of P_L leads to

$$\begin{aligned}
\|\!|\Pi_0^z v_1|\!\|^2 = \|\!|\Pi_0^z v_1|\!\|^2_{\omega_L(z)} &\overset{(2.6)}{\leq} \sup_{y \in \omega_L(z)} \lambda_{\max}(\mathbf{K}(y)) \|\nabla \Pi_0^z v_1\|^2 \\
&\overset{(5.38)}{\lesssim} \sup_{y \in \omega_L(z)} \lambda_{\max}(\mathbf{K}(y)) \big(\|\nabla v_1\|^2_{\omega_L(z)} + h_{L,z}^{-2} \|v_1\|^2_{\omega_L(z)} \big) \\
&\overset{\substack{(5.36)\\(5.37)}}{\lesssim} \sup_{y \in \omega_L(z)} \lambda_{\max}(\mathbf{K}(y)) \|\nabla v_L\|^2_{\omega_L^2(z)} \overset{(2.6)}{\leq} \frac{\sup_{y \in \omega_L(z)} \lambda_{\max}(\mathbf{K}(y))}{\inf_{y \in \omega_L^2(z)} \lambda_{\min}(\mathbf{K}(y))} \|\nabla v_L\|^2_{\omega_L^2(z)}.
\end{aligned}$$

Summing over the vertices yields

$$\sum_{z \in \mathcal{V}_L^\Omega} \|\!|\Pi_0^z v_1|\!\|^2 \lesssim C_{\mathrm{loc}}^{(2)} \|\!| v_L |\!\|^2.$$

Step 3 (Edge contributions): Let us define the set of interior edges

$$\mathcal{E}_L^\Omega := \{E \in \mathcal{E} : E = \mathrm{conv}\{z_1, z_2\} \text{ and } z_1 \in \mathcal{V}_L^\Omega \text{ or } z_2 \in \mathcal{V}_L^\Omega\}.$$

In [SMP+08, eq.8] following prior work of [BCM+91], averaging operators Π_0^E corresponding to edges $E \in \mathcal{E}_{L,\mathrm{in}}$ are defined. More precisely, we have

$$\Pi_0^E : \mathcal{X}_{L,0}^p := \{v \in \mathcal{X}_L^p : v(z) = 0 \text{ for all } z \in \mathcal{V}_L\} \to H_0^1(\omega_L(E)) \cap \mathcal{X}_L^p.$$

For $v \in \mathcal{X}_{L,0}^p$ and $\omega \subseteq \Omega$, we can define the following norm

$$\|v\|^2_{r,\omega} := \|\nabla v\|^2_\omega + \|r_{\mathcal{V}_L}^{-1} v\|^2_\omega, \tag{5.39}$$

where $r_{\mathcal{V}_L}(x) := \min_{z \in \mathcal{V}_L} |x - z|$. Then, the averaging operators are stable [SMP+08, Lemma 3.6] in the following sense

$$\|\nabla \Pi_0^E v\|_{\omega_L(E)} \lesssim \|v\|_{r,\omega_L(E)} \quad \text{for all } v \in \mathcal{X}_{L,0}^p, \tag{5.40}$$

where the hidden constant depends only on γ-shape regularity. We denote by $\varphi_{L,z}$ the hat function at vertex z on level L. The goal is further to decompose the function v_2 from the previous step. In [SMP+08], it is established that $v_2 \in \mathcal{X}^p_{L,0}$. Hence, we can apply the operators Π^E_0 and obtain

$$v_2 = \sum_{E\in\mathcal{E}^\Omega_L} \Pi^E_0 v_2 + v_3 \tag{5.41}$$

for some $v_3 \in \mathcal{X}^p_L$. From the norm equivalence (2.6) and the stability (5.40) it follows that

$$\begin{aligned} \|\Pi^E_0 v_2\|^2_{\omega_L(E)} &\overset{(2.6)}{\leq} \sup_{y\in\omega_L(E)} \lambda_{\max}(\mathbf{K}(y)) \|\nabla \Pi^E_0 v_2\|^2_{\omega_L(E)} \\ &\overset{(5.40)}{\lesssim} \sup_{y\in\omega_L(E)} \lambda_{\max}(\mathbf{K}(y)) \|v_2\|^2_{r,\omega_L(E)}. \end{aligned} \tag{5.42}$$

By definition we have $v_2 = v_1 - \sum_{z\in\mathcal{V}^\Omega_L} \Pi^z_0 v_1$. Utilizing the partition of unity provided by the hat functions and considering their local support, we are led to

$$\begin{aligned} \|v_2\|^2_{r,\omega_L(E)} &= \Big\| v_1 - \sum_{z\in\mathcal{V}^\Omega_L} \Pi^z_0 v_1 \Big\|^2_{r,\omega_L(E)} \\ &= \Big\| \sum_{z\in\mathcal{V}_L\cap\partial\Omega} \varphi_{L,z} v_1 + \sum_{z\in\mathcal{V}^\Omega_L} \big(\varphi_{L,z} v_1 - \Pi^z_0 v_1\big) \Big\|^2_{r,\omega_L(E)} \\ &\lesssim \sum_{z\in\mathcal{V}_L\cap\partial\Omega} \|\varphi_{L,z} v_1\|^2_{r,\omega_L(E)} + \sum_{z\in\mathcal{V}^\Omega_L} \|\varphi_{L,z} v_1 - \Pi^z_0 v_1\|^2_{r,\omega_L(E)} \\ &\leq \sum_{z\in\overline{\omega_L(E)}\cap\mathcal{V}_L\cap\partial\Omega} \|\varphi_{L,z} v_1\|^2_{r,\omega_L(z)} + \sum_{z\in\overline{\omega_L(E)}\cap\mathcal{V}^\Omega_L} \|\varphi_{L,z} v_1 - \Pi^z_0 v_1\|^2_{r,\omega_L(z)}. \end{aligned}$$

In [SMP+08, Theorem 3.4], it is shown that

$$\|\varphi_{L,z} v_1\|^2_{r,\omega_L(z)} \lesssim \|\nabla v_1\|^2_{\omega_L(z)} \quad \text{for all } z \in \mathcal{V}_L \cap \partial\Omega, \tag{5.43}$$

where the hidden constant depends only on γ-shape regularity. Moreover, from [SMP+08, Lemma 3.3], we have

$$\|\varphi_{L,z} v_1 - \Pi^z_0 v_1\|^2_{r,\omega_L(z)} \lesssim \|\nabla v_1\|^2_{\omega_L(z)} \quad \text{for all } z \in \mathcal{V}_{L,\mathrm{in}}, \tag{5.44}$$

where the hidden constant depends only on γ-shape regularity. The estimates (5.43) and (5.44) provide

$$\|v_2\|^2_{r,\omega_L(E)} \lesssim \sum_{z\in\overline{\omega_L(E)}\cap\mathcal{V}_L} \|\nabla v_1\|^2_{\omega_L(z)}.$$

Let z_E be one of the two vertices of E. The H^1-stability (5.36) of the Scott-Zhang projection for $v_1 = (1 - P_L)v_L$ and the finite patch overlap imply

$$\|v_2\|^2_{r,\omega_L(E)} \lesssim \sum_{z\in\overline{\omega_L(E)}\cap\mathcal{V}_L} \|\nabla v_1\|^2_{\omega_L(z)} \overset{(5.36)}{\lesssim} \sum_{z\in\overline{\omega_L(E)}\cap\mathcal{V}_L} \|\nabla v_L\|^2_{\omega^2_L(z)} \lesssim \|\nabla v_L\|^2_{\omega^3_L(z_E)}. \tag{5.45}$$

Together with (5.42), we obtain

$$\|\Pi_0^E v_2\|^2_{\omega_L(E)} \overset{(5.42)}{\lesssim} \sup_{y\in\omega_L(E)} \lambda_{\max}(\mathbf{K}(y))\|\nabla v_L\|^2_{\omega_L^3(z_E)} \overset{(2.6)}{\leq} \frac{\sup_{y\in\omega_L(E)} \lambda_{\max}(\mathbf{K}(y))}{\inf_{y\in\omega_L^3(z_E)} \lambda_{\min}(\mathbf{K}(y)} \|v_L\|^2_{\omega_L^3(z_E)}$$

and hence also

$$\sum_{E\in\mathcal{E}_L^\Omega} \|\Pi_0^E v_2\|^2 \lesssim C_{\mathrm{loc}}^{(2)} \|v_L\|^2.$$

Step 4 (Element contributions): Due to the construction (5.41), it holds that $v_3 \in \mathcal{X}_L^p$ and $v_3 = 0$ on $\bigcup_{E\in\mathcal{E}_{L,\mathrm{in}}} E$, see [SMP+08, Theorem 3.7]. Thus, we can define the element contributions

$$v_{3,T}(x) := \begin{cases} v_3(x) & x \in T, \\ 0 & x \in \Omega\backslash T \end{cases}$$

for all $T \in \mathcal{T}_L$ and it holds that $v_{3,T} \in \mathcal{X}_L^p$. The definition (5.39), the stability of Π_0^E (5.40), and the estimate (5.45) lead to

$$\begin{aligned}
\|v_{3,T}\|_T^2 &\overset{(5.41)}{=} \Big\|v_2 - \sum_{E\in\mathcal{E}_L^\Omega} \Pi_0^E v_2\Big\|_T^2 \overset{(2.6)}{\leq} \sup_{y\in T} \lambda_{\max}(\mathbf{K}(y))\Big\|\nabla\big(v_2 - \sum_{E\in\mathcal{E}_L^\Omega} \Pi_0^E v_2\big)\Big\|_T^2 \\
&\lesssim \sup_{y\in T} \lambda_{\max}(\mathbf{K}(y))\Big(\|\nabla v_2\|_T^2 + \sum_{\substack{E\in\mathcal{E}_L^\Omega \\ E\subseteq T}} \|\nabla\Pi_0^E v_2\|_T^2\Big) \\
&\overset{\substack{(5.39)\\(5.40)}}{\lesssim} \sup_{y\in T} \lambda_{\max}(\mathbf{K}(y))\Big(\sum_{\substack{E\in\mathcal{E}_L^\Omega \\ E\subseteq T}} \|v_2\|^2_{r,\omega_L(E)}\Big) \\
&\overset{(5.45)}{\lesssim} \sup_{y\in T} \lambda_{\max}(\mathbf{K}(y))\Big(\sum_{\substack{E\in\mathcal{E}_L^\Omega \\ E\subseteq T}} \|\nabla v_L\|^2_{\omega_L^3(z_E)}\Big).
\end{aligned}$$

Introducing the sum over the elements and using the norm equivalence (2.6) gives us

$$\begin{aligned}
\sum_{T\in\mathcal{T}_L} \|v_{3,T}\|_T^2 &\lesssim \sum_{T\in\mathcal{T}_L} \sum_{\substack{E\in\mathcal{E}_L^\Omega \\ E\subseteq T}} \sup_{y\in T} \lambda_{\max}(\mathbf{K}(y))\|\nabla v_L\|^2_{\omega_L^3(z_E)} \\
&\overset{(2.6)}{\leq} C_{\mathrm{loc}}^{(2)} \sum_{T\in\mathcal{T}_L} \sum_{\substack{E\in\mathcal{E}_L^\Omega \\ E\subseteq T}} \|v_L\|^2_{\omega_L^3(z_E)} \lesssim C_{\mathrm{loc}}^{(2)} \|v_L\|^2.
\end{aligned}$$

Step 5: Combining all the previous steps results in

$$v_L = v_L^1 + \sum_{z\mathcal{V}_L^\Omega} \Pi_0^z v_1 + \sum_{E\in\mathcal{E}_L^\Omega} \Pi_0^E v_2 + \sum_{T\in\mathcal{T}_L} v_{3,T}$$

and

$$\|v_L^1\|^2 + \sum_{z\mathcal{V}_L^\Omega} \|\Pi_0^z v_1\|^2 + \sum_{E\in\mathcal{E}_L^\Omega} \|\Pi_0^E v_2\|^2 + \sum_{T\in\mathcal{T}_L} \|v_{3,T}\|^2 \lesssim C_{\mathrm{loc}}^{(2)} \|v_L\|^2.$$

We can assign edge and element components to a vertex such that their support is contained in the vertex patch. This concludes the proof. □

Remark 5.25. *For $d = 3$, a construction of a p-robust one-level decomposition that is stable in the H^1-seminorm is presented in [SMP+08]. However, this construction is more intricate than the one in Lemma 5.24, as it also requires considering the faces of the simplices. Further investigation is needed to extend the result to the energy norm, with a stability constant that depends only on the local diffusion-contrast.*

5.5 *hp*-robust decomposition for $d = 2$

In this section, we combine the results from Section 5.3 and Section 5.4 to obtain a *hp*-robust decomposition in 2D, where the constant depends only on local variations of the diffusion coefficient.

Lemma 5.26. *For any $v_L \in \mathcal{X}_L^p$, there exist functions $v_0 \in \mathcal{X}_0^1$, $\{v_{\ell,z}\}_{z\in\mathcal{V}_\ell^+} \in \mathcal{X}_{\ell,z}^1$, and $\{v_{L,z}\}_{z\in\mathcal{V}_L} \in \mathcal{X}_{L,z}^p$ such that*

$$v_L = v_0 + \sum_{\ell=1}^{L-1} \sum_{z\in\mathcal{V}_\ell^+} v_{\ell,z} + \sum_{z\in\mathcal{V}_L} v_{L,z}. \tag{5.46}$$

Furthermore, there holds the estimate

$$\|v_0\|^2 + \sum_{\ell=1}^{L-1} \sum_{z\in\mathcal{V}_\ell^+} \|v_{\ell,z}\|^2 + \sum_{z\in\mathcal{V}_L} \|v_{L,z}\|^2 \le \widetilde{C}_{\mathrm{SD}} (C_{\mathrm{loc}}^{(2)})^2 \|v_L\|^2, \tag{5.47}$$

where $C_{\mathrm{loc}}^{(2)} > 0$ is defined in (5.6) and $\widetilde{C}_{\mathrm{SD}} > 0$ depends only on the initial mesh $\mathcal{T}_0$ and γ-shape regularity (2.15).

Proof. Let $v_L \in \mathcal{X}_L^p$. From Lemma 5.24, we obtain a decomposition on the finest level L. Applying Proposition 5.19 to the lowest-order contribution v_L^1 from (5.34), we are led to

$$\begin{aligned} v_L \overset{(5.34)}{=} v_L^1 + \sum_{z\in\mathcal{V}_L} v_{L,z}^p \overset{(5.28)}{=} v_0^1 + \sum_{\ell=1}^{L} \sum_{z\in\mathcal{V}_L^+} v_{\ell,z}^1 + \sum_{z\in\mathcal{V}_L} v_{L,z}^p \\ = v_0^1 + \sum_{\ell=1}^{L-1} \sum_{z\in\mathcal{V}_\ell^+} v_{\ell,z}^1 + \sum_{z\in\mathcal{V}_L^+} v_{L,z}^1 + \sum_{z\in\mathcal{V}_L} v_{L,z}^p. \end{aligned}$$

Defining the contributions $v_0 := v_0^1$, $v_{\ell,z} := v_{\ell,z}^1 \in \mathcal{X}_{\ell,z}^1$ for $z \in \mathcal{V}_\ell^+$ and $\ell = 1, \dots, L-1$, and $v_{L,z} := v_{L,z}^1 + v_{L,z}^p \in \mathcal{X}_{L,z}^p$ for $z \in \mathcal{V}_L^+$ and $v_{L,z} := v_{L,z}^p \in \mathcal{X}_{L,z}^p$ for $z \in \mathcal{V}_L \backslash \mathcal{V}_L^+$ gives the

desired decomposition (5.46). Next, we show the estimate (5.47). On the finest level, the Young inequality gives us

$$\begin{aligned}\sum_{z\in\mathcal{V}_L} |||v_{L,z}|||^2 &\leq \sum_{z\in\mathcal{V}_L\setminus\mathcal{V}_L^+} |||v_{L,z}^p|||^2 + 2\sum_{z\in\mathcal{V}_L^+}\Big(|||v_{L,z}^1|||^2 + |||v_{L,z}^p|||^2\Big)\\ &\leq 2\Big(\sum_{z\in\mathcal{V}_L^+} |||v_{L,z}^1|||^2 + \sum_{z\in\mathcal{V}_L} |||v_{L,z}^p|||^2\Big).\end{aligned}$$

With the estimate (5.29), stability (5.35), and $C_{\mathrm{loc}}^{(2)} \geq 1$, we therefore have

$$\begin{aligned}&|||v_0|||^2 + \sum_{\ell=1}^{L-1}\sum_{z\in\mathcal{V}_\ell^+} |||v_{\ell,z}|||^2 + \sum_{z\in\mathcal{V}_L} |||v_{L,z}|||^2\\ &\leq 2\Big(|||v_0^1|||^2 + \sum_{\ell=1}^{L-1}\sum_{z\in\mathcal{V}_\ell^+} |||v_{L,z}^1|||^2 + \sum_{z\in\mathcal{V}_L^+} |||v_{L,z}^1|||^2 + \sum_{z\in\mathcal{V}_L} |||v_{L,z}^p|||^2\Big)\\ &= 2\Big(|||v_0^1|||^2 + \sum_{\ell=1}^{L}\sum_{z\in\mathcal{V}_\ell^+} |||v_{\ell,z}^1|||^2 + \sum_{z\in\mathcal{V}_L} |||v_{L,z}^p|||^2\Big)\\ &\overset{(5.29)}{\lesssim} C_{\mathrm{loc}}^{(2)}|||v_L^1|||^2 + \sum_{z\in\mathcal{V}_L} |||v_{L,z}^p|||^2 \overset{(5.35)}{\lesssim} (C_{\mathrm{loc}}^{(2)})^2|||v_L|||^2.\end{aligned}$$

This concludes the proof. □

5.6 Proof of Theorem 5.1

We can use the improved results from this chapter to prove Theorem 5.1.

Proof of Theorem 5.1. We note that the properties (5.1) and (5.4) follow immediately from Theorem 4.13 as well as the equivalence of reliability of the estimator (5.2) and contraction of the solver (5.3). Lastly, the proof of reliability of the estimator ζ_L follows with the same arguments as in the proof of Theorem 4.13. However, let us summarize the main arguments for the case $d = 2$ and $p \in \mathbb{N}$ in order to highlight the improved constant. Decomposing the algebraic error $u_L^* - u_L \in \mathcal{X}_L^p$ with Lemma 5.26 yields functions $v_0 \in \mathcal{X}_0^1$, $\{v_{\ell,z}\}_{z\in\mathcal{V}_\ell^+} \in \mathcal{X}_{\ell,z}^1$ and $\{v_{L,z}\}_{z\in\mathcal{V}_L} \in \mathcal{X}_{L,z}^p$ such that

$$u_L^* - u_L = v_0 + \sum_{\ell=1}^{L-1}\sum_{z\in\mathcal{V}_\ell^+} v_{\ell,z} + \sum_{z\in\mathcal{V}_L} v_{L,z} \quad \text{and}$$

$$|||v_0|||^2 + \sum_{\ell=1}^{L-1}\sum_{z\in\mathcal{V}_\ell^+} |||v_{\ell,z}|||^2 + \sum_{z\in\mathcal{V}_L} |||v_{L,z}|||^2 \leq \widetilde{C}_{\mathrm{SD}}(C_{\mathrm{loc}}^{(2)})^2|||u_L^* - u_L|||^2.$$

Note that this improves (4.49) by the use of the *local diffusion-contrast* constant $C_{\mathrm{loc}}^{(2)}$. The above decomposition and the solver construction is then used to obtain

$$\begin{aligned}\|\!|u_L^* - u_L|\!\|^2 &= \Big\langle\!\!\Big\langle \rho_0, v_0 + \sum_{\ell=1}^{L-1}\sum_{z\in\mathcal{V}_\ell^+} v_{\ell,z} + \sum_{z\in\mathcal{V}_L} v_{L,z}\Big\rangle\!\!\Big\rangle + \sum_{\ell=1}^{L-1}\sum_{z\in\mathcal{V}_\ell^+}\langle\!\langle \rho_{\ell,z}, v_{\ell,z}\rangle\!\rangle \\ &\quad + \sum_{z\in\mathcal{V}_L}\langle\!\langle \rho_{L,z}, v_{L,z}\rangle\!\rangle + \sum_{\ell=1}^{L-1}\sum_{k=1}^{\ell-1}\Big\langle\!\!\Big\langle \lambda_k\rho_k, \sum_{z\in\mathcal{V}_\ell^+} v_{\ell,z}\Big\rangle\!\!\Big\rangle + \sum_{k=1}^{L-1}\Big\langle\!\!\Big\langle \lambda_k\rho_k, \sum_{z\in\mathcal{V}_L} v_{L,z}\Big\rangle\!\!\Big\rangle.\end{aligned}$$

As in Theorem 4.13, we use the Young inequality (4.51) to estimate the five terms constituting the algebraic error. Next, the strengthened Cauchy–Schwarz inequality with *a local diffusion-contrast* dependence from Proposition 5.9 is used instead of the estimate from Proposition 4.12. Rearranging the terms, this leads to

$$\begin{aligned}\|\!|u_L^* - u_L|\!\|^2 &\le \frac{1}{2}\|\!|\rho_0|\!\|^2 + \frac{1}{2}\|\!|u_L^* - u_L|\!\|^2 + \frac{1}{4}(\widetilde{C}_{\mathrm{rel}})^2\Big(\sum_{\ell=1}^{L-1}\lambda_\ell\sum_{z\in\mathcal{V}_\ell^+}\|\!|\rho_{\ell,z}|\!\|^2 + \lambda_L\sum_{z\in\mathcal{V}_L}\|\!|\rho_{L,z}|\!\|^2\Big) \\ &\quad + \frac{1}{4\widetilde{C}_{\mathrm{SD}}(C_{\mathrm{loc}}^{(2)})^2}\Big(\sum_{\ell=1}^{L-1}\sum_{z\in\mathcal{V}_\ell^+}\|\!|v_{\ell,z}|\!\|^2 + \sum_{z\in\mathcal{V}_L}\|\!|v_{L,z}|\!\|^2\Big),\end{aligned}$$

where the constant $\widetilde{C}_{\mathrm{rel}}$ is defined in (5.7). Finally, the stability of the decomposition and the definition of the estimator $\zeta_L(u_L)$ give

$$\begin{aligned}\|\!|u_L^* - u_L|\!\|^2 &\le \frac{3}{4}\|\!|u_L^* - u_L|\!\|^2 + \frac{1}{4}(\widetilde{C}_{\mathrm{rel}})^2\Big(\|\!|\rho_0|\!\|^2 + \sum_{\ell=1}^{L-1}\lambda_\ell\sum_{z\in\mathcal{V}_\ell^+}\|\!|\rho_{\ell,z}|\!\|^2 + \lambda_L\sum_{z\in\mathcal{V}_L}\|\!|\rho_{L,z}|\!\|^2\Big) \\ &= \frac{3}{4}\|\!|u_L^* - u_L|\!\| + \frac{1}{4}(\widetilde{C}_{\mathrm{rel}})^2\zeta_L(u_L)^2\end{aligned}$$

and hence

$$\|\!|u_L^* - u_L|\!\|^2 \le (\widetilde{C}_{\mathrm{rel}})^2\zeta_L(u_L)^2.$$

The proof for $d = 3$ and $p = 1$ is analogous (while $d = 3$ and $p > 1$ remains open; see Remark 5.25). This concludes the proof. □

6 Multigrid as inexact solver for AFEM

The multigrid solver of Algorithm 3.7 can be used as an iterative solver in the module SOLVE of the adaptive finite element method presented in Algorithm 2.11. Moreover, this application fits into the framework of [GHP+21], which will allow us to prove optimal complexity of the resulting adaptive algorithm.

6.1 AFEM with multigrid solver

In this section, we first introduce the algorithm for AFEM employing the multigrid solver of Algorithm 3.7. Afterwards, the computational cost of the algorithm is discussed. We will use the residual error estimator η_L from Section 2.4.2 in the stopping criterion of the algebraic solver. Therefore, the modules SOLVE and ESTIMATE from Algorithm 2.11 are combined in the following algorithm.

Algorithm 6.1 (AFEM with multigrid solver)**.** ***Input:*** *Initial mesh $\mathcal{T}_0$, polynomial degree $p \in \mathbb{N}$, adaptivity parameters $0 < \theta \leq 1$, $C_{\mathrm{mark}} \geq 1$, and $\mu > 0$, as well as the initial guess $u_0^0 := 0$.*
Adaptive loop: *Iterate the following steps* (I)–(III) *for all $L = 0, 1, 2, \dots$:*

(I) SOLVE & ESTIMATE: *For all $k = 1, 2, 3, \dots$* **repeat** (i)–(ii):

(i) *Do one step of the multigrid solver starting from $u_L^{k-1} \in \mathcal{X}_L^p$ to obtain the improved approximation $u_L^k = \Phi_L(u_L^{k-1}) \in \mathcal{X}_L^p$ and the associated a-posteriori estimator $\zeta_L(u_L^{k-1})$ of the algebraic error, i.e.,*

$$\{u_L^k, \zeta_L(u_L^{k-1})\} := \mathtt{SOLVE}(u_L^{k-1}, \{\mathcal{T}_\ell\}_{\ell=0}^L, p).$$

(ii) *Compute local contributions $\eta_L(T, u_L^k)$ of the residual error estimator for all $T \in \mathcal{T}_L$ and define*

$$\eta_L(u_L^k) := \Big(\sum_{T \in \mathcal{T}_L} \eta_L(T, u_L^k)\Big)^{1/2}.$$

until

$$\zeta_L(u_L^{k-1}) \leq \mu \eta_L(u_L^k). \tag{6.1}$$

Upon termination of the k-loop, define the index $\underline{k}[L] := k \in \mathbb{N}$ and $u_L^{\underline{k}} := u_L^k$.

(II) MARK: *Employ Dörfler marking to determine a set $\mathcal{M}_L \in \mathbb{M}(\mathcal{T}_L, \theta, u_L^{\underline{k}}) := \{\mathcal{U}_L \subset \mathcal{T}_L \mid \theta \eta_L(u_L^{\underline{k}})^2 \leq \eta_L(\mathcal{U}_L, u_L^{\underline{k}})^2\}$ that fulfills*

$$\#\mathcal{M}_L \leq C_{\mathrm{mark}} \min_{\mathcal{U}_L \in \mathbb{M}[\mathcal{T}_L, \theta, u_L^{\underline{k}}]} \#\mathcal{U}_L.$$

(III) `REFINE`: *Generate the new mesh* $\mathcal{T}_{L+1} := \texttt{REFINE}(\mathcal{T}_L, \mathcal{M}_L)$ *and use nested iteration* $u_{L+1}^0 := u_L^{\underline{k}}$.

Output: *Sequence of successively refined simplicial triangulations* $\mathcal{T}_L$*, discrete approximations* $u_L^{\underline{k}}$*, and error estimators* $\eta_L(u_L^{\underline{k}})$ *and* $\zeta_L(u_L^{\underline{k}-1})$.

Note that we omit the mesh level L in the notation $\underline{k}[L]$ if the dependency is clear from the context, e.g., $u_L^{\underline{k}} = u_L^{\underline{k}[L]}$ as defined in Algorithm 6.1. Moreover, we define the stopping index for the outer loop of Algorithm 6.1 by $\underline{L} := \sup\{L \in \mathbb{N}_0 : u_L^0$ is defined in Algorithm 6.1$\}$ with the typical case being $\underline{L} = \infty$. Let us make some remarks concerning nested iterations and the stopping criterion (6.1).

Remark 6.2 (Nested iterations)**.** *We use the last iteration* $u_L^{\underline{k}}$ *as the initial guess on the newly-refined mesh* $\mathcal{T}_{L+1}$*. This ensures optimal computational cost of the algorithm. We can also look at this from the algebraic solver perspective. Recalling the full multigrid algorithm from Section 3.1.2, we see that Algorithm 6.1 is just a full multigrid method over the evolving hierarchy of meshes. Moreover, the number of V-cycles on a mesh is determined by the adaptive stopping criterion. Hence, the choice of the parameter* α_0 *in Algorithm 3.3 is inherently taken care of.*

Remark 6.3. *The core idea of Algorithm 6.1 is to balance different error components using a-posteriori analysis; see, e.g., [EV13]. We have shown* $\|u_L^* - u_L^{\underline{k}}\| \leq q_{\mathrm{ctr}}\, C'_{\mathrm{rel}}\, \zeta_L(u_L^{\underline{k}-1})$ *in Theorem 4.13. Hence, the* k*-loop is stopped in* (6.1) *once the algebraic error is controlled by the estimator* $\eta_L(u_L^{\underline{k}})$ *associated to the discretization error* $\|u^* - u_L^*\|$*, i.e.,* $\|u_L^* - u_L^{\underline{k}}\| \lesssim \eta_L(u_L^{\underline{k}})$*. Thus, the termination criterion balances the algebraic and discretization error. Meaning, that once the algebra is sufficiently resolved compared to the discretization, the solver is stopped, and the next step in Algorithm 6.1 is the mesh refinement.*

Lemma 6.4 (A-posteriori control of the overall error)**.** *Let* $L \in \mathbb{N}_0$ *and* $\underline{k} = \underline{k}[L]$ *be the termination index of the iterative solver in Algorithm 6.1. Then, it holds that*

$$\|u^* - u_L^{\underline{k}}\| \lesssim \eta_L(u_L^{\underline{k}}).$$

Proof. Due to reliability (A3) and stability (A1) of the residual error estimator η_L, the discretization error satisfies

$$\|u^* - u_L^*\| \overset{\text{(A3)}}{\lesssim} \eta_L(u_L^*) \overset{\text{(A1)}}{\lesssim} \eta_L(u_L^{\underline{k}}) + \|u_L^* - u_L^{\underline{k}}\|. \tag{6.2}$$

From Remark 6.3 we know that the stopping criterion (6.1) yields $\|u_L^* - u_L^{\underline{k}}\| \lesssim \eta_L(u_L^{\underline{k}})$ and therefore $\|u^* - u_L^*\| \lesssim \eta_L(u_L^{\underline{k}})$. This concludes the proof. □

Next, we compare the given stopping criterion (6.1) to the one employed in [GHP+21] and [BFM+24]. Therein a contractive solver with iteration operator $\Psi_L : \mathcal{X}_L^p \to \mathcal{X}_L^p$ guaranteeing $\|u_L^* - \Psi_L(u_L)\| \leq q_{\mathrm{ctr}}\, \|u_L^* - u_L\|$ for all $u_L \in \mathcal{X}_L^p$ and an $\mathcal{X}_L^p$-independent constant $0 < q_{\mathrm{ctr}} < 1$ is used. Moreover, the iterative solver is terminated within AFEM if

$$\|u_L^{\underline{k}} - u_L^{\underline{k}-1}\| \leq \nu\, \eta_L(u_L^{\underline{k}}), \tag{6.3}$$

where $\nu > 0$ is a given adaptivity parameter. From now on, we will always denote by $\nu > 0$ the parameter used in the termination criterion (6.3). Compared to (6.1) in Algorithm 6.1, not all solvers have a built-in algebraic error estimator, hence, the computable quantity $\|u_L^k - u_L^{k-1}\|$ is utilized instead. Indeed, the triangle inequality and contraction lead to

$$\|u_L^* - u_L^{k-1}\| \leq \|u_L^* - u_L^k\| + \|u_L^k - u_L^{k-1}\| \leq q_{\mathrm{ctr}} \|u_L^* - u_L^{k-1}\| + \|u_L^k - u_L^{k-1}\|$$

and hence

$$\|u_L^* - u_L^k\| \leq q_{\mathrm{ctr}} \|u_L^* - u_L^{k-1}\| \leq \frac{q_{\mathrm{ctr}}}{1 - q_{\mathrm{ctr}}} \|u_L^k - u_L^{k-1}\|. \tag{6.4}$$

Thus, the expression $\|u_L^k - u_L^{k-1}\|$ is indeed an a-posteriori estimator of the algebraic error. This means that the two criteria (6.1) and (6.3) differ only in the choice of the a-posteriori estimator. Moreover, the observations from Remark 6.3 and Lemma 6.4 can also be applied to the criterion (6.3). In summary, the solver in Algorithm 6.1 is stopped once $\|u_L^* - u_L^k\| \leq q_{\mathrm{ctr}} C'_{\mathrm{rel}} \mu \eta_L(u_L^k)$, while the criterion (6.3) leads to $\|u_L^* - u_L^k\| \leq (1 - q_{\mathrm{ctr}})^{-1} q_{\mathrm{ctr}} \nu \eta_L(u_L^k)$. Hence, the two criteria are formally equivalent up to a constant.

Now, that AFEM incorporates MG as a solver in Algorithm 6.1, we want to discuss the notion of computational cost. For this purpose, we define the countably infinite set

$$\mathcal{Q} := \{(L,k) \in \mathbb{N}_0^2 : u_L^k \text{ is defined in Algorithm 6.1}\}$$

The set $\mathcal{Q}$ can be equipped with the natural order

$$(L',k') \leq (L,k) :\Longleftrightarrow u_{L'}^{k'} \text{ is computed earlier than or equal to } u_L^k \text{ in Algorithm 6.1.}$$

Furthermore, we define the total step counter by

$$|L,k| := \#\{(L',k') \in \mathcal{Q} : (L',k') \leq (L,k)\} \in \mathbb{N}_0 \quad \text{for all } (L,k) \in \mathcal{Q}.$$

In order to discuss the computational cost of Algorithm 6.1, we first consider the cost of steps (I)–(III) separately:

- `SOLVE & ESTIMATE`: The calculations of the error indicators $\eta_L(T, u_L^k)$ for all $T \in \mathcal{T}_L$ can be performed in $\mathcal{O}(\#\mathcal{T}_L)$ operations as these consist of element-wise operations. Moreover, Remark 3.10 classifies that one solver step can be realized in linear complexity $\mathcal{O}(\#\mathcal{T}_L)$.
- `MARK`: We recall that the Dörfler marking can be implemented with linear cost $\mathcal{O}(\#\mathcal{T}_L)$. This was shown in [Ste07] for $C_{\mathrm{mark}} = 2$ and in [PP20] for $C_{\mathrm{mark}} = 1$.
- `REFINE`: Newest vertex bisection can be realized in $\mathcal{O}(\#\mathcal{T}_L)$ operations; see, e.g., [BDD04; Ste07].

Due to the cumulative structure of Algorithm 6.1 the total computational cost to compute u_L^k is therefore proportional to

$$\mathrm{cost}(L,k) := \sum_{\substack{(L',k') \in \mathcal{Q} \\ |L',k'| \leq |L,k|}} \#\mathcal{T}_{L'}. \tag{6.5}$$

Indeed, to reach a given step (L,k) of the Algorithm, one needs to consider all costs from the coarse mesh and subsequently add costs taking place at each refined mesh prior to reaching the given level L and iteration step k. For a fixed polynomial degree p, it also holds that $\dim \mathcal{X}_L^p \simeq \#\mathcal{T}_L$, where the constants depend only on p and d. Thus, convergence rates with respect to the degrees of freedom and with respect to the number of elements are equivalent. In the next section, we go into more detail regarding convergence rates and optimal complexity.

6.2 Optimal complexity of AFEM with multigrid solver

Let us first introduce the notion of optimal convergence rates. To this end, we define nonlinear approximation classes following [BDD04; CKN$^+$08]. The set of triangulations with at most N additional elements compared to the initial mesh $\mathcal{T}_0$ is given by $\mathbb{T}_N(\mathcal{T}_0) := \{\mathcal{T}_H \in \mathbb{T}(\mathcal{T}_0) : \#\mathcal{T}_H - \#\mathcal{T}_0 \leq N\}$. For any rate $s > 0$, define the approximation class $\mathbb{A}_s$ as

$$\|u^*\|_{\mathbb{A}_s} := \sup_{N\in\mathbb{N}_0} \big((N+1)^s \min_{\mathcal{T}_{\mathrm{opt}}\in\mathbb{T}_N(\mathcal{T}_0)} \eta_{\mathrm{opt}}(u^*_{\mathrm{opt}})\big).$$

The minimum ensures that we take some optimal triangulation in the set $\mathcal{T}_N(\mathcal{T}_0)$ where the error estimator is smallest. If $\|u^*\|_{\mathbb{A}_s} < \infty$, then the error decreases with rate $-s$ along the sequence of unknown optimal meshes with respect to the additional number N of simplices. Thus, $s > 0$ is an attainable convergence rate. However, up to this point, we have not discussed whether any algorithm can actually achieve these rates.

Definition 6.5. We say that an adaptive algorithm is *rate-optimal* if the generated sequence of successively refined triangulations $\{\mathcal{T}_\ell\}_{\ell\in\mathbb{N}_0}$ satisfies

$$\forall s > 0 : \big(\|u^*\|_{\mathbb{A}_s} < \infty \Longrightarrow \sup_{\ell\in\mathbb{N}_0} (\#\mathcal{T}_\ell)^s \eta_\ell(u^*_\ell) < \infty\big),$$

i.e., the adaptive algorithm attains indeed all possible rates.

Indeed, the standard adaptive Algorithm 2.11 is rate-optimal for sufficiently small $0 < \theta \ll 1$; see, e.g., [CFP$^+$14]. Note that rate-optimality refers to the quality of the approximation per invested degree of freedom, without providing information on computational costs invested in calculating the said approximation. Since the module `SOLVE` in Algorithm 2.11 is generally not of linear complexity $\mathcal{O}(\#\mathcal{T}_\ell)$, we instead examine Algorithm 6.1 regarding its optimal complexity, i.e., optimality with respect to the overall computational cost. In the spirit of [BFM$^+$24] this leads to the introduction of the following quasi-error

$$\mathrm{H}_L^k := |\!|\!| u_L^* - u_L^k |\!|\!| + \eta_L(u_L^k) \overset{\text{(A1)}}{\simeq} |\!|\!| u_L^* - u_L^k |\!|\!| + \eta_L(u_L^*) \quad \text{for all } (L,k) \in \mathcal{Q}.$$

The proposed quasi-error H_L^k can hence be seen as a representation of the algebraic and discretization error. Recall that (6.2) ensures that $|\!|\!| u_L^* - u_L^k |\!|\!| + |\!|\!| u^* - u_L^* |\!|\!| \lesssim \mathrm{H}_L^k$ and, therefore, the quasi-error controls the overall error $|\!|\!| u^* - u_L^k |\!|\!|$. We say that the quasi-error decays with rate $-s$ with respect to the overall computational cost if

$$\sup_{(L,k)\in\mathcal{Q}} \mathrm{cost}(L,k)^s\, \mathrm{H}_L^k = \sup_{(L,k)\in\mathcal{Q}} \Big(\sum_{\substack{(L',k')\in\mathcal{Q}\\ |L',k'|\leq|L,k|}} \#\mathcal{T}_{L'} \Big)^s \mathrm{H}_L^k < \infty. \tag{6.6}$$

Thus, an adaptive algorithm is of optimal complexity if all possible convergence rates s with respect to the degrees of freedom are also achieved with respect to the overall computational cost, i.e., $\|u^*\|_{\mathbb{A}_s} < \infty \Leftrightarrow \sup_{(L,k)\in\mathcal{Q}} \mathrm{cost}(L,k)^s\, \mathrm{H}_L^k < \infty$. Let us formulate the optimal complexity result for Algorithm 6.1.

Theorem 6.6 (Full R-linear convergence)**.** *Let $0 < \theta \le 1$, $C_{\mathrm{mark}} \ge 1$ and $\mu > 0$ be arbitrary. Suppose that the sequence of meshes $\{\mathcal{T}_L\}_{L\in\mathbb{N}_0}$ is generated by Algorithm 6.1. Then, there holds full R-linear convergence of the quasi-error, i.e., there exist constants $0 < q_{\mathrm{lin}} < 1$ and $C_{\mathrm{lin}} > 0$ such that*

$$\mathrm{H}_L^k \le C_{\mathrm{lin}}\, q_{\mathrm{lin}}^{|L,k|-|L',k'|}\, \mathrm{H}_{L'}^{k'} \quad \text{for all } (L',k'),(L,k) \in \mathcal{Q} \text{ with } |L',k'| \le |L,k|. \tag{6.7}$$

For the proof of full R-linear convergence, we need the subsequent statement from [BFM+24].

Lemma 6.7 (Tail summability vs. R-linear convergence [BFM+24, Lemma 11])**.** *For any sequence $(a_\ell)_{\ell\in\mathbb{N}_0}$ in $\mathbb{R}_{\ge 0}$ and $m > 0$, the following two statements are equivalent:*

(i) ***tail summability:*** *There exists a constant $C_m > 0$ such that*

$$\sum_{\ell'=\ell+1}^{\infty} a_{\ell'}^m \le C_m a_\ell^m \quad \text{for all } \ell \in \mathbb{N}_0.$$

(ii) ***R-linear convergence:*** *There exists constants $0 < q_{\mathrm{lin}} < 1$ and C_{lin} such that*

$$a_{\ell+n} \le C_{\mathrm{lin}} q_{\mathrm{lin}}^n a_\ell \quad \text{for all } \ell, n \in \mathbb{N}_0. \qquad \square$$

To show full R-linear convergence (6.7), we follow the proof of [BFM+24, Theorem 7].

Proof of Theorem 6.6. The proof is split into three steps.
Step 1 (Estimator reduction): Let $L \in \mathbb{N}_0$. Using stability (A1) and reduction (A2), we get

$$\begin{aligned}
\eta_{L+1}(u_L^k)^2 &= \eta_{L+1}(\mathcal{T}_{L+1}\cap\mathcal{T}_L, u_L^k)^2 + \eta_{L+1}(\mathcal{T}_{L+1}\backslash\mathcal{T}_L, u_L^k)^2 \\
&\overset{\substack{(A1)\\(A2)}}{\le} \eta_L(\mathcal{T}_{L+1}\cap\mathcal{T}_L, u_L^k)^2 + q_{\mathrm{red}}^2\, \eta_L(\mathcal{T}_L\backslash\mathcal{T}_{L+1}, u_L^k)^2 \\
&= \eta_L(u_L^k)^2 - (1-q_{\mathrm{red}}^2)\, \eta_L(\mathcal{T}_L\backslash\mathcal{T}_{L+1}, u_L^k)^2.
\end{aligned}$$

Furthermore, Dörfler marking (2.18) and $\mathcal{M}_L \subseteq \mathcal{T}_L\backslash\mathcal{T}_{L+1}$ give us

$$\theta\eta_L(u_L^k)^2 \overset{(2.18)}{\le} \eta_L(\mathcal{M}_L, u_L^k)^2 \le \eta_L(\mathcal{T}_L\backslash\mathcal{T}_{L+1}, u_L^k)^2.$$

Since $0 < (1-q_{\mathrm{red}}^2)\,\theta < 1$, it follows that

$$\eta_{L+1}(u_L^k) \le q_\theta\, \eta_L(u_L^k) \quad \text{with} \quad 0 < q_\theta := [1-(1-q_{\mathrm{red}}^2)\,\theta]^{1/2} < 1. \tag{6.8}$$

This and stability (A1) lead to the estimator reduction

$$\eta_{L+1}(u_{L+1}^k) \overset{(A1)}{\le} \eta_{L+1}(u_L^k) + C_{\mathrm{stab}}|\!|\!| u_{L+1}^k - u_L^k |\!|\!| \overset{(6.8)}{\le} q_\theta \eta_L(u_L^k) + C_{\mathrm{stab}}|\!|\!| u_{L+1}^k - u_L^k |\!|\!|. \tag{6.9}$$

Step 2 (Tail summability with respect to L): Let $L \in \mathbb{N}$ with $(L+1, \underline{k}) \in \mathcal{Q}$. Due to nested iteration $u_{L+1}^0 = u_L^{\underline{k}}$ with $\underline{k}[L+1] \geq 1$ and contraction of the multigrid solver (4.1), we obtain

$$\|u_{L+1}^* - u_{L+1}^{\underline{k}}\| \overset{(4.1)}{\leq} q_{\mathrm{ctr}}^{\underline{k}[L+1]} \|u_{L+1}^* - u_L^{\underline{k}}\| \leq q_{\mathrm{ctr}} \|u_{L+1}^* - u_L^{\underline{k}}\|. \tag{6.10}$$

Combining this with the estimator reduction from Step 1 results in

$$\begin{aligned} \eta_{L+1}(u_{L+1}^{\underline{k}}) &\overset{(6.9)}{\leq} q_\theta\, \eta_L(u_L^{\underline{k}}) + C_{\mathrm{stab}} \|u_{L+1}^{\underline{k}} - u_L^{\underline{k}}\| \\ &\leq q_\theta \eta_L(u_L^{\underline{k}}) + C_{\mathrm{stab}} \big(\|u_{L+1}^* - u_{L+1}^{\underline{k}}\| + \|u_{L+1}^* - u_L^{\underline{k}}\| \big) \\ &\overset{(6.10)}{\leq} q_\theta \eta_L(u_L^{\underline{k}}) + (q_{\mathrm{ctr}} + 1) C_{\mathrm{stab}} \|u_{L+1}^* - u_L^{\underline{k}}\|. \end{aligned} \tag{6.11}$$

Let us define $a_{L+1} := \|u_{L+1}^* - u_{L+1}^{\underline{k}}\| + \gamma\, \eta_{L+1}(u_{L+1}^{\underline{k}})$ for some $\gamma > 0$ and $\widetilde{q} := \max\{q_{\mathrm{ctr}} + \gamma(q_{\mathrm{ctr}}+1)C_{\mathrm{stab}}, q_\theta\}$. It follows immediately that $a_L \simeq \mathrm{H}_L^{\underline{k}}$. Furthermore, with the triangle inequality there holds

$$\begin{aligned} a_{L+1} &\overset{(6.10)}{\overset{(6.11)}{\leq}} q_{\mathrm{ctr}} \|u_{L+1}^* - u_L^{\underline{k}}\| + \gamma \big[q_\theta\, \eta_L(u_L^{\underline{k}}) + (q_{\mathrm{ctr}}+1)\, C_{\mathrm{stab}} \|u_{L+1}^* - u_L^{\underline{k}}\| \big] \\ &\leq \widetilde{q} \big[\|u_{L+1}^* - u_L^{\underline{k}}\| + \gamma\, \eta_L(u_L^{\underline{k}}) \big] \\ &\leq \widetilde{q} \big[\|u_L^* - u_L^{\underline{k}}\| + \gamma\, \eta_L(u_L^{\underline{k}}) \big] + \widetilde{q} \|u_{L+1}^* - u_L^*\| = \widetilde{q}\, a_L + \widetilde{q} \|u_{L+1}^* - u_L^*\|. \end{aligned}$$

Finally, the Young inequality gives us

$$a_{L+1}^2 \leq (1+\delta)\, \widetilde{q}^2\, a_L^2 + (1+\delta^{-1})\, \widetilde{q}^2\, \|u_{L+1}^* - u_L^*\|^2 \quad \text{for all } \delta > 0.$$

We can choose $0 < \gamma \ll 1$ and $0 < \delta \ll 1$ sufficiently small so that $0 < q := (1+\delta)\widetilde{q}^2 < 1$ and $C := (1+\delta^{-1})\widetilde{q}^2 > 0$ yield

$$a_{L+1}^2 \leq q\, a_L^2 + C\, \|u_{L+1}^* - u_L^*\|^2. \tag{6.12}$$

Summing over the levels and applying the Pythagorean identity (2.12) leads to

$$\begin{aligned} \sum_{L'=L+1}^{\underline{L}-1} a_{L'}^2 = \sum_{L'=L}^{\underline{L}-2} a_{L'+1}^2 &\overset{(6.12)}{\leq} q \sum_{L'=L}^{\underline{L}-2} a_{L'}^2 + C \sum_{L'=L}^{\underline{L}-2} \|u_{L'+1}^* - u_{L'}^*\|^2 \\ &\overset{(2.12)}{=} q \sum_{L'=L}^{\underline{L}-2} a_{L'}^2 + C \sum_{L'=L}^{\underline{L}-2} \big(\|u^* - u_{L'}^*\|^2 - \|u^* - u_{L'+1}^*\|^2 \big). \end{aligned}$$

Exploiting that the second sum is a telescoping series, we use reliability (A3) of the error estimator to obtain

$$\begin{aligned} \sum_{L'=L+1}^{\underline{L}-1} a_{L'}^2 &\leq q \sum_{L'=L}^{\underline{L}-2} a_{L'}^2 + C \big(\|u^* - u_L^*\|^2 - \|u^* - u_{\underline{L}-1}^*\|^2 \big) \\ &\overset{(A3)}{\leq} q \sum_{L'=L}^{\underline{L}-2} a_{L'}^2 + C C_{\mathrm{rel}}^2 \eta_L(u_L^*)^2. \end{aligned} \tag{6.13}$$

Owing to stability (A1), we also have

$$\eta_L(u_L^*) \overset{\text{(A1)}}{\leq} \eta_L(u_L^k) + C_{\mathrm{stab}}\|u_L^* - u_L^k\| \simeq \mathrm{H}_L^k \simeq a_L.$$

Due to $0 < q < 1$, we can rearrange the terms in (6.13) so that

$$\sum_{L'=L+1}^{\underline{L}-1} a_{L'}^2 \leq (1-q)^{-1}(q + CC_{\mathrm{stab}}^2 C_{\mathrm{rel}}^2 \gamma^{-2})\, a_L^2 \quad \text{for all } 0 \leq L < \underline{L}.$$

Ultimatly, Lemma 6.7 yields tail summability of a_L and thus also of H_L^k, i.e.,

$$\sum_{L'=L+1}^{\underline{L}-1} \mathrm{H}_{L'}^k \lesssim \mathrm{H}_L^k \quad \text{for all } 0 \leq L < \underline{L}. \tag{6.14}$$

Step 3 (Tail summability with respect to L and k): Let $0 \leq k < k' < \underline{k}$. Then, the failure of the stopping criterion (6.1), efficiency (4.43) of the estimator ζ_L, and contraction of the solver (4.1) provide us with

$$\begin{aligned}\mathrm{H}_L^{k'} &= \|u_L^* - u_L^{k'}\| + \eta_L(u_L^{k'}) \overset{(6.1)}{\leq} \|u_L^* - u_L^{k'}\| + \mu^{-1}\zeta_L(u_L^{k'-1}) \\ &\overset{(4.43)}{\leq} \|u_L^* - u_L^{k'}\| + \mu^{-1}\|u_L^* - u_L^{k'-1}\| \\ &\overset{(4.1)}{\leq} (1 + (q_{\mathrm{ctr}}\mu)^{-1})q_{\mathrm{ctr}}^{k'-k}\|u_L^* - u_L^k\| \lesssim q_{\mathrm{ctr}}^{k'-k}\mathrm{H}_L^k.\end{aligned}$$

It is left to consider $(L, \underline{k}) \in \mathcal{Q}$. In this case, stability (A1), the triangle inequality, and the contraction of the solver imply

$$\mathrm{H}_L^k \overset{\text{(A1)}}{\lesssim} \|u_L^* - u_L^k\| + \eta_L(u_L^{k-1}) + \|u_L^{k-1} - u_L^k\| \leq \mathrm{H}_L^{k-1} + 2\|u_L^* - u_L^k\| \leq (1 + 2q_{\mathrm{ctr}})\mathrm{H}_L^{k-1}.$$

Hence, it follows that

$$\mathrm{H}_L^{k'} \lesssim q_{\mathrm{ctr}}^{k'-k}\mathrm{H}_L^k \quad \text{for all } 0 \leq k \leq k' \leq \underline{k}. \tag{6.15}$$

With quasi-monotonicity (QM), reliability (A3), and stability (A1), we prove

$$\begin{aligned}\|u_{L+1}^* - u_L^*\| \leq\ & \|u_{L+1}^* - u^*\| + \|u^* - u_L^*\| \overset{\text{(A3)}}{\lesssim} \eta_{L+1}(u_{L+1}^*) + \eta_L(u_L^*) \overset{\text{(QM)}}{\lesssim} \eta_L(u_L^*) \\ &\overset{\text{(A1)}}{\lesssim} \eta_L(u_L^k) + \|u_L^* - u_L^k\| = \mathrm{H}_L^k.\end{aligned}$$

Due to nested iteration and the triangle inequality, it therefore holds that

$$\mathrm{H}_{L+1}^0 = \|u_{L+1}^* - u_L^k\| + \eta_{L+1}(u_L^k) \leq \mathrm{H}_L^k + \|u_{L+1}^* - u_L^*\| \lesssim \mathrm{H}_L^k \quad \text{for all } (L, \underline{k}) \in \mathcal{Q}. \tag{6.16}$$

Finally, we obtain tail summability using the geometric series

$$\sum_{\substack{(L',k')\in\mathcal{Q}\\ |L',k'|>|L,k|}} \mathrm{H}_{L'}^{k'} = \sum_{k'=\underline{k}[L]}^{k'} \mathrm{H}_L^{k'} + \sum_{L'=L+1}^{\underline{L}} \sum_{k'=0}^{\underline{k}[L']} \mathrm{H}_{L'}^{k'} \overset{(6.15)}{\lesssim} \mathrm{H}_L^k \sum_{k'=\underline{k}[L]}^{k'} q_{\mathrm{ctr}}^{k'-k} + \sum_{L'=L+1}^{\underline{L}} \mathrm{H}_{L'}^0 \sum_{k'=0}^{\underline{k}[L']} q_{\mathrm{ctr}}^{k'}$$
$$\overset{(6.16)}{\lesssim} \mathrm{H}_L^k + \sum_{L'=L}^{\underline{L}-1} \mathrm{H}_{L'}^k \overset{(6.14)}{\lesssim} \mathrm{H}_L^k + \mathrm{H}_L^k \overset{(6.15)}{\lesssim} \mathrm{H}_L^k \quad \text{for all } (L,k)\in\mathcal{Q}.$$

Since $\mathcal{Q}$ is countable and linearly ordered, Lemma 6.7 concludes the proof of full R-linear convergence. □

Theorem 6.8 (Optimal complexity of AFEM with multigrid solver)**.** *With the assumptions from Theorem 6.6 it follows that*

$$\sup_{(L,k)\in\mathcal{Q}} (\#\mathcal{T}_L)^s\, \mathrm{H}_L^k \le \sup_{(L,k)\in\mathcal{Q}} \mathrm{cost}(L,k)^s\, \mathrm{H}_L^k \le C_{\mathrm{cost}} \sup_{(L,k)\in\mathcal{Q}} (\#\mathcal{T}_L)^s\, \mathrm{H}_L^k \quad \text{for all } s>0, \tag{6.17}$$

where the constant C_{cost} depends only on C_{lin}, q_{lin}, and s. Moreover, for sufficiently small adaptivity parameters, i.e.,

$$0<\mu<\mu^* := \frac{1-q_{\mathrm{ctr}}}{(1+q_{\mathrm{ctr}})q_{\mathrm{ctr}}C_{\mathrm{stab}}C'_{\mathrm{rel}}} \tag{6.18}$$

and

$$0<\frac{(\theta^{1/2}+\mu/\mu^*)^2}{(1-\mu/\mu^*)^2}<\theta^* := (1+C_{\mathrm{stab}}^2C_{\mathrm{drel}}^2)^{-1/2}, \tag{6.19}$$

Algorithm 6.1 guarantees, for all $s>0$, that

$$c_{\mathrm{opt}}\|u^*\|_{\mathbb{A}_s} \le \sup_{(L,k)\in\mathcal{Q}} \mathrm{cost}(L,k)^s\, \mathrm{H}_L^k \le C_{\mathrm{opt}} \max\{\|u^*\|_{\mathbb{A}_s}, \mathrm{H}_0^0\}. \tag{6.20}$$

The constants $c_{\mathrm{opt}}, C_{\mathrm{opt}}>0$ depend only on C_{stab}, q_{red}, C_{rel}, C_{drel}, C_{child}, C_{mark}, C_{lin}, q_{lin}, the polynomial degree p, the initial triangulation $\mathcal{T}_0$, s, θ, μ, and q_{ctr}. Importantly, this provides the equivalence

$$\|u^*\|_{\mathbb{A}_s}<\infty \iff \sup_{(L,k)\in\mathcal{Q}} \mathrm{cost}(L,k)^s\, \mathrm{H}_L^k<\infty,$$

hence Algorithm 6.1 is of optimal complexity.

Remark 6.9. *Since the constants c_{opt} and C_{opt} depend on q_{ctr}, they also depend on $\Lambda_{\max}/\Lambda_{\min}$ and $\max_{T\in\mathcal{T}_0}\|\operatorname{div}(\mathbf{K})\|_{L^\infty(T)}/\Lambda_{\min}$; see in Theorem 4.13.*

Remark 6.10. *This section is based on the framework of [GHP+21], where optimal complexity was achieved by combining AFEM with a contractive iterative solver. We also refer to [BFM+24] for more recent and improved results. For the model problem (2.4), both [GHP+21] and [BFM+24] ensure parameter-robust full R-linear convergence of the quasi-error, i.e., (6.7) holds for all parameters $0<\theta\le 1$ and $\nu>0$. Moreover, [BFM+24]*

extends this to inf-sup stable problems. Hence, we follow their approach here, too. Though, at first glance, different quasi-errors are used in [GHP+21] and [BFM+24], they are actually equivalent owing to reliability (A3)*, stability* (A1)*, and Céa's lemma* (2.13)*. Note that the so-called quasi-orthogonality plays an important role in [BFM+24]. However, for our model problem, there holds the Pythagorean identity* (2.12)*, which is even a stronger property.*

Proof of Theorem 6.8. **Step 1:** Let us recall some properties of Algorithm 6.1. As discussed in Section 2.4, we use the residual error estimator, which fulfills the assumptions (A1)–(A4). Furthermore, since we employ NVB as the mesh refinement, also the assumptions (R1)–(R3) are satisfied. Additionally, the multigrid solver is contractive (4.1), Dörfler marking of Section 2.4.3 is used, and nested iterations are employed. Ultimately, we recall the stopping criterion (6.1) balancing the algebraic and discretization errors.

Step 2: As a consequence of full R-linear convergence [BFM+24, Corollary 11] proves the equivalence of convergence rates with respect to the degrees of freedom and to the computational cost, i.e., the identity (6.17).

Step 3: To show optimal complexity, we follow the proof in [GHP+21, Theorem 7] and rely on full R-linear convergence (6.7), assumptions (A1)–(A4), (R1)–(R3), contraction of the inexact solver, Dörfler marking with a quasi-minimal set of marked elements, and the fulfilled stopping criterion $\|\!|u_L^k - u_L^{k-1}|\!\| \leq \nu\eta_L(u_L^k)$. Then, from Step 1, we only need to show that Algorithm 6.1 satisfies the last assumption. Using the triangle inequality, contraction of the multigrid solver (4.44), reliability of the algebraic error estimator ζ_L (4.43) and the stopping criterion (6.1) leads to

$$\begin{aligned}\|\!|u_L^k - u_L^{k-1}|\!\| &\leq \|\!|u_L^k - u_L^*|\!\| + \|\!|u_L^* - u_L^{k-1}|\!\| \overset{(4.44)}{\leq} (1+q_{\mathrm{ctr}})\|\!|u_L^* - u_L^{k-1}|\!\| \\ &\overset{(4.43)}{\leq} C'_{\mathrm{rel}}(1+q_{\mathrm{ctr}})\zeta_L(u_L^{k-1}) \overset{(6.1)}{\leq} C'_{\mathrm{rel}}(1+q_{\mathrm{ctr}})\mu\,\eta_L(u_L^k).\end{aligned}$$

Thus, we define $\nu := C'_{\mathrm{rel}}(1+q_{\mathrm{ctr}})\mu$ and recognize that Algorithm 6.1 guarantees

$$\|\!|u_L^k - u_L^{k-1}|\!\| \leq \nu\,\eta_L(u_L^k).$$

Following the analysis of [BFM+24, Theorem 13], the parameters ν and θ are required to fulfill

$$0 < \nu < \frac{1-q_{\mathrm{ctr}}}{q_{\mathrm{ctr}}C_{\mathrm{stab}}} =: \nu^* \quad \text{and } 0 < \frac{(\theta^{1/2}+\nu/\nu^*)^2}{(1-\nu/\nu^*)^2} < (1+C_{\mathrm{stab}}^2C_{\mathrm{drel}}^2)^{-1} = \theta^*. \tag{6.21}$$

So in order for Algorithm 6.1 to satisfy (6.21), there needs to hold

$$\nu = C'_{\mathrm{rel}}(1+q_{\mathrm{ctr}})\mu < \nu^* = (1-q_{\mathrm{ctr}})/(q_{\mathrm{ctr}}C_{\mathrm{stab}})$$

and

$$\frac{(\theta^{1/2}+\nu_2/\nu^*)^2}{(1-\nu_2/\nu^*)} < \theta^*.$$

Let us define $\mu^* := \nu^*/((1+q_{\mathrm{ctr}})C'_{\mathrm{rel}})$. Then, the conditions can be simplified to

$$\mu < \mu^* \quad \text{and} \quad \frac{(\theta^{1/2}+\mu/\mu^*)^2}{(1-\mu/\mu^*)^2} < \theta^*.$$

This concludes the proof. □

Remark 6.11. *If Algorithm 6.1 is implemented in a way that ensures linear complexity for each module as discussed in Section 6.1, one can also achieve optimal convergence rates with respect to the cumulative time. An example of this is shown in Chapter 7 in Figure 7.7 and Figure 7.8.*

7 Numerical experiments

In this chapter, we investigate the numerical performance of the proposed multigrid solver in Algorithm 3.7 and the adaptive Algorithm 6.1 employing this solver. First, we want to explore the behavior of the multigrid solver. More precisely, the interest lies in the dependence of the contraction factor q_{ctr} and subsequently also the reliability constant C'_{rel} on the local diffusion-contrast. Indeed, since the analysis was improved in Chapter 5 compared to [IMP+24], we aim to highlight numerically that the dependence of the solver contraction on the diffusion-contrast is *local* instead of *global*. Afterwards, some experiments concerning the optimality of the adaptive algorithm will be presented. The experiments are done in MATLAB using the implementation of the multigrid solver from [IMP+24] which is embedded into the MooAFEM framework from [IP23].

7.1 Performance of the multigrid solver

The goal is to numerically confirm the main result from Theorem 5.1. To this end, we want to design an experiment that can support that only the local variations of the diffusion coefficient influence the contraction factor q_{ctr}. In the following, we will describe the chosen setting and give insight into the choice of the parameters. The diffusion problem (2.4) is considered on the unit square $\Omega = (0,1)^2$ with the right-hand side $f \equiv 1$. Furthermore, we opt for "striped" diffusion, i.e., we consider a piecewise constant diffusion tensor where the value changes across four regions/stripes of the domain; see Figure 7.1. The idea is to compare the following two test cases.

Experiment 7.1. *The value of* $\mathbf{K}$ *on the first stripe is* 10^0*, on the second stripe* 10^2*, on the third stripe* 10^4*, and on the last stripe* 10^6*. For an initial mesh* $\mathcal{T}_0$ *satisfying that any three-layer patch lies at most across two different stripes, it follows that* $\Lambda_{\max}/\Lambda_{\min} = 10^6$ *as well as* $C_{\mathrm{loc}}^{(1)} = C_{\mathrm{loc}}^{(2)} = 100$ *(i.e., local jumps of the diffusion* $\ll$ *global jump); see Figure 7.1 (left).*

Experiment 7.2. *The value of* $\mathbf{K}$ *is 1 on the first and third stripe and* 10^6 *on the other two. This leads to* $\Lambda_{\max}/\Lambda_{\min} = C_{\mathrm{loc}}^{(1)} = C_{\mathrm{loc}}^{(2)} = 10^6$ *(i.e., local jumps of the diffusion = global jump); see Figure 7.1 (right).*

The analysis from Chapter 5 implies that the contraction factor in the first case is smaller than in the second case under the assumption that the same initial mesh is used. However, conducting different experiments, it became clear that it is not easy to isolate the influence of the diffusion coefficient alone. Indeed, many parameters enter (e.g., how the mesh hierarchy is generated, i.e., which choice of θ is employed; how the discretization error influences the mesh generation process, i.e., which choice of p is used; to which precision the solver is iterating, i.e., for AFEM with certain μ in the stopping criterion). Since discretization and

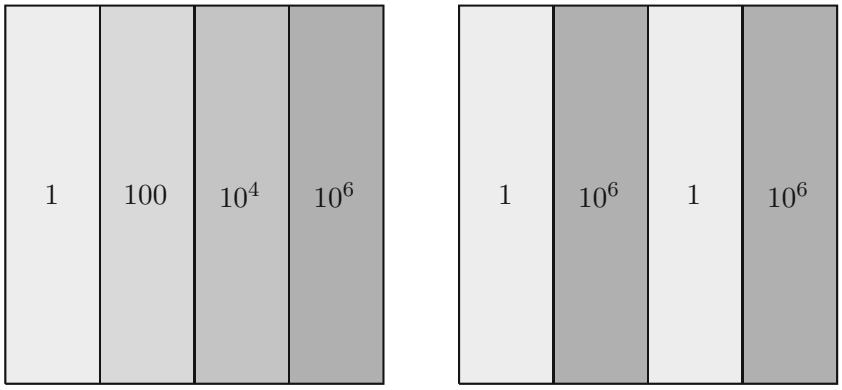

Figure 7.1: Striped diffusion. We display the diffusion coefficient from Experiment 7.1 (left) and the diffusion coefficient from Experiment 7.2 (right).

algebra cross-influence each other, we opt to fix a pre-computed mesh hierarchy (of $L = 10$) generated via Algorithm 6.1 and study therein the behavior of the solver of Algorithm 3.7. Assuming the mesh hierarchy is given, the solver yields a new approximation u_L^{k+1} after one step on the current approximation u_L^k (after k iterations, $k \geq 0$). Then, the experimental contraction factor is given by

$$q_{\mathrm{ctr},k} = \frac{|||u_L^* - u_L^{k+1}|||}{|||u_L^* - u_L^k|||}. \tag{7.1}$$

This is iterated until the stopping criterion $\zeta_L(u_L^k) < \mathrm{tol}$ is reached. We use $\mathrm{tol} = 10^{-13}$, which results in the computation of enough iterations to be able to draw some insights from the solver contraction.

7.1.1 Pre-computed meshes

Let us now explain how the mesh hierarchy $\{\mathcal{T}_\ell\}_{\ell=0}^{10}$ is generated utilizing Algorithm 6.1. We expect to see the biggest influence of the diffusion-contrast on the contraction factor when a mesh hierarchy is used, which is mostly refined along the lines where the diffusion coefficient changes value. Hence, we choose appropriate input parameters of Algorithm 6.1:

- Initial mesh $\mathcal{T}_0$: The requirements of the initial mesh are rather clear from the analysis of Chapter 5 as it needs to be fine enough such that its 3-patches are at most contained in two stripes. In practice, this is achieved by initially considering a coarse mesh and possibly performing a limited number of uniform refinements (in our case 3).
- Adaptivity parameter θ: Since the goal is to eventually use the solver within an adaptive framework, the generated meshes should be rather locally refined in the vicinity of singularities. Hence, we change to $\theta = 0.3$ from the usual $\theta = 0.5$.
- Solver stopping parameter μ: Since this section focuses on the solver, we use $\mu = 10^{-3}$, thus oversolving the algebraic problem.

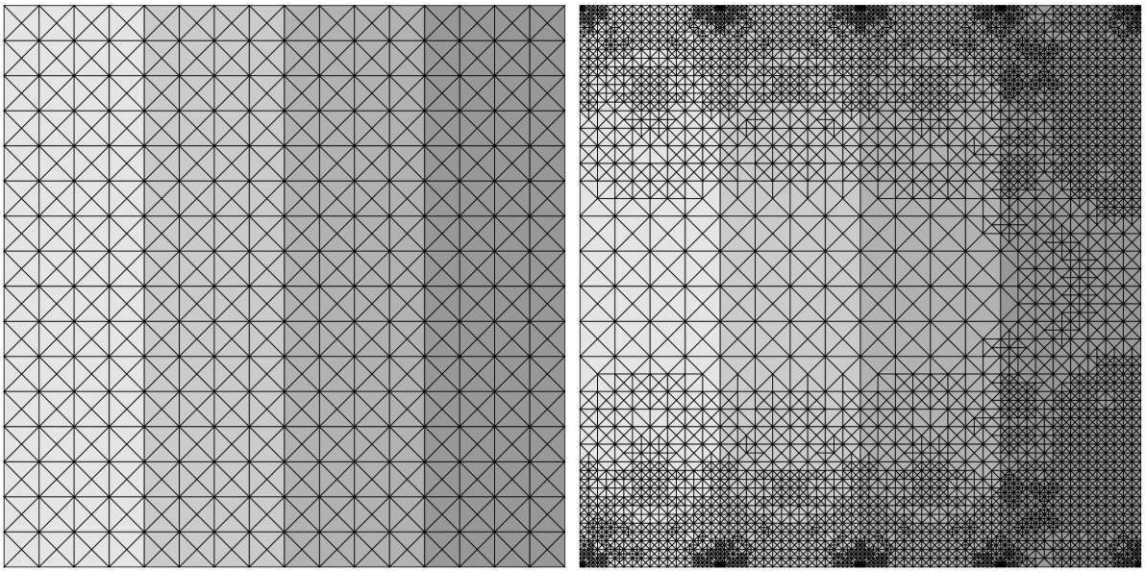

Figure 7.2: Adaptively-refined meshes. Left: The initial mesh $\mathcal{T}_0$ with $\#\mathcal{T}_0 = 1024$ elements which is fine enough so that any 3-patch only goes across two stripes at most but coarse enough so that a direct solve is inexpensive. Right: The mesh $\mathcal{T}_{10}$ with $\#\mathcal{T}_{10} = 9854$ elements that is obtained with Algorithm 6.1 using the described parameters.

- Polynomial degree p: Since we need to decide a polynomial degree for the pre-computed mesh-generation and since we later want to test the solver for different polynomial degrees, we choose $p = 2$ here.
- Diffusion coefficient $\mathbf{K}$: We also need to choose a diffusion coefficient for the generation of the mesh hierarchy. Since we do not want to favor one of the two Experiments 7.1 or 7.2, but want nonetheless refinement along the stripes, we use another "striped" diffusion: set $\mathbf{K} \equiv 1$ on the first and third stripe and 10^3 on the rest.

In Figure 7.2, the initial and final meshes are displayed.

Utilizing the precomputed mesh hierarchy, we calculate the experimental contraction factor (7.1) of Algorithm 3.7 for the diffusion coefficients from Experiment 7.1 and Experiment 7.2 on the final level $L = 10$ until the proposed tolerance $\zeta_L(u_L^k) < 10^{-13}$ is reached. The results for $p = 1, 2, 5$ are presented in Figure 7.3. These results corroborate the analysis in Chapter 5 since the contraction factor is reduced when the jumps in the diffusion coefficient are gradual as in Experiment 7.1, compared to the scenario of Experiment 7.2, where the local jumps coincide with the global jump. To showcase the h-robustness of the contraction factor, we also pre-compute a mesh hierarchy with 15 levels (i.e., $L = 15$) and repeat the aforementioned experiment. To this end, we display the experimental contraction factor (7.1) of Algorithm 3.7 for the diffusion coefficients from Experiment 7.1 and Experiment 7.2 on the final level $L = 15$ until the proposed tolerance $\zeta_L(u_L^k) < 10^{-13}$ is reached for $p = 5$ in Figure 7.3. We observe that the experimental contraction factor is still

of the same size as for $L = 10$, which confirms h-robustness. However, the difference between the two diffusion coefficients from Experiment 7.1 and Experiment 7.1 is less noticable.

7.1.2 Other mesh hierarchies

Algorithm 3.7 requires a sequence of meshes as input, which is assumed to be available. In the last section, we gave one reasonable example of how this could be done. However, other options of meshes can be used and we now discuss how this influences the behavior of the solver with respect to the diffusion coefficient.

Remark 7.3 (Studying the diffusion jumps)**.** *Though in the previous tests, we indeed see better contraction factors for problems where the local jumps of the diffusion coefficient are lower than the global jump, the improvements are rather mild. This by no means discourages the analytical improvements, we set in place. It may well be that more sophisticated singular problems (exhibiting e.g. cross points) need to be engineered to truly see a degradation of contraction factors. However, it is not straightforward to construct* comparable *singular test cases where the only difference is the locality of the jumps.*

Remark 7.4. *Another reason why the gap between Experiment 7.1 and Experiment 7.2 in Figure 7.3 is not as large as one might expect, may stem from the analysis being overly pessimistic. Recall the norm equivalence* (2.6)*, i.e.,*

$$\Lambda_{\min}^{1/2}\|\nabla u\| \leq |\!|\!| u |\!|\!| \leq \Lambda_{\max}^{1/2}\|\nabla u\| \quad \text{for all } u \in \mathcal{X}.$$

The analysis in Chapter 4, using essentially this estimate to extend the framework from the H^1-seminorm analysis, yields that the contraction factor depends on $\Lambda_{\max}/\Lambda_{\min}$. However, the above equivalence indicates that q_{ctr} possibly depends only on $(\Lambda_{\max}/\Lambda_{\min})^{1/2}$ instead.

Remark 7.5 (Parameters for the pre-computed meshes)**.** *For the comparison of the diffusion coefficient from Experiment 7.1 to the one from Experiment 7.2 on a pre-computed mesh hierarchy, we explored different choices of the adaptivity parameter θ and polynomial degree p. Whenever the generated meshes were rather uniform the history plots for the contraction factor became almost identical for the two diffusion coefficients. We believe this happens because the almost uniform meshes make it so that the geometry is resolved rather too well. In Figure 7.4, we show an example of this phenomenon for $\theta = 0.5$ and $p = 1$.*

Remark 7.6 (Choice of meshes)**.** *It is curious to see that when running tests where the algebra and the discretization mutually influence each other, the situation overall improves. This is to say, in the typical AFEM setting with multigrid as the inexact solver, the mesh becomes more tailored to the singularities stemming from the jumps in the diffusion coefficient. As a result, the contraction factors improve even when the local jumps are the same as the global jump. We want to give an example here. Let us consider the diffusion coefficient from Experiment 7.2 and compare it to $\mathbf{K} \equiv 1$. We construct the meshes with Algorithm 6.1 but use the corresponding diffusion coefficients and polynomial degrees $p = 2, 4, 6$ already for the generation of the mesh hierarchy. Furthermore, we set $\theta = 0.5$ and $\mu = 10^{-5}$ in the stopping criterion* (6.1)*. In Figure 7.5, we can see that the contraction factors for the two diffusion coefficients are not comparable. We believe this is due to the cross-influence of the discretization and algebra since we are not pre-computing the meshes anymore.*

7.1.3 Step-sizes

In this section, we use an additional diffusion coefficient which is introduced in the following experiment.

Experiment 7.7. *The value of* $\mathbf{K}$ *on the first stripe is 1, on the second stripe 10, on the third stripe* 100*, and on the last stripe* 1000*. For an initial mesh* $\mathcal{T}_0$ *satisfying that any three-layer patch lies at most across two different stripes, it follows that* $\Lambda_{\max}/\Lambda_{\min} = 1000$ *as well as* $C_{\mathrm{loc}}^{(1)} = C_{\mathrm{loc}}^{(2)} = 10$.

Our objective is to check the bounds of the step-size λ_ℓ as already promised in Chapter 4. In the numerical experiments, the optimal step-size s_ℓ never crosses the limit $d+1$. Hence, the case distinction in Algorithm 3.7 never takes place in practice. In order to observe this, Algorithm 6.1 is used and set to terminate if 10^6 degrees of freedom are reached. Moreover, we use $\theta = 0.5$ and $\mu = 10^{-5}$ in the stopping criterion (6.1) thus oversolving the algebra. Furthermore, the diffusion coefficient introduced in Experiment 7.7 is utilized. In Figure 7.6 (left), the maximal step-size on a level ℓ for the polynomial degrees $p = 1, 2, 3, 4$ is shown as well as the upper bound $d+1$. Throughout, the values of λ_ℓ lie well below this bound. In Figure 7.6 (right), the minimal step-size on a level and the lower bound $(d+1)^{-1}$ are displayed.

7.2 Optimality of AFEM with multigrid solver

The objective of this section is to confirm Theorem 6.8 of Chapter 6. As discussed in Remark 6.9 the constants c_{opt} and C_{opt} depend on q_{ctr} and hence Chapter 5 implies that they depend on local variations of the diffusion coefficient. Therefore, we again use the diffusion coefficients described in Experiment 7.1 and Experiment 7.2. We set $\mu = 0.1$ in Algorithm 6.1 and study the decrease of the discretization error estimator $\eta_L(u_L^k)$ with respect to the cumulative time and cumulative degrees of freedom

$$\sum_{\substack{(L'k')\in\mathcal{Q}\\ |L',k'|\leq|L,k|}} \dim \mathcal{X}_{L'}$$

which is equivalent to the overall computational cost (6.5). Theorem 6.8 guarantees optimal rates for the quasi error H_L^k in terms of the overall computational cost. However, for the final iterate, the error estimator is equivalent to the quasi-error, i.e., $\mathrm{H}_\ell^k \simeq \eta_\ell(u_\ell^k)$ as follows directly from Lemma 6.4. Let us first consider the diffusion coefficient from Experiment 7.1. Furthermore, we use $\theta = 0.5$ and polynomial degrees $p = 1, 2, 3, 4$. After a pre-asymptotic phase, one can observe the optimal convergence rates $-p/2$ in Figure 7.7 both with respect to the cumulative degrees of freedom and with respect to the cumulative time.

We perform the same experiments for the diffusion coefficient described in Experiment 7.2 and also observe optimal convergence rates in Figure 7.8. This is not surprising since the analysis in Chapter 6 ensures optimal complexity for all diffusion coefficients that satisfy the assumptions in Section 2.2. Furthermore, the influence of c_{opt} and C_{opt} is rather seen in the longer pre-asymptotic regime in Figure 7.8 compared to Figure 7.7.

7.2.1 Nested iterations

Finally, we repeat the experiments from this section but omit nested iteration, i.e., $u_{L+1}^0 = u_L^k$, and instead set $u_L^0 := 0$ for all levels $L \in \mathbb{N}$. Furthermore, we use $\mu = 10^{-2}$ in the stopping criterion (6.1). The results for the diffusion coefficient from Experiment 7.1 can be seen in Figure 7.9 and for the diffusion coefficient described in Experiment 7.2 in Figure 7.10. Since the analysis in Chapter 6 explicitly uses nested iteration, we observe suboptimal rates with respect to the cumulative degrees of freedom, as well as a considerably worse pre-asymptotic regime; see Figure 7.9 and Figure 7.10 (top left). Furthermore, as shown in Figure 7.9 and Figure 7.10 (top right), the convergence rates with respect to time are noticeably suboptimal starting at polynomial degree $p = 3$. Therefore, nested iteration is not only needed for the analysis but also necessary in practice to achieve optimal complexity. However, the convergence rates with respect to the degrees of freedom remain optimal, as demonstrated in Figure 7.9 and Figure 7.10 (bottom left). Finally, the number of iterations of the multigrid solver with respect to the degrees of freedom increases, as we always start with the same initial guess $u_L^0 := 0$. This is shown in Figure 7.9 and Figure 7.10 (bottom right).

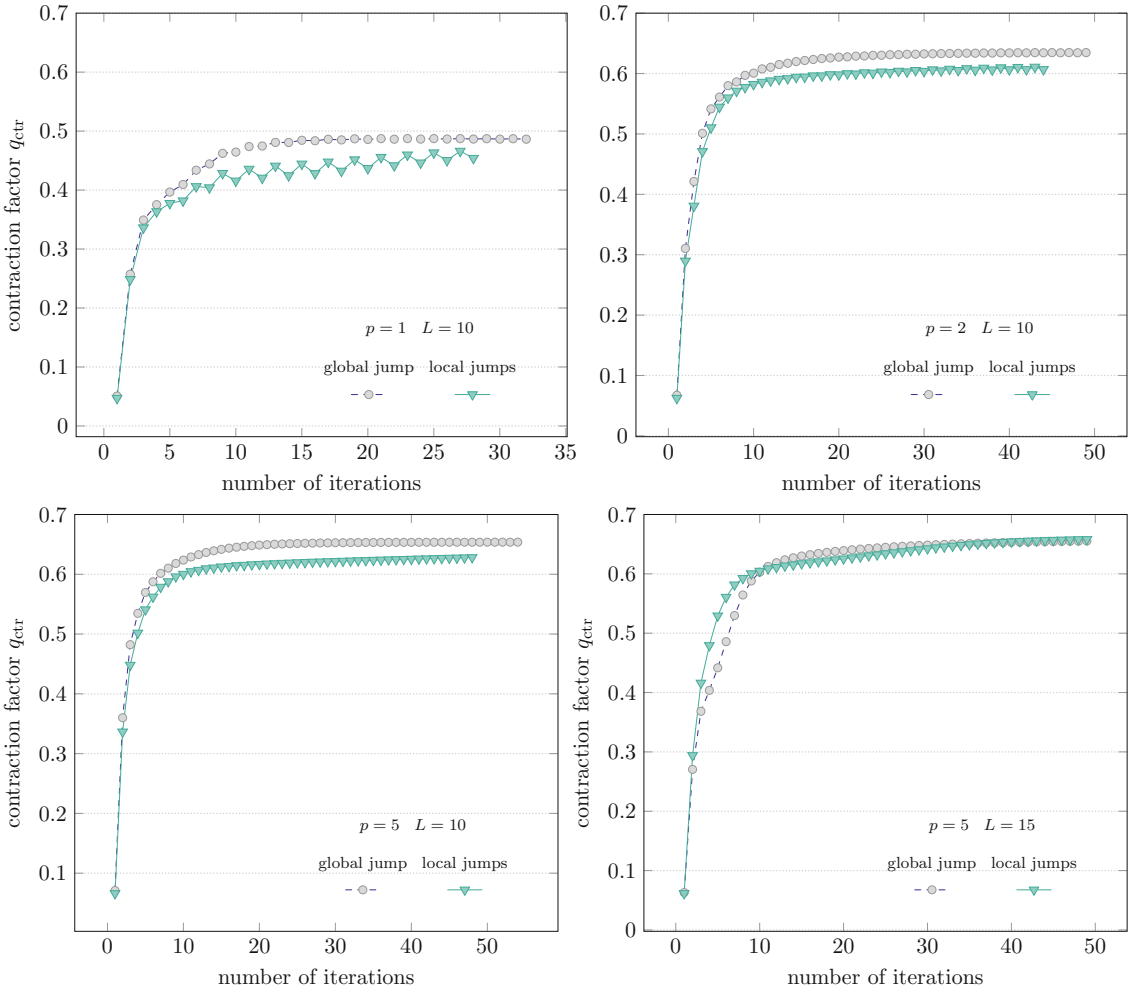

Figure 7.3: Contraction factor of the multigrid solver. History plot of the experimental contraction factor for the diffusion coefficient from Experiment 7.1 in green compared to the diffusion coefficient from Experiment 7.2 in grey calculated on the pre-computed mesh hierarchy introduced in Section 7.1.1, where $\dim(\mathbb{S}^1_0(\mathcal{T}_{10})) = 5078$, $\dim(\mathbb{S}^2_0(\mathcal{T}_{10})) = 20009$ and $\dim(\mathbb{S}^5_0(\mathcal{T}_{10})) = 123926$.

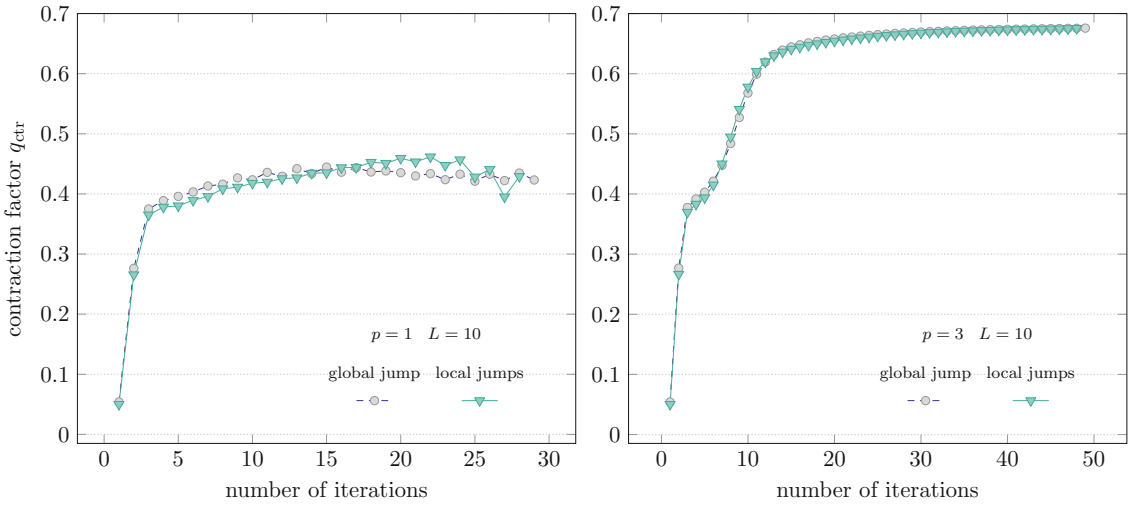

Figure 7.4: Contraction factor of the multigrid solver. History plot of the experimental contraction factor for diffusion coefficient from Experiment 7.1 in green compared to the diffusion coefficient from Experiment 7.2 in grey calculated on the pre-computed mesh hierarchy described in Remark 7.5.

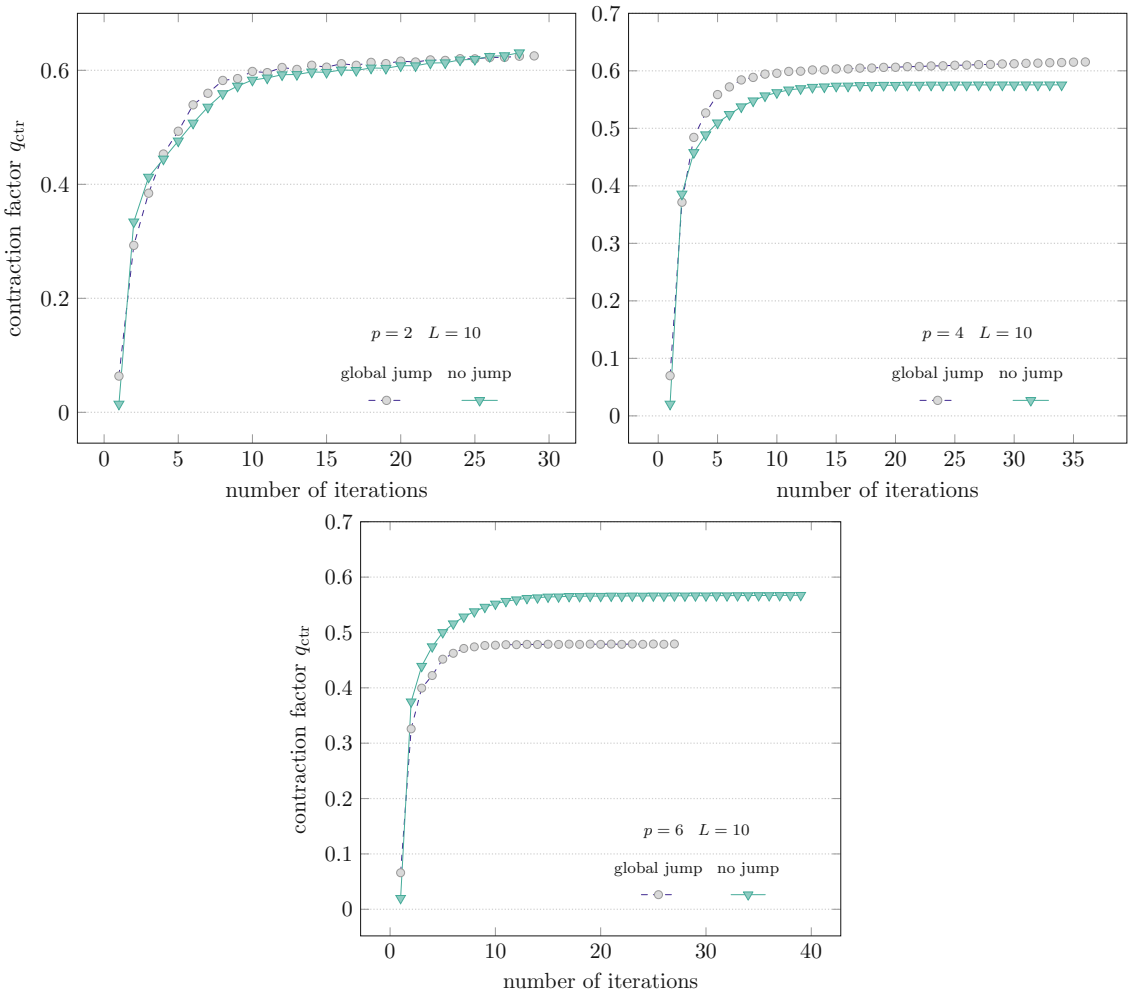

Figure 7.5: Contraction factor of the multigrid solver. History plot of the experimental contraction factor for the identity as diffusion coefficient in green and for the diffusion coefficient from Experiment 7.2 in grey computed on the respective adaptive meshes; see Remark 7.6.

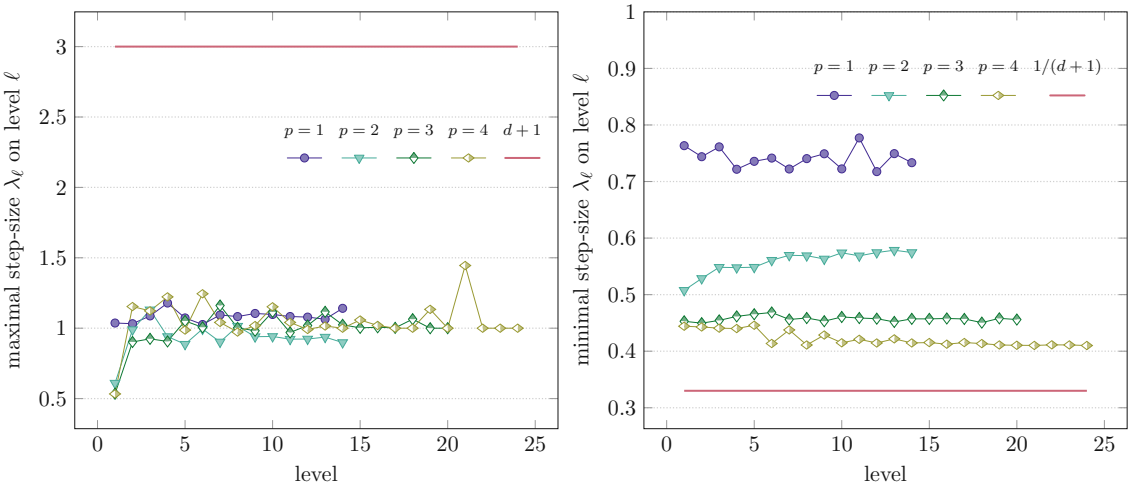

Figure 7.6: Step-size of the multigrid solver. History plot of the maximal step-size (left) and the minimal step-size (right) compared to the corresponding bounds calculated for the diffusion coefficient from Experiment 7.7 introduced in Section 7.1.3.

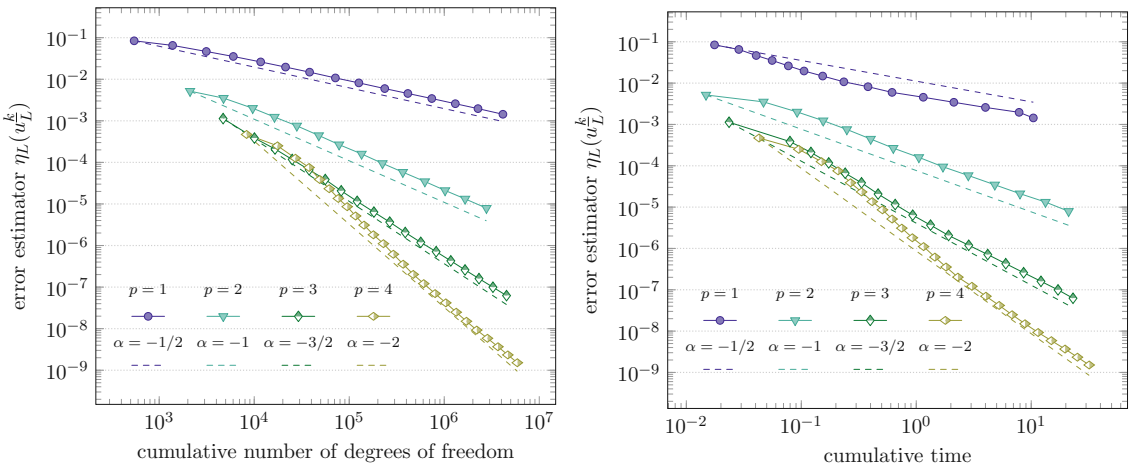

Figure 7.7: Optimality of AFEM for the striped diffusion with local jumps from Experiment 7.1. The convergence history plot of the discretization error $\eta_L(u_L^k)$ with respect to the cumulative degrees of freedom (left) and with respect to the cumulative time (right); see Section 7.2.

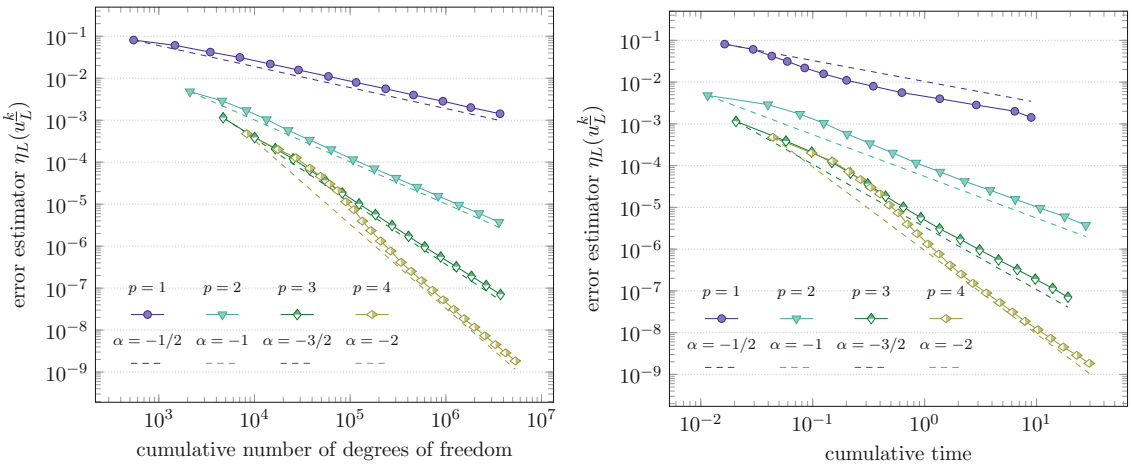

Figure 7.8: Optimality of AFEM for the striped diffusion with global jumps from Experiement 7.2. The convergence history plot of the discretization error $\eta_L(u_L^k)$ with respect to the cumulative degrees of freedom (left) and with respect to the cumulative time (right); see Section 7.2.

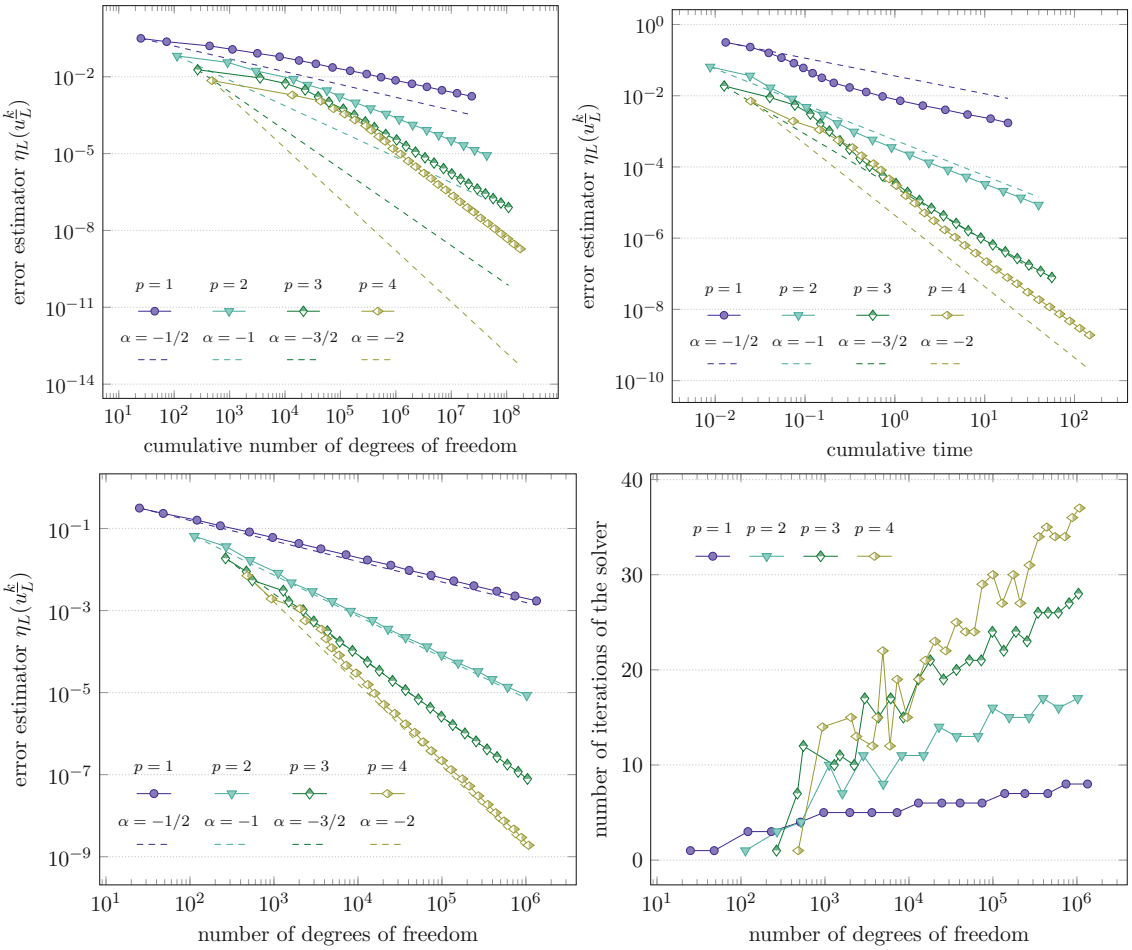

Figure 7.9: AFEM without nested iteration for the striped diffusion with local jumps from Experiment 7.1. The convergence history plot of the discretization error $\eta_L(u_L^k)$ with respect to the cumulative degrees of freedom (top left), with respect to the cumulative time (top right), and with respect to the degrees of freedom (bottom left), as well as the number of iterations of the algebraic solver with respect to the degrees of freedom (bottom right); see Section 7.2.1.

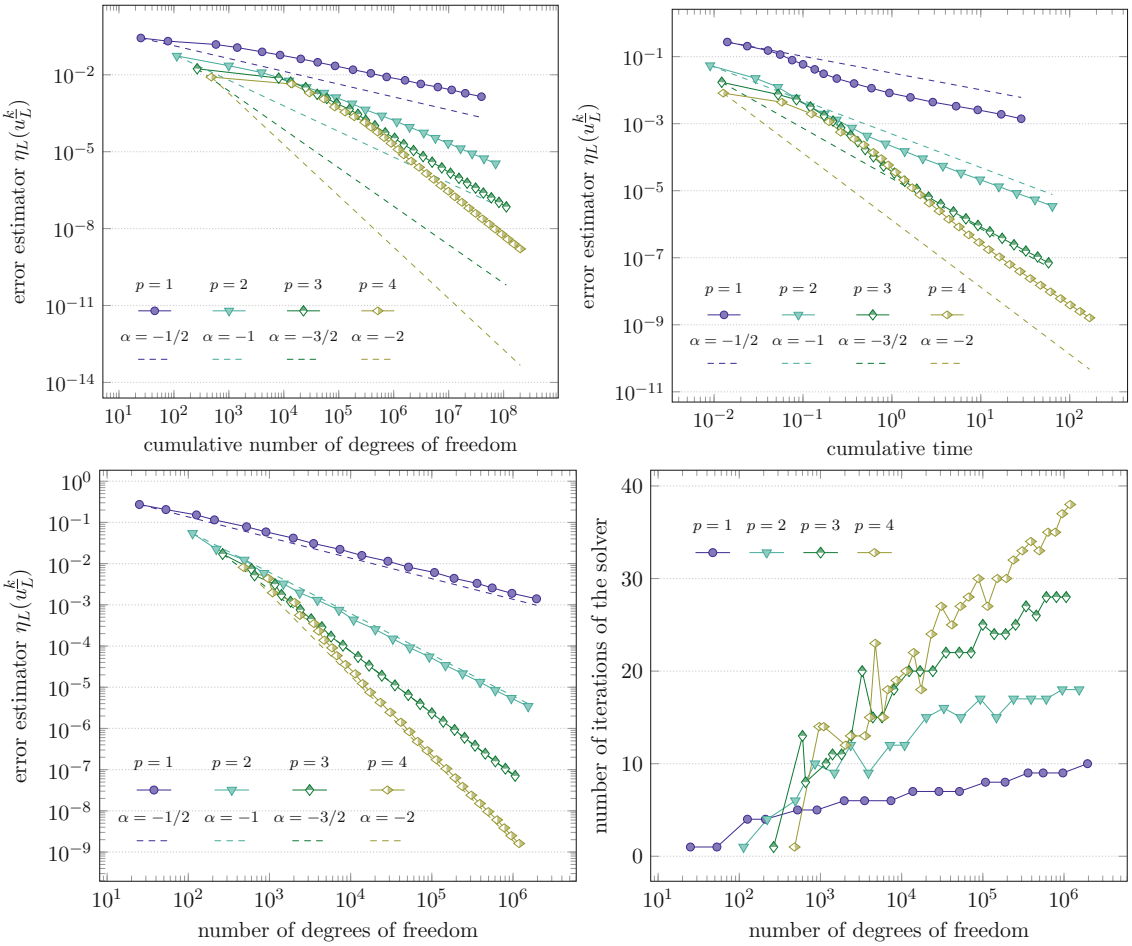

Figure 7.10: AFEM without nested iteration for the striped diffusion with global jumps from Experiment 7.2. The convergence history plot of the discretization error $\eta_L(u_L^k)$ with respect to the cumulative degrees of freedom (top left), with respect to the cumulative time (top right), and with respect to the degrees of freedom (bottom left), as well as the number of iterations of the algebraic solver with respect to the degrees of freedom (bottom right); see Section 7.2.1.

References

[AF03] Robert A. Adams and John J. F. Fournier. *Sobolev spaces*. Second. Vol. 140. Pure and Applied Mathematics (Amsterdam). Elsevier/Academic Press, Amsterdam, 2003, pp. xiv+305. ISBN: 0-12-044143-8.

[AFF+13] Markus Aurada, Michael Feischl, Thomas Führer, Michael Karkulik, and Dirk Praetorius. "Efficiency and optimality of some weighted-residual error estimator for adaptive 2D boundary element methods". In: *Comput. Methods Appl. Math.* 13.3 (2013), pp. 305–332. ISSN: 1609-4840,1609-9389. DOI: 10.1515/cmam-2013-0010.

[BCM+91] Ivo Babuška, Alan W. Craig, Jan Mandel, and Juhani Pitkäranta. "Efficient preconditioning for the p-version finite element method in two dimensions". In: *SIAM J. Numer. Anal.* 28.3 (1991), pp. 624–661. ISSN: 0036-1429. DOI: 10.1137/0728034.

[BDD04] Peter Binev, Wolfgang Dahmen, and Ron DeVore. "Adaptive finite element methods with convergence rates". In: *Numer. Math.* 97.2 (2004), pp. 219–268. ISSN: 0029-599X,0945-3245. DOI: 10.1007/s00211-003-0492-7.

[BFM+24] Philipp Bringmann, Michael Feischl, Ani Miraci, Dirk Praetorius, and Julian Streitberger. *On full linear convergence and optimal complexity of adaptive FEM with inexact solver*. Preprint, 2024. arXiv: 2311.15738 [math.NA].

[BHM00] William L. Briggs, Van Emden Henson, and Steve F. McCormick. *A multigrid tutorial*. Second. Society for Industrial and Applied Mathematics (SIAM), Philadelphia, PA, 2000, pp. xii+193. ISBN: 0-89871-462-1. DOI: 10.1137/1.9780898719505.

[BS08] Susanne C. Brenner and L. Ridgway Scott. *The mathematical theory of finite element methods*. Third. Vol. 15. Texts in Applied Mathematics. Springer, New York, 2008, pp. xviii+397. ISBN: 978-0-387-75933-3. DOI: 10.1007/978-0-387-75934-0.

[Bur99] Victor Burenkov. "Extension theorems for Sobolev spaces". In: *The Maz'ya anniversary collection, Vol. 1 (Rostock, 1998)*. Vol. 109. Oper. Theory Adv. Appl. Birkhäuser, Basel, 1999, pp. 187–200. ISBN: 3-7643-6201-4.

[BY93] Folkmar Bornemann and Harry Yserentant. "A basic norm equivalence for the theory of multilevel methods". In: *Numer. Math.* 64.4 (1993), pp. 455–476. ISSN: 0029-599X,0945-3245. DOI: 10.1007/BF01388699.

[CFP+14] Carsten Carstensen, Michael Feischl, Marcus Page, and Dirk Praetorius. "Axioms of adaptivity". In: *Comput. Math. Appl.* 67.6 (2014), pp. 1195–1253. ISSN: 0898-1221,1873-7668. DOI: 10.1016/j.camwa.2013.12.003.

[CKN+08] J. Manuel Cascon, Christian Kreuzer, Ricardo H. Nochetto, and Kunibert G. Siebert. "Quasi-optimal convergence rate for an adaptive finite element method". In: *SIAM J. Numer. Anal.* 46.5 (2008), pp. 2524–2550. ISSN: 0036-1429,1095-7170. DOI: 10.1137/07069047X.

[CNX12] Long Chen, Ricardo H. Nochetto, and Jinchao Xu. "Optimal multilevel methods for graded bisection grids". In: *Numer. Math.* 120.1 (2012), pp. 1–34. ISSN: 0029-599X,0945-3245. DOI: 10.1007/s00211-011-0401-4.

[DGS24] Lars Diening, Lukas Gehring, and Johannes Storn. *Adaptive mesh refinement for arbitrary initial triangulations*. Preprint, 2024. arXiv: 2306.02674 [math.NA].

[DJN15] Victorita Dolean, Pierre Jolivet, and Frédéric Nataf. *An introduction to domain decomposition methods*. Algorithms, theory, and parallel implementation. Society for Industrial and Applied Mathematics (SIAM), Philadelphia, PA, 2015, pp. x+238. ISBN: 978-1-611974-05-8. DOI: 10.1137/1.9781611974065.ch1.

[Dör96] Willy Dörfler. "A convergent adaptive algorithm for Poisson's equation". In: *SIAM J. Numer. Anal.* 33.3 (1996), pp. 1106–1124. ISSN: 0036-1429. DOI: 10.1137/0733054.

[EG21a] Alexandre Ern and Jean-Luc Guermond. *Finite elements I—Approximation and interpolation*. Vol. 72. Texts in Applied Mathematics. Springer, Cham, 2021, pp. xii+325. ISBN: 978-3-030-56340-0; 978-3-030-56341-7. DOI: 10.1007/978-3-030-56341-7.

[EG21b] Alexandre Ern and Jean-Luc Guermond. *Finite elements II—Galerkin approximation, elliptic and mixed PDEs*. Vol. 73. Texts in Applied Mathematics. Springer, Cham, 2021, pp. ix+492. ISBN: 978-3-030-56922-8; 978-3-030-56923-5. DOI: 10.1007/978-3-030-56923-5.

[EV13] Alexandre Ern and Martin Vohralík. "Adaptive inexact Newton methods with a posteriori stopping criteria for nonlinear diffusion PDEs". In: *SIAM J. Sci. Comput.* 35.4 (2013), A1761–A1791. DOI: 10.1137/120896918.

[FFP+17] Michael Feischl, Thomas Führer, Dirk Praetorius, and Ernst P. Stephan. "Optimal additive Schwarz preconditioning for hypersingular integral equations on locally refined triangulations". In: *Calcolo* 54.1 (2017), pp. 367–399. ISSN: 0008-0624,1126-5434. DOI: 10.1007/s10092-016-0190-3.

[GHP+21] Gregor Gantner, Alexander Haberl, Dirk Praetorius, and Stefan Schimanko. "Rate optimality of adaptive finite element methods with respect to overall computational costs". In: *Math. Comp.* 90.331 (2021), pp. 2011–2040. ISSN: 0025-5718,1088-6842. DOI: 10.1090/mcom/3654.

[Gil07] William Gilbert Strang. "Multigrid Methods". MIT. Lecture Notes. 2007. URL: https://math.mit.edu/classes/18.086/2006/am63.pdf.

[GSS14] Dietmar Gallistl, Mira Schedensack, and Rob P. Stevenson. "A remark on newest vertex bisection in any space dimension". In: *Comput. Methods Appl. Math.* 14.3 (2014), pp. 317–320. ISSN: 1609-4840,1609-9389. DOI: 10.1515/cmam-2014-0013.

[Hac85] Wolfgang Hackbusch. *Multi-Grid Methods and Applications*. Vol. 4. Jan. 1985. ISBN: 3-540-12761-5. DOI: 10.1007/978-3-662-02427-0.

[HWZ12] Ralf Hiptmair, Haijun Wu, and Weiying Zheng. "Uniform convergence of adaptive multigrid methods for elliptic problems and Maxwell's equations". In: *Numer. Math. Theory Methods Appl.* 5.3 (2012), pp. 297–332. ISSN: 1004-8979,2079-7338. DOI: 10.4208/nmtma.2012.m1128.

[IMP+24] Michael Innerberger, Ani Miraçi, Dirk Praetorius, and Julian Streitberger. "*hp*-robust multigrid solver on locally refined meshes for FEM discretizations of symmetric elliptic PDEs". In: *ESAIM Math. Model. Numer. Anal.* 58.1 (2024), pp. 247–272. ISSN: 2822-7840,2804-7214. DOI: 10.1051/m2an/2023104.

[IP23] Michael Innerberger and Dirk Praetorius. "MooAFEM: an object oriented Matlab code for higher-order adaptive FEM for (nonlinear) elliptic PDEs". In: *Appl. Math. Comput.* 442 (2023), Paper No. 127731, 17. ISSN: 0096-3003,1873-5649. DOI: 10.1016/j.amc.2022.127731.

[KPP13] Michael Karkulik, David Pavlicek, and Dirk Praetorius. "On 2D newest vertex bisection: optimality of mesh-closure and H^1-stability of L_2-projection". In: *Constr. Approx.* 38.2 (2013), pp. 213–234. ISSN: 0176-4276,1432-0940. DOI: 10.1007/s00365-013-9192-4.

[Leo09] Giovanni Leoni. *A first course in Sobolev spaces*. Vol. 105. Graduate Studies in Mathematics. American Mathematical Society, Providence, RI, 2009, pp. xvi+607. ISBN: 978-0-8218-4768-8. DOI: 10.1090/gsm/105.

[PP20] Carl-Martin Pfeiler and Dirk Praetorius. "Dörfler marking with minimal cardinality is a linear complexity problem". In: *Math. Comp.* 89.326 (2020), pp. 2735–2752. ISSN: 0025-5718,1088-6842. DOI: 10.1090/mcom/3553.

[Pra17] Dirk Praetorius. "Finite element method". TU Wien. Lecture Notes. 2017. URL: https://www.tuwien.at/index.php?eID=dumpFile&t=f&f=180713&token=a213dc70491e4a5a1139ff6e46be20fdb445248f.

[Sch17] Patrick Schön. "Scalable adaptive bisection algorithms on decomposed simplicial partitions for efficient discretizations of nonlinear partial differential equations". PhD thesis. University of Freiburg, 2017.

[SMP+08] Joachim Schöberl, Jens M. Melenk, Clemens Pechstein, and Sabine Zaglmayr. "Additive Schwarz preconditioning for p-version triangular and tetrahedral finite elements". In: *IMA J. Numer. Anal.* 28.1 (2008), pp. 1–24. ISSN: 0272-4979,1464-3642. DOI: 10.1093/imanum/drl046.

[Ste07] Rob P. Stevenson. "Optimality of a standard adaptive finite element method". In: *Found. Comput. Math.* 7.2 (2007), pp. 245–269. ISSN: 1615-3375,1615-3383. DOI: 10.1007/s10208-005-0183-0.

[Ste08] Rob P. Stevenson. "The completion of locally refined simplicial partitions created by bisection". In: *Math. Comp.* 77.261 (2008), pp. 227–241. ISSN: 0025-5718,1088-6842. DOI: 10.1090/S0025-5718-07-01959-X.

[Tra97] Christoph T. Traxler. "An algorithm for adaptive mesh refinement in n dimensions". In: *Computing* 59.2 (1997), pp. 115–137. ISSN: 0010-485X,1436-5057. DOI: 10.1007/BF02684475.

[WC06] Haijun Wu and Zhiming Chen. "Uniform convergence of multigrid V-cycle on adaptively refined finite element meshes for second order elliptic problems". In: *Sci. China Ser. A* 49.10 (2006), pp. 1405–1429. ISSN: 1006-9283,1862-2763. DOI: 10.1007/s11425-006-2005-5.

[WZ17] Jinbiao Wu and Hui Zheng. "Uniform convergence of multigrid methods for adaptive meshes". In: *Appl. Numer. Math.* 113 (2017), pp. 109–123. ISSN: 0168-9274,1873-5460. DOI: 10.1016/j.apnum.2016.11.005.

[Xu97] Jinchao Xu. "An introduction to multigrid convergence theory". In: *Iterative methods in scientific computing (Hong Kong, 1995)*. Springer, Singapore, 1997, pp. 169–241. ISBN: 981-3083-08-5.